Ministry of Education and Science of the Russian Federation

NOVOSIBIRSK STATE TECHNICAL UNIVERSITY

INTERNATIONAL SUMMERSCHOOL ON COMPUTER SCIENCE, COMPUTER ENGINEERING AND EDUCATION TECHNOLOGY 2018

Proceedings of the ISCSET-2018 workshop (Novosibirsk, Russia, 12-18 of August)

NOVOSIBIRSK

2018

CONTENTS

BlackPearl: Extended Automotive Multi-ECU Demonstrator Platform

Mirko Lippmann[1], Batbayar Battseren[2], Ariane Heller[3], Wolfram Hardt[4]

[1,2,3,4]*TU Chemnitz*

[4]*hardt@cs.tu-chemnitz.de*

***Abstract* - Today's Advanced Driver Assistance Systems (ADAS) use more and more image based sensors. Image preprocessing, feature detection and feature recognition cannot be computed by typical Electronic Control Unit (ECU) hardware. Although multi-ECU systems are used for automotive control systems the capacity and the architecture features don`t meet the needs of such image processing tasks. Thus, we extended our automotive multi-ECU demonstrator platform named YellowCar. Standard multicore prototyping boards are introduced. The multicore processors provide high computation power and enables parallel computing techniques. The implementation of the image processing change is comfortable and high performant. The computed information is packed into CAN (Controller Area Network) messages and passed to the multi-ECU AUTOSAR system implementing the ADAS functions. First applications have been mapped to the extended automotive multi-ECU demonstrator platform BlackPearl.**

Keywords - Automotive demonstrator platform, image processing, multicore, feature point detection, advanced driver assistance system development, AUTOSAR.

I. INTRODUCTION

The YellowCar automotive multi-ECU demonstrator platform is the basis for our ADAS prototyping. This demonstrator platform has been developed for functional tests, performance evaluation, and optimizations of the software architecture for hardware independent implementation of ADAS functions. But ADAS algorithms use more and more image based sensors. This leads to a change of algorithms and introduces the need of high performant image processing tasks. The extended platform is composed as a multi board rack which is mounted on a miniature model of a car, well known from the market for kid´s toys. The electric power infrastructure is battery based. Standard ultrasonic distance sensors in front and back side and speed sensors provide control information. Additional cameras are mounted as well. Actors are a powertrain unit, which consists an electric motor

which can move the car and a steering unit. Additionally, the platform has several lights that can be switched and a horn for acoustic signals.

Image processing is a complex task typically divided into several steps. Artificial intelligence approaches as deep learning and machine learning can be applied. On the other hand, feature point oriented algorithms can be used to identify and extract relevant information. The image processing chain for this kind of algorithms consist of three steps: image preprocessing, feature point (FP) detection, and target recognition. These steps are depicted in Fig. 1.

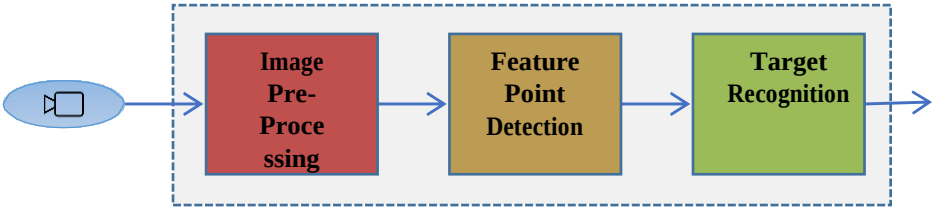

Fig. 1: Image processing chain for feature point algorithms

The processing platform for the image processing chain must be high performant. Therefore we separated the image processing from the automotive multi-ECU control system. This requires a new architecture modularization and adequate communication. This concept is described next.

II. MODULARIZATION

The BlackPearl extended automotive multi-ECU demonstrator platform combines four aspects. First, sensor data is read in and actor data is written. Second, ADAS algorithms and the automotive system control is implemented by the multi-ECU network interconnected by CAN bus. Third, the image processing chain is implemented on one or more multicore processors. Forth, control information and process status can be visualized by the display module. This modularization is depicted in Fig. 2. All units are interconnected by CAN bus. The cameras are connected directly to the image processing module, due to bandwidth issues. All units are implemented on separate boards. This boards can be plugged into our new rack design. Actual, the rack design allows up to three ECU units and three additional image processing units. Future extensions may double the number of units. Thus, the rack design is very flexible and supports image processing tasks as well as automotive control tasks.

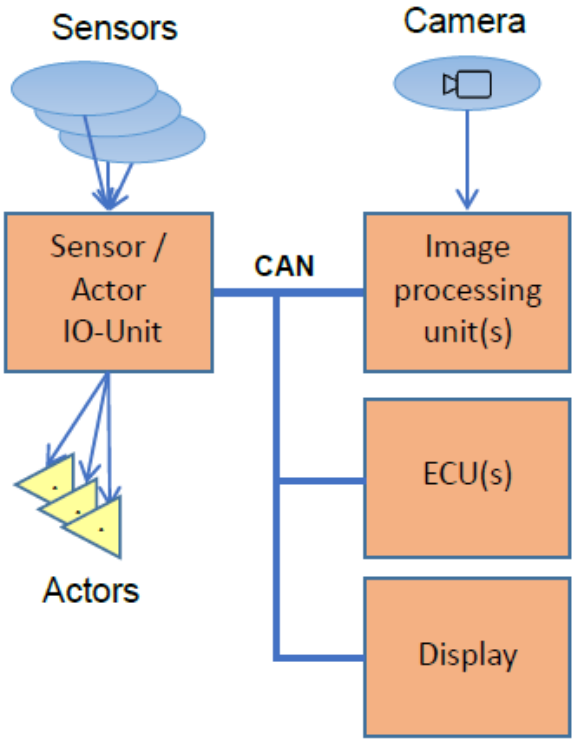

Fig. 2: Modularized rack architecture

The sensor unit handles all sensor inputs. In total six ultrasonic distance sensors (USS) are installed. Three USSs are used for front distance control and three USSs are used for back distance control. Also for steering control and light control sensors are added. The same unit handles the actors as well. Various motors and some control LEDs can be activated. Fig. 3 shows the details. Also, the implementation of the sensor unit has been modularized. We developed a printed circuit board and driver modules, processing modules, and interfaces can be plugged in. This allows easy adaptation to further sensors and new actors as well. And for communications the CAN bus interface is added. Fig. 4 shows the sensor unit implementation.

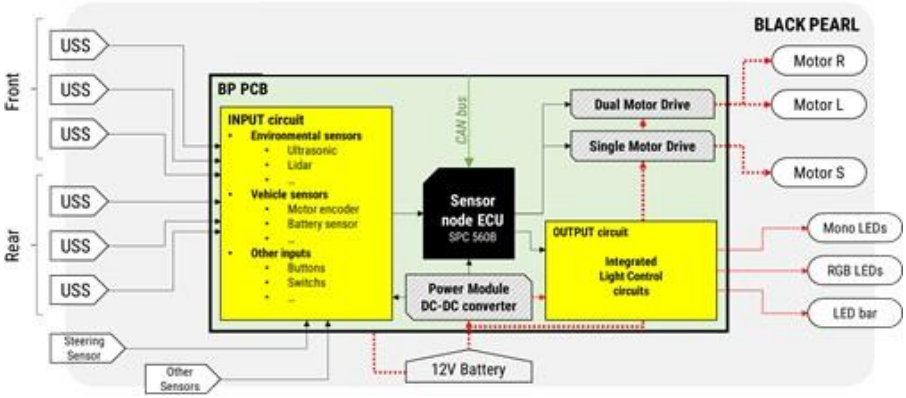

Fig. 3: Sensor unit concept

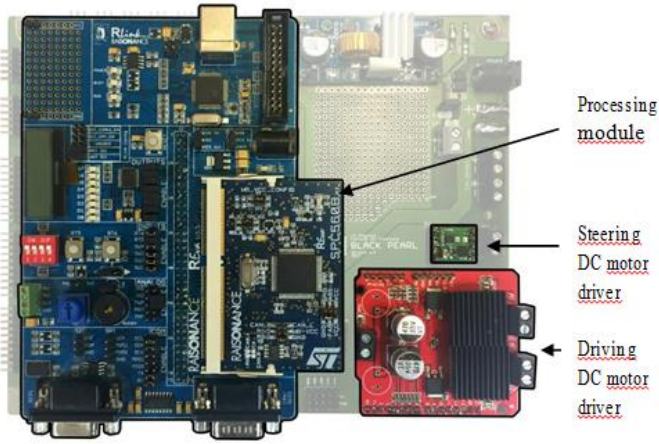

Fig. 4: Sensor unit implementation

The BlackPearl extended automotive multi-ECU demonstrator platform combines image processing and automotive control and ADAS applications. We defined all requirements similar to a real world modern car. Thus, BlackPearl becomes a viable demonstration platform for evaluation of different image processing algorithms in combination with ADAS applications. For details about hardware and software architecture of the multi ECU units see [12].

For the software architecture we implemented the AUTOSAR standard [1]. In recent development strategies in the automotive industry as well as to latest research activities in test automation and evaluation where AUTOSAR is a widely used standard [3, 5, 9] Well-developed tools like Matlab-Simulink [7], dSPACE SystemDesk [8] can be used for implementation of ADAS applications on the extended automotive multi-ECU demonstrator platform BlackPearl. In this way, validation and testing of applications are easily achieved. It is also possible to test by modifying/designing architectural and behavioral aspects before implementing and realizing the actual application on BlackPearl. Similar to a modern car essential applications are distributed to various ECUs of the demonstration platform and image processing applications are implemented beyond the AUTOSAR ECUs.

BlackPearl with modularized rack is shown in Fig. 5.

Fig. 5: BlackPearl extended automotive multi-ECU demonstrator platform

III. IMAGE PROCESSING APPLICATIONS

A typical application of image processing based sensors is the High Way Traffic Analysis (HWTA). In HWTA the following aspects are of interest:

- Vehicles Detection
- Vehicles Speed Estimation
- Highway Traffic Monitoring

We implemented the HWTA by feature point image processing algorithms on the extended automotive multi-ECU demonstrator platform BlackPearl. The first step is image data preprocessing. This step is implemented by Gaussian filtering which is a standard method [11]. The second step, identification of region if interest

eliminates unnecessary information. This reduces the complexity of the following tasks. For feature point extraction the algorithms Blob Detection, SIFT Detection, and SURF Detection are implemented. All vehicles and the lane markings are found and visualized. The implementation is done on multicore Raspberry Pi 3 prototyping boards. This boards are plugged into the BlackPearl rack as image processing unit. Fig. 6 visualizes the successful image processing application. The original image is given, the detected region of interest and the identified vehicles are depicted.

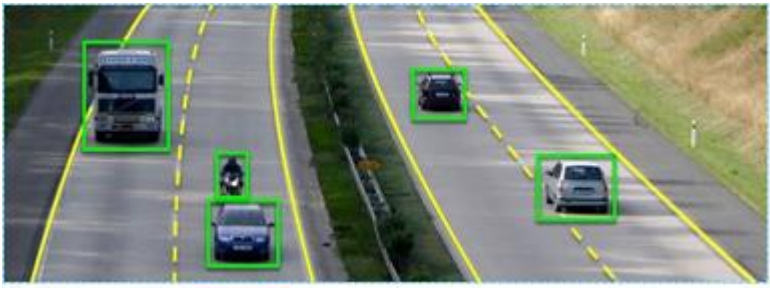

Fig. 6: High Way Traffic Analysis

IV. SUMMARY

The extended automotive demonstrator BackPearl is a research platform with similar behavioral and architectural properties as modern real world cars, developed at Chemnitz University of Technology. Advanced Driver Assistance Systems (ADAS) use more and more image based sensors. Image preprocessing, feature detection and feature recognition cannot be computed by typical ECU hardware. Although multi-ECU systems are used for automotive control systems the capacity and the architecture features don`t meet the needs of such image processing tasks. Thus, we extended our automotive multi-ECU demonstrator platform named YellowCar. Standard multicore prototyping boards are introduced. The multicore processors provide high computation power and enables parallel computing techniques. The implementation of the image processing change is comfortable and high performant. The computed information is packed into can messages and passed to the multi ECU AUTOSAR system implementing the ADAS functions. First applications have been mapped to the extended automotive multi-ECU demonstrator platform BlackPearl.

REFERENCES

[1] AUTOSAR, Layered Software Architecture; Date: 26.06.2017: http://www.autosar.org/fileadmin/files/standards/classic/4-2/software-architecture/general/auxiliary/AUTOSAR_EXP_LayeredSoftwareArchitecture.pdf.

[2] A. Spillner, T. Linz and H. Schaefer: “Software Testing Foundations: A Study Guide for the Certified Tester Exam”, Rocky Nook, 2014, ISBN 978-1937538422.

[3] O. Kindel und M. Friedrich: Softwareentwicklung mit AUTOSAR: Grundlagen, Engineering, Management in der Praxis, dpunkt Verlag, 2009, ISBN 978-3898645638.

[4] N. Englisch et al.: “Application-Driven Evaluation of AUTOSAR Basic Software on Modern ECUs”; Proceedings of the 13th IEEE/IFIP International Conference on Embedded and Ubiquitous Computing, 2015. ISBN: 978-1-4673-8299-1.

[5] N. Englisch et al.: “Efficiently Testing AUTOSAR Software Based on an Automatically Generated Knowledge Base”; 7th Conference on Simulation and Testing for Vehicle Technology; Springer International Publishing, 2016; ISBN: 978-3-319-32344-2.

[6] M. Di Natale: “Scheduling the CAN bus with earliest deadline techniques”, 21st IEEE Proceedings of Real-Time Systems Symposium, 2000.

[7] Soltani, Saeed: “Dynamic Architectural Simulation Model of YellowCar in MATLAB/Simulink Using AUTOSAR System”, 2016.

[8] dSPACE SystemDesk Product page; Date: 26.06.2017: https://www.dspace.com/de/gmb/home/products/sw/system_architecture_software/systemde sk.cfm.

[9] L. Hatton: “Safer language subsets: an overview and a case history”, MISRA C, Information and Software Technology (2004).

[10] M. Deicke, W. Hardt and M. Martinus: “Virtual Validation of ECU Software with Hardware Dependent Components Using an Abstraction Layer; Simulation und Test für die Automobilelektronik”, 2012.

[11] E. Jauregi, E. Lazkano and B. Sierra. “Object Recognition Using Region Detection and Feature Extraction.” Towards Autonomous Robotic Systems, 2009.

[12] N. Englisch et all: “ YellowCar Automotive Multi-ECU Demonstrator Platform“ Lecture Notes in Informatics (LNI) - Proceedings, Volume P-275, IN INFORMATIK 2017, 15. GI Workshop Automotive Software Engineering, page 1517 - 1522, September 2017. ISBN: 978-3-88579-669-5, ISSN: 1617-5468

Experiences of using ICT for Teaching Courses of "Mechanics of Materials"

Danaa Ganbat[1], Radnaa Naidandorj[2]

[1,2]*Mongolian University of Science and Technology (MUST)*

ganbatda@must.edu.mn[1], naidan@must.edu.mn[2]

Abstract **- In line with the changes in human approaches and methods of obtaining information and acquiring knowledge in the modern world, it has become necessary to improve and develop educational training environments using progress in computers, internet and telecommunication technologies. In order to organize "outcome based teaching and learning" processes with "active learning" using modern advanced technology, "digital-professors" or "digital lecturers" have been created who satisfy interests and needs of "digital-students". These concepts are demanding changes in conventional facilities and laboratories and leading to establishment of a combination of virtual and real training environments. Mongolian University of Science and Technology is developing and working on innovative ideas and initiatives by experimenting them on the example of teaching courses on "Mechanics of Materials".**

In this article, we report the current status and results on the integration of the above mentioned concepts: establishing active learning processes through "digital student", "digital professor", "active teaching and learning environment", "virtual teaching and learning environment", lectures and classes using "light board technologies."

Keywords – digital student, digital professor, flipped class, facilities for active learning, virtual class, light board

I. INTRODUCTION

Higher education quality is the most important factor in producing highly competitive professionals and engineers in technical and technological fields [1].

The main tool to prepare competent specialists who are capable and flexible to adapt to practical requirements irrespective of their study majors is the outcome based education with active learning processes [2].

The world's top universities have launched development and distribution of "Massive Open Online Courses" /MOOC/ that are not only expanding educational provision and access to the public but also having significant impact on raising quality of education systems throughout the world [2]. Therefore Mongolian University of Science and Technology (MUST) also considers that it is required to prepare materials for Massive Open Online Courses, make them available on the internet and use in a "flipped" way during "Flipped Class" lectures and seminars to improve the effectiveness and outcome of education. To this end we are conducting experiments for integrating active learning concepts on the example of "Mechanics of Materials" course by combining creation of appropriate class, lab and virtual environments equipped with computers, internet and telecommunication tools that utilize latest capabilities of modern technologies, with new ideas and ways of organizing and conducting educational activities. This presentation introduces such ideas and tools like the "triangular smart table" that facilitates team work of students and "light board" used for preparation of video lectures within "Flipped Class" teaching and learning processes [3].

In the rapidly changing society, there is a great demand for highly competent specialists with knowledge, creativity, social intelligence and flexibility to meet the changing requirements in all job fields [4]. In order to prepare such lifelong learner-creator-professional-humans who can use advantages of modern technologies, it is becoming increasingly important for education sector to utilize new concepts of outcome-based active learning and teaching methodology techniques and technologies. The advances in ICT have brought extensive new possibilities to improve educational environment and processes along with requirements based on modern students' interest in using modern technologies and the fact that we live in the time of widespread use of portable computers, tablets and smart phones. They provide opportunities for different learning and teaching ways including virtual environments. Students today differ from students from a decade ago. Perhaps they better should be called "Digital Students" and we need to think of how we can stimulate their motivation and studying based on their interests while simultaneously developing skills to effectively use ICT technologies in their education and learning [5], [6].

In connection with the above circumstances, to improve the quality and efficiency of engineering education, and the outcome of educational activities we are introducing a "Digital professor" concept for teaching and learning processes for the essential basic engineering course in "Mechanics of Materials" at the MUST. This concept requires the development of real and virtual facilities for organizing teaching and learning processes. This article describes some of the possibilities and implementation experiment experiences in creating educational classes, labs and virtual environments. For example, a "smart table" which

facilitates teamwork for different numbers of students and encourages their active participation, online training materials that are prepared using a light board (Fig. 1) etc.

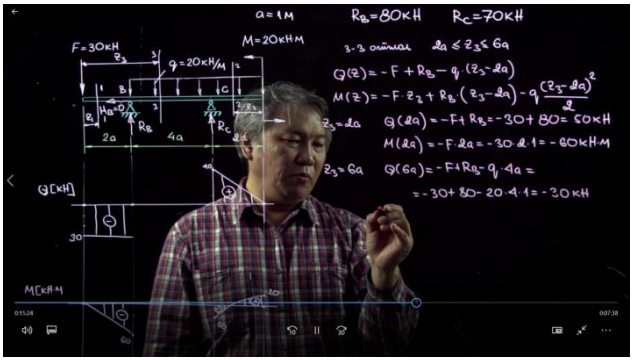

Fig. 1. Example of video lectures by “Digital Professor”

II. MATERIALS AND METHODS

Concepts of “Digital professor” and “Digital Student”

The Digital Professor is a Virtual professor who has prepared video lectures and seminar materials in advance in a modular form, ideally consisting of modules of no longer length than 15 to 20 minutes. These materials are then made available in online platforms, such as at our university website “unimis.must.edu.mn”, online classroom “classroom.google.com” or public social networks such as “facebook.com”, “youtube.com” etc. Students can use these video materials in combination with textbooks and workbooks for seminar and laboratory classes. The preliminary course materials made accessible through online sources makes it possible to organize a “Flipped Class”. This class is different from a traditional one, where teachers dictate the material and students write passively by listening to the teacher.

The “Flipped Class” gives an opportunity for students to participate and learn actively during the class. Since they have studied the online materials before coming to the class, there is more time during class for discussions, solving problems and issues on related topics, working in teams, holding competitions between students and teams etc. [7].

In the “Flipped class”, the “Digital Professor” is a manager for organizing course classes based on previously prepared materials, an evaluator of students’ participation in class and an assessor of their knowledge [8] and [9].

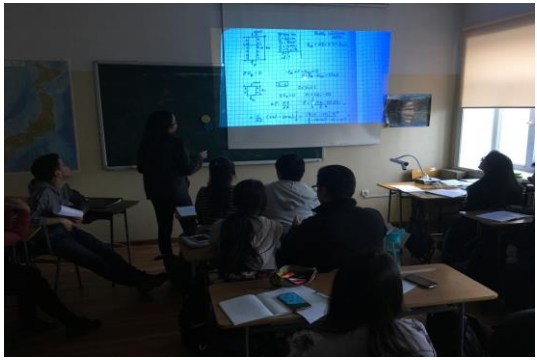

Fig. 2a. Seminar class of Digital Students

In order to participate in the “Flipped class” and study the subject students need to use notebooks, tablets and/or smart phones in preparation for the class as well as during the class. Therefore those students can be called “Digital Students”. (Fig. 2a,b and Fig. 3).

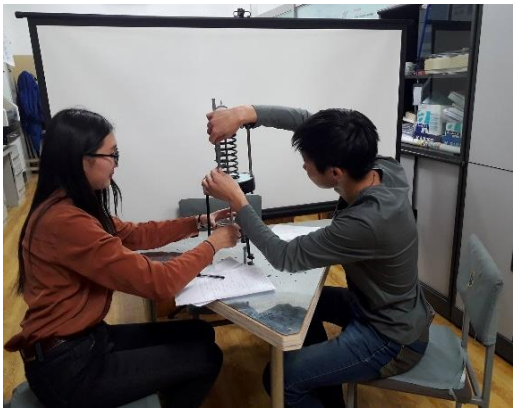

Fig. 2b. Laboratory class of Digital Students

Facilities for Active Learning

Implementation of outcome based education requires convenient facilities appropriate for active learning process.

The environment should be conducive to students being divided into several teams and giving them opportunities to learn and solidify new knowledge

on a subject matter through talking, sharing information and exchanging ideas with each other. It helps them to become confident during competitions of solving practical and theoretical problems as well as finding correct and optimal answers. With the idea to facilitate this type of environment we use classrooms equipped with triangular-smart-tables, document cameras, projectors and other tools. The triangular-smart-table is a newly designed and developed tool that we received a patent for.

Fig. 3. The laboratory equipped with triangular-smart-table.

Facilities for Virtual Learning

Nowadays, there is a heightened necessity to create facilities for virtual learning in order to improve efficiency of the teachers' teaching process as well as to stimulate and satisfy the need of students for active and independent learning. Depending on the subject nature and other influencing factors the facilities can be in different forms. For instance, www.classroom.google.com is an online platform that could be used as a virtual class. It allows numerous possibilities such as sending and sharing information with students, uploading questions, problems and quizzes on relevant topics for homework, student self-progression-control, student feedback, sending completed homework, self-assessments, holding and submission

of mid-term exams online etc. Compared to a traditional class, managing a virtual class requires different pedagogical concepts, teaching techniques and use of equipment from teachers. Lecture notes, classwork and homework materials should be prepared by teachers that should support and stimulate active and efficient learning of students. In addition, modern ICT technologies, such as tablets, smart phones and virtual reality (VR) headsets can all be productively used in a virtual class.

Fig. 4. VR Smart Phone Headset can be used in virtual class

Light board

One of several inventions for active learning in a virtual class is the "Light Board". It has LED lights installed in the frame around a transparent-glass-board. The light-board is used to prepare video-lectures by a digital professor. It gives digital students real feeling similar to the digital professor giving a lecture in a real class. It is very comfortable for students to see all the written lecture notes when the digital professor is talking and writing on the light-board since the teacher does not cover the board, and digital professors and digital students can see each other face to face. Advances in modern technology are allowing us to prepare and provide such kind of video-lectures to students. Conventionally when a video lecture using the glass board is recorded, the written texts and pictures will be shown to students in a wrong way. But flipping functions in the recording devices such as cameras, smart phones and projectors can be used to show it in the right way on the glass light board. Fig. 5 shows the flipped and un-flipped views made with the recording device.

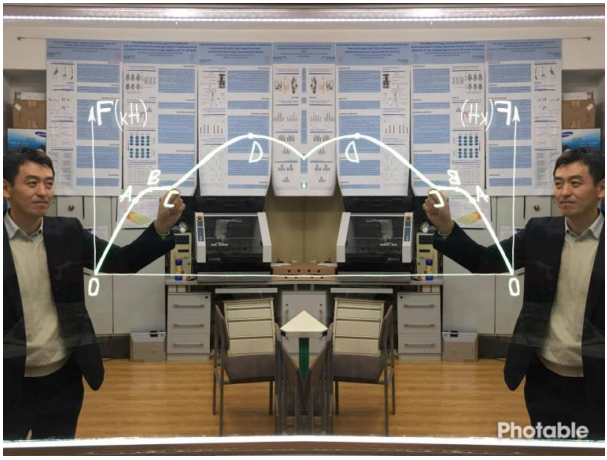

Fig. 5. Flipped and un-flipped views of lecture using the light board

III. CONCLUSIONS

Rapidly changing progression of modern advanced technology should be used in training and educating students today so that they become future highly-skilled professionals and specialists capable of independent, creative thinking and life-long learning. In order for us to efficiently organize teaching and learning processes it is necessary to utilize modern engineering education concepts, pedagogical approaches, technology and equipment. Students nowadays are more interested in using modern ICT technologies and want to learn in an efficient manner. Satisfying those needs requires changes to traditional pedagogical approaches by efficient methods and technologies. In this field some inventions and innovations have been initiated, developed and are being tested in teaching and learning processes of the course on "Mechanics of Materials" at the MUST, some of which were presented in this article.

In the near future, more work needs to be done in this field, such as preparing text books and lecture notes for using in combination with modern ICT technologies, developing applications for smart phones etc.

REFERENCES

[1] Biggs J.B. and Tang C., Teaching for quality Learning at University, McGrawHill, 2011.

[2] Badarch D. Innovation on Higher Education Reform.Ulaanbaatar, 2013; 213-235.

[3] Ganbat D., Delgermaa S. Case study of ICT usage for active learning processes. IBS Scientific Workshop Proceedings, 2017; 60-63.

[4] Anderson L.W., Krathwohl D.R. A Taxonomy for Learning, Teaching, and Assessing: A Revision of Bloom's Taxonomy of Educational Objectives, A bridged Edition, 2001.

[5] Ganbat D., Naidandorj R. CDIO – Approach to create the creators, “Outcome based Education" Conference Proceeding No.3, 2017; 12-15.

[6] Viau R. La motivation en contexte scolaire, De Boeck Supérieur, 1995; 154-155

[7] Chi M. T. H. Active-constructive-interactive: A conceptual framework for differentiating learning activities. Topics in Cognitive Science 1(1), 2009; 73–105.

[8] Mazur E., Peer Instruction: Getting students to think class, AIP Conference Proceedings, 1997; 981.

[9] Kember D., McNaught C., Enhancing University Teaching, London: Routledge, 2007

A SIFT-based Image Retrieval system

Haibin Wu[1], Beiyi Wang[2], Dewei Guan[3], Liwei Liu[4]

[1,2]*Harbin University of Science and Technology (HUST)*

[3,4] *Harbin Third Power Plant of Huadian Energy*

23402891@qq.com [1], 63918600@qq.com [3]

***Abstract*—With the rapid development of information technology, the amount of image media information is ever increasing. Recently, the traditional text based image retrieval has been a lot of problems. As a result, it is required to support content-based image retrieval efficiently on such image data. A new image retrieval system-iSee, which can be used to accurately search the image features, is developed by using the SIFT algorithm with good robustness to image scale, rotation, cover, visual angle, brightness change and noise etc.. It is based on the key technology of image content retrieval, and combined with the contrast of the algorithm. The iSee system can be used in several applications such as fingerprint recognition, face recognition, video key frame search and medical image retrieval.**

Keywords—image retrieval; SIFT; isee system; content based system

I. INTRODUCTION

Being a main form of expression for multimedia information. The greatest advantage of image information is to be able to describe the scene or objects visually and vividly [1]. However, due to the popularity of digital cameras, scanners and other digital devices led to an increase in the amount of image information. Hence, there is a dire need of some expert technique to manage image information effectively.

The image feature is the attribute or characteristic of an image, which can distinguish from other image and the normal image feature extraction is the guarantee to the stable and efficient operation of the content based image retrieval(CBIR) system [2].

In this paper, we analyze the three kinds of image feature description and extraction methods. There are Harris algorithm, SUSAN algorithm and SIFT algorithm. Harris detector is a detector that is used for feature point extraction. It is an improvement of Moravec corner detecting algorithm, which uses the first partial derivative to describe the intensity change. Harris detector is enlightened by the autocorrelation function of the signal process, which is able to give the matrix M that is related to the autocorrelation function. As a more effective algorithm, SIFT

local feature detecting algorithm can be regarded as a significant achievement in the field of image feature detection. The idea of the algorithm originates from Lindeberg's scale space theory. In Lindeberg's paper, the normalized Gaussian-Laplace operator is proved to have the real scale invariance. However, the Gaussian-Laplace transformation needs massive calculation, and therefore the Gaussian difference operator is used to replace the Gaussian-Laplace transformation. Primarily, the image is converted into gray scale. Then, the converted image is processed with the Gaussian smoothing filter from different scales, and consequently, the description of the image in the Gaussian difference scale space is obtained. Finally, the extreme point in the scale space is selected as the feature point of the image. The algorithm not only improves the feature extracting speed, but owns the stability and invariance to scale changes, intensity and rotation. Therefore, we choose SIFT as the feature extracting algorithm for our research project.

According to the results, SIFT algorithm is selected as the feature extraction scheme of the system in the paper and a set of CBIR test system is developed by using MATLAB platform.

II. AN OVERVIEW OF RETRIEVAL SYSTEM BASED ON IMAGE CONTENT

CBIR is a new technology with high inheritance, which mainly includes the following aspects.

A. Feature Extraction

The visual features are divided into general visual features and field-related visual features. The general visual features refer to the common feature of all images, including point features, color, texture, shape, spatial position relationship etc.; The field-related visual features refer to the special features based on some experience and professional knowledge, such as facial feature, fingerprint feature etc. [3]. Feature extraction is the fundamental step of CBIR technology, which is the standard of distinguishing from different types of image retrieval system [4].

B. Feature Matching and Similarity Measure

The template is used to format your paper and style the text. All margins, column widths, line spaces, and text fonts are prescribed; please do not alter them. You may note peculiarities. For example, the head margin in this template measures proportionately more than is customary. This measurement and others are deliberate, using specifications that anticipate your paper as one part of the entire proceedings, and not as an independent document. Please do not revise any of the current designations.

C. Feature Indexhe

When dealing with the large image library, the extracted image features have the following features: huge data, complex structure and various types. So, using the reasonable and effective data structure to store the feature information is very important to save the storage space and improve the retrieval efficiency. The frequently-used index methods include B-tree and Kd-tree.

D. Query Mode

Query mode refers to what type of information the user submits to the system, there are a few mainly modes as following: provide a query image to retrieve the QBE by the user. Query by sketch is that the user draws a simple graphic as standard to inquiry. Described query is based on specifying the search criteria described by the user.

E. Relevance Feedback

According to the users requirements, after the system making the initial research, the user can submit the correction information on the system based on the results of the preliminary inquiry for better search results, this process is relevance feedback. In this way we can improve the accuracy of research, and make up the semantic gap between the user and the computer to a certain degree.

F. Performance Evaluation

CBIR is a highly integrated technology, and has a rich theoretical and complex classification, therefore, different algorithms evaluation and comparison method is an important tool for determining the merits of the CBIR, which is conductive to exchange between researchers and algorithms promotion, and jointly promote the development of CBIR technology.

A typical CBIR system block chart is shown in Figure 1 :

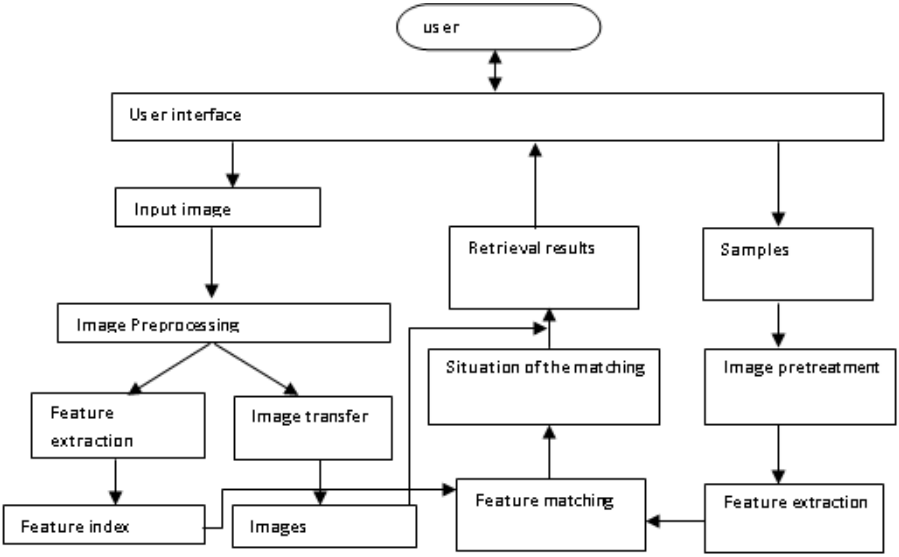

Fig. 1. Typical CBIR system block chart

III. COMPARATIVE ANALYSIS OF THREE KINDS OF FEATURE EXTRACTION ALGORITHMS

Compared with other image features, point feature has the virtue of little mount of account and great amount of image information. At the present stage, the research of local feature algorithm is mainly based on the extraction and matching of feature points. In this paper, the Harris algorithm, SUSAN algorithm and SIFT algorithm are compared and analyzed, and we have mainly discussed the SIFT algorithm.

A.Smallest Univalue Segment Assimilating Nucleus(SUSAN) algorithm

SUSAN is a simple and effective method to get feature points based on the gray value character. Firstly, move approximately circular template. In the image, make template core coincide and each pixel together; secondly, count the number of the similarity pixel between the template and the gray value to get the USAN value of and to calculate the corresponding value of the corner; finally, the feature extraction is implemented by using non maximum suppression method to calculate the feature point. This method is mainly used in edge-detection and corner–detection in image, and it is robust to noise interference. The SUSAN algorithm don't need to segment the image, so there is no need to calculate the image gradient

data, at the same time, the USAN region is obtained by the pixel accumulation of similar gray value in the template and the center of the template, actually, in the process, the pixel accumulation is similar to the integral, from which Gauss noise can be effectively suppressed [5].

B.Harris Algorithm

Harris operator can give the autocorrelation matrix of a pixel in an image, which is inspired by the autocorrelation function in signal processing. And the characteristic value of autocorrelation matrix is the first order curvature of autocorrelation function [6]. Rectangular window w from the image to be processed to an arbitrary direction makes a slight displacement(x, y), then, the amount of change of gradation is calculated by the formula 1:

$$\begin{aligned} E_{x,y} &= \sum_{u,v} W_{u,v}\left[I_{x+u,y+v} - I_{u,v}\right]^2 \\ &= \sum_{u,v} W_{u,v}\left[xX + yY + o(x^2 + y^2)\right]^2 \\ &= Ax^2 + By^2 + 2C_{xy} \\ &= (x,y)M(x,y)^T \end{aligned} \tag{1}$$

Where M is the point (x, y) autocorrelation function matrix, and is the coefficient of gauss window. Judge whether the point is the corner by calculating whether the curvature value of XY two directions is high. However in the practical implementation of the algorithm, the trace and determinant of the matrix M are used to replace the eigenvalue for simplifying the calculation and improving the efficiency of retrieval. The algorithm has many advantages, including simple calculation, the feature of extraction point is uniform and reasonable. It can be quantitatively extracted feature points and it has better robustness for image rotation, brightness change, perspective changes and the effects of noise. However the scale is very sensitive, and it does not have the scale invariance and corner point extraction is the pixel level.

C.SIFT Algorithm

SIFT is a local feature description algorithm based on the scale space, which can keep invariant in the image transformation of scale, rotation and affine distortion. Describe the local features of the image, that is, the pixel gray gradient distribution in the vicinity of image feature points by establishing the DOG scale space, searching and locating the key points, and by feature points direction assignment and the key point descriptor. In order to verify the superiority of the SIFT algorithm, the performance test of SIFT is designed in this paper [7]. In the performance test, the feature points in the image are marked by green arrow, the direction of the arrow is the main direction of the feature point, and the length of

the arrow indicates the scale of the characteristic point [8]. It is clear that the SIFT algorithm has good robustness to scale changes, translation, rotation and brightness changes, but it has some limitations in the fuzzy retrieval for similar images [9,10]. The experimental results are as follows.

Fig. 2. Feature detection of the same objects under different scale

Fig.3. Feature matching under different scale

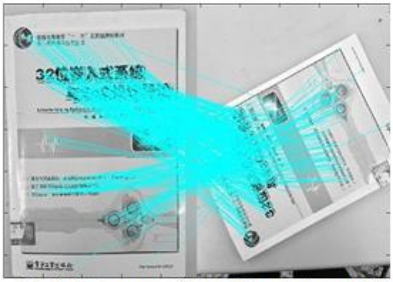

Fig. 4. Feature matching under rotation condition

Fig. 5. Feature matching under perspective transformation

Fig. 6. Feature matching under the conditions of noise

Fig. 7. Feature matching under the condition change of brightness

Fig. 8. Feature matching under the condition of rotation, cover, translation and scale changes

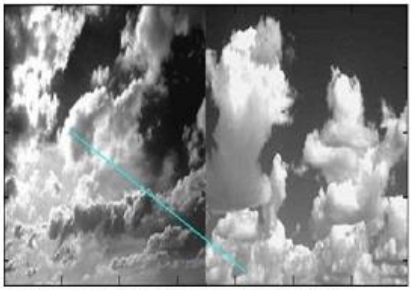

Fig. 9. The similar images matching result

In addition to validate the point feature extraction, the feature extraction and matching features and time were statistically tested in experiment. Limited space, only a few groups of typical images of the experimental results are listed in table I:

TABLE 1: SIFT feature extraction and machine time of typical images

Number	Type	Thumbnail	Feature extraction time /ms	Matching time /ms	Amount of feature point
L1	Contrast		457	0	0
S1	Simple Texture		457	<1	20
S2			471	1	32
M1	Medium texture		541	5	139
M2			562	7	173
M3			541	7	203
F1	Complex Texture		697	27	415
F2			963	277	1010

We use feature extraction time, matching time and amount of feature point to compare the different type images. These results show that (1) SIFT feature extraction capability is insufficient for low contrast image, as shown in l1, that (2) SIFT has good feature extraction ability for the image with complex texture but cannot get enough feature points for the image with simple texture and slow change of gray value, as shown in F1 and F2, and that (3) SIFT spends a lot of time on feature extraction, while feature matching time is very little, as shown in S1 and S2.

IV.CBIR SYSTEM BASED ON SIFT ALGORITHM

In this paper, a simple image retrieval system (iSee) was implemented in the MATLAB. The system uses the query by example, takes SIFT algorithm as feature extraction method and matches according to the distance-ratio criterion using exhaustive method.

ISee system operation is divided into offline and online two processes. The offline process is the generation and management of the image database feature index. In this process, the system uses SIFT algorithm to extract the features of each image in the original image database and generates feature information. The feature information includes three parts: first, the image itself, second, the position, scale and main direction information of the feature points, which is represented as a vector set with K dimensional vector , and K is the number of feature points, and third, the description vector of the feature points, which is represented as K vectors with 128-dimensional. The online process is the image retrieval process. In this process: First, some features are obtained from the object pictures. Second, match the features in the retrieval index which is generated by the offline process. Finally, display the result based on retrieval result. System can display pictures, where N is for the number of the image database, P is for the confidence defined by the user, and the proposed value is 0.01.

In this paper, we designed the corresponding iSee system image retrieval experiment to test the performance of iSee.

In the experiment, join three types of pictures, each type with 10 groups and each group with 20 pictures to form a picture library. There are the pictures X such as the similar images, flowers, cars and so on. Also, similar texture images Y and the images Z of the same object taken at different scales, viewing angles, brightness and rotation angles. The images in the same groups have similar characteristic and those in different groups are independence. From the image database, select an image input into the iSee system to make an image retrieval as a query image in each group of image. Then, statistical search results and statistical results are shown in table II.

TABLE II: Statistical results

	groups	1	2	3	4	5
X-type	*R*	0.15	0.25	0.20	0.05	0.30
	P	0.16	0.14	0.24	0.18	0.22
Y-type	*R*	0.45	0.55	0.40	0.35	0.55
	P	0.46	0.44	0.48	0.56	0.54
Z-type	*R*	1.00	0.95	1.00	0.90	1.00
	P	1.00	0.98	0.99	0.96	1.00
	groups	6	7	7	9	10
X-type	*R*	0.25	0.20	0.25	0.20	0.25
	P	0.24	0.16	0.18	0.24	0.30
Y-type	*R*	0.60	0.45	0.40	0.50	0.65
	P	0.60	0.48	0.48	0.50	0.58
Z-type	*R*	1.00	0.95	1.00	1.00	1.00
	P	1.00	0.94	0.98	1.00	0.99

The precision P and recall R can be calculated by following formula 2:

$$R = A/A+C \qquad (2)$$
$$P = A/A+B$$

Where A is the number of images to be retrieved and the number of images similar to the reference image; B is the number of images that are retrieved but not associated with the reference image; C is the number of images that are not retrieved but similar to the reference image.

From table 1 statistical data shows, iSee retrieval ability is not good for X images. It can only retrieve the query image itself and the images containing the same object with the query image. Other results are returned as error results, and only a few feature points are identified as the same feature points; For Y images, the retrieval ability is some better than X image, but still not ideal, mainly because the SIFT algorithm has trouble understanding and extracting features of the image completely, so it is hard to match the same type but different characteristics of images such as landscapes, flowers, cars and other visual. The visual features of the texture include strategic line shape, color distribution, so it is difficult to produce the similarity of the same with the human body for SIFT algorithm; For Z images, SIFT algorithm shows its excellent retrieval performance, which can detect almost all of the relevant images, that is associated with the SIFT algorithm. The image of the scale, rotation, occlusion, perspective change, brightness and noise changes have good robustness.

The SIFT algorithm is a favorable local feature descriptor, which owns a good invariance to translation, scale, rotation, noise, angle change, and intensity change. It is able to match the same object of two images accurately. These properties of SIFT make it to have advantages over other algorithms in accurately retrieving the target image. However, there is a huge limitation for SIFT when implementing the fuzzy retrieval for similar images, which is shown in the following figure.

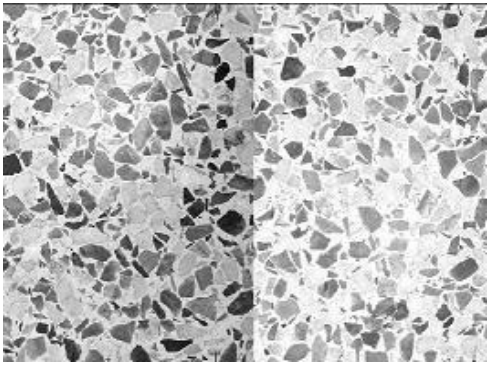

Fig. 10. Matching result of similar images with SIFT

Figure 10 displays the matching result of two similar images with SIFT. These are images of two marble bricks of the same kind. According to the figure, we can get that although the two images are extremely similar, SIFT can hardly find the same features (there are more than 5,000 features in both images, but none of them are the same). The reason why SIFT is unable to find the same features is that SIFT can only describe the low level visual feature, and cannot understand the meaning of the image. Therefore, despite the fact that what shows on the images are the same kind of object, the gray values of pixels around each feature are different due to different backgrounds and object distributions. Consequently, SIFT generates different feature descriptors, which is unable to detect the matching features.

SIFT owns a huge advantage in some CBIR systems which need to accurately retrieve the target image, such as fingerprint recognition, face recognition, key frame retrieval, and medical image retrieval, etc. The sample image of this kind of retrieving system has the same scene or object with the target image, and only scale change, angle change or rotation happens. However, when it comes to material retrieval which needs to retrieve the image that is in accord with human's judgment in visual and semantic aspects, SIFT does not seem to have a good performance.

V. CONCLUSIONS

Based on the analysis of algorithm, a CBIR system based on the SIFT algorithm was designed, and then an experiment proved the availability of the system. Because the system has good robustness to scale changes, translation, rotation and brightness changes, it has broad application prospects in the field of accurate image retrieval, such as pattern recognition, face recognition, video key frame search and medical image retrieval.

ACKNOWLEDGEMENT

This work was financially supported by National Natural Science Foundation of China (Grant No. 61671190).

REFERENCES

[1] Chang T, Kuo C J. Texture analysis and classification with tree-structured wavelet transform[J]. IEEE Transactions on Image Processing A Publication of the IEEE Signal Processing Society, 1993, 2(4):429-441.

[2] Pentland A P, Picard R W, Scarloff S. Photobook: tools for content-based manipulation of image databases[J]. Proceedings of SPIE - The International Society for Optical Engineering, 1994, 2185:34-47.

[3] Jing F, Zhang B, Lin F, et al. A novel region-based image retrieval method using relevance feedback[C]// 2001:28-31.

[4] Pass G, Zabih R. Histogram refinement for content-based image retrieval[C]// IEEE Workshop on Applications of Computer Vision. IEEE Computer Society, 1996:96. .

[5] Smith S M, Brady J M. SUSAN—A New Approach to Low Level Image Processing[J]. International Journal of Computer Vision, 1997, 23(1):45-78. .

[6] Harris C. A combined corner and edge detector[J]. Proc Alvey Vision Conf, 1988, 1988(3):147-151.

[7] Lowe D G, Lowe D G. Distinctive Image Features[J]. 2004.

[8] Zhu Y, Li J, Yang W, et al. A feature points description and matching algorithm for edge in IR/visual images[J]. Jisuanji Fuzhu Sheji Yu Tuxingxue Xuebao/Journal of Computer-Aided Design and Computer Graphics, 2013, 25(6):857-864.

[9] Ma J. A scene matching approach based on edge signal between IR and visible image[D]. The Huazhong University of Science and Technology, Wuhan, China, 2006.

[10] Wang S. SIFT based image matching algorithm research[D]. Xidian University, Xian, China, 2013.

Decoding of digital holograms

Vladimir I. Guzhov[1], Ekaterina E. Serebryakova[2]

[1,2]*Novosibirsk State Technical University (NSTU)*

vigguzhov@gmail.com[1], silver-kate94@mail.ru[2]

Abstract **- The article describes a system for recording digital holograms. The Fresnel transformation is used for decoding.**

Keywords - holography, optical microscopy, interference, digital holography, Fresnel transform, Fourier transform**.**

I. INTRODUCTION

To register classical thin holograms it is necessary to use high-resolution photographic media. This is due to the fact that when the real and imaginary images are restored they overlap with the central beam. E. Leith and Yu. Upatnieks solved the problem of separation of beam overlap as follows [1]: they directed an object beam of light onto a photographic plate at a rather large angle with a beam of light diffracted by the object; this made it possible to obtain images that, when observed, do not overlap. To record a hologram at an angle between interfering strips of 30 degrees, a recording material with a resolution of at least 2000 lines / mm is required for recording only the carrier frequency.

Digital matrices used in digital holography can't at the moment provide such a high spatial resolution. Therefore, in digital holographic reconstruction, it is necessary to reduce the angle between the interfering wave fields, which inevitably leads to overlapping of the spectra in different diffraction orders.

II. THEORY

The existing methods for decoding holograms are based on the fact that we can register only the intensity of the hologram. However, in contrast to recording classical holograms that represent a picture of intensities, using digital holography one can obtain a complex mathematical hologram [2], which consists of the amplitude and phase of the object field:

$$G(x,y) = a_p(x,y)\exp\left(\varphi_p(x,y)\right) \quad (1)$$

$a_p(x,y)$ - field amplitude, $\varphi_p(x,y)$ phase of the field propagated from the object in the plane of the hologram (η,ξ).

The amplitude and phase values can be found from the set of holograms using phase-shifting interferomet

The stepwise phase shift method is based on recording several interference patterns when the reference wave phase changes by a certain amount. The phase shift between interfering beams can be realized in various ways. The phase shift is most often set using a mirror fixed to a piezoceramic. Depending on the number of phase shifts, there are various decoding algorithms.ry (PSI) methods.

In [3] it is shown how to obtain computational procedures which, using combinations of intensity of interference patterns, obtain the distribution of the phase difference $\phi(x,y)$ of interfering beams for arbitrary angles of displacement. In [4-6], a generalized scheme of the algorithm for a different number of shifts is obtained. Knowing the phase difference $\phi(x,y)$ and the phase of the reference wave $\varphi_r(x,y)$, it is possible to determine the initial phase distribution $\varphi_p(x,y)$.

$$\varphi_p(x,y) = \phi(x,y) - \varphi_r(x,y) \tag{2}$$

To form a mathematical hologram it is also necessary to determine the amplitude of the wave field $a_p(x,y)$ reflected from the object in the plane of the hologram. The values of the amplitudes of the object and reference beam can be determined by overlapping the corresponding beams in the optical circuit. But if we already have a set of registered holograms with a phase shift used to determine the phase values, then we can obtain the amplitude of the object beam by the stepwise shift method using the same set of holograms [7,8].

If you can find a mathematical hologram $G(x,y)$, then in the image plane you can restore the complex amplitude of the field scattered from the object. For this, it is necessary to carry out the Fresnel transformation over $G(x,y)$ [9].

$$\Gamma(r,s) = \frac{1}{i\lambda d} exp\left[i\frac{2\pi d}{\lambda} \right] \exp\left[i\frac{\pi\left[(r\Delta\xi)^2 + (s\Delta\eta)^2 \right]}{\lambda d} \right] \times \tag{3}$$

$$\times \sum_{k}^{N_x-1} \sum_{l}^{N_y-1} b_1(k,l) \exp\left[i\frac{\pi}{\lambda d}\left[\left(k\Delta\xi\right)^2 + \left(l\Delta\eta\right)^2 \right] \right] \exp\left[-i\frac{2\pi}{N}\left(kr + ls\right) \right]$$

In expression (3), d - the distance to the object. The Fresnel transformation algorithm provides a simple scaling of the reconstructed image, but this imposes a number of limitations on the design of the measuring system, in particular, the upper and lower limits of the permissible recording distance of the hologram become a significant factor.

It is necessary to determine at what distances we can use the discrete Fresnel transform. It was shown in [10] that discrete Fresnel and Fourier transforms can be used when the distance to the object is comparable with the size of the object and hologram, while the object is in the near zone of diffraction. When recording digital holograms, the optical scheme shown in Fig. 1.

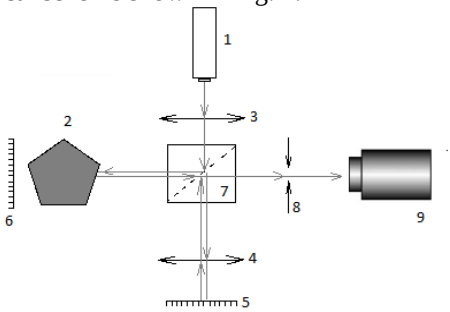

Fig. 1. Scheme of recording a digital hologram

The beam of light from the laser expands (3) and hits the separation cube. Part of the beam hits the mirror fixed to the piezoceramic (5). When reflecting from this mirror, an object beam is formed. Another part of the beam hits the object. When reflecting from the object (2), a reference beam is formed. To equalize the intensities of the reference and object beams, a light filter is used to form the hologram (4). The interference of the reference and object beams and the formation of holograms occurs on the camera array (9).

III. EXPERIMENTS AND RESULTS

The object was a jubilee silver badge with the emblem of the university. In Fig. 2 shows the results of interference between the reference and object beams when the phase angle of the shift is changed . Interference patterns were projected directly onto the digital array of photodetectors.

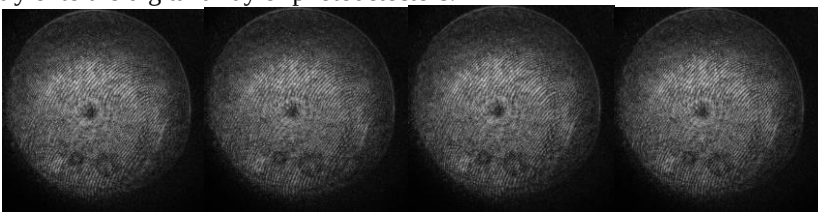

Figure 2. Interference patterns with a change in the phase angle of shear

$$\delta_1 = 0^\circ,\ \delta_2 = 90^\circ,\ \delta_3 = 180^\circ,\ \delta_3 = 270^\circ$$

For these pictures, the phase distribution and amplitude were determined. Then a mathematical hologram was formed using the expression (1). In Fig. 3 shows the amplitude and phase of the mathematical hologram.

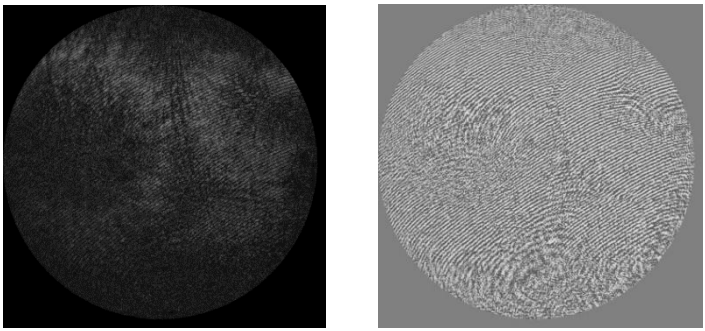

Figure 3. Amplitude and phase of the mathematical hologram.

The actual image was reconstructed from the mathematical hologram using the Fresnel transform. The size of the object is 7 mm, the distance to the object is 135 mm. The result of the restoration is shown in Fig. 4.

Figure 4. Left source object, right: the result of restoring the actual image from the mathematical hologram.

The noise in Fig. 4 are caused by the deflection of the reference beam from the plane beam. By improving the quality of optical elements, this factor can be eliminated.

This work was supported by the Russian Foundation for Basic Research "Development and research of computer holographic interferometry methods for complex objects" (Grant No. 18-08-00580).

REFERENCES

[1] Leith, E.N. Reconstructed wavefronts and communication theory [Text] E.N. Leith, J. Upatnieks. Journal of the Optical Society of America, 1962, Vol. 52, pp. 1123-1130.

[2] YAroslavskij, L.P. Cifrovaya golografiya [Tekst]. L.P. YAroslavskij, N.S. Merzlyakov. – M.: Nauka, 1982, P. 219 .

[3] Guzhov V.I., Il'inyh S.P. Opticheskie izmereniya. Komp'yuternaya interferometriya: Ucheb. posobie. - Moskva: Izd-vo YUrajt, 2018. (ISBN: 978-5-534-06855-9), P.258.

[4] Guzhov V., Ilinykh S., Kuznetsov R., Haydukov D. Generic algorithm of phase reconstruction in phase-shifting interferometry. Optical Engineering, 2013, Vol.52(3), pp. 030501-1 – 030501-2.

[5] Guzhov V.I., Il'inyh S.P., Hajdukov D.S., Vagizov A.R. Universal'nyj algoritm rasshifrovki. Nauchnyj vestnik NGTU, 2010, №4(41), pp. 51-58.

[6] Il'inyh S.P., Guzhov V.I. Obobshchennyj algoritm rasshifrovki interferogramm s poshagovym sdvigom. Avtometriya, 2002, №3, pp.123-126.

[7] Guzhov V.I., Il'inyh S.P., Hajbulin S.V. Vosstanovlenie fazovoj informacii na osnove metodov poshagovogo fazovogo sdviga pri malyh uglah mezhdu interferiruyushchimi puchkami. Avtometriya, 2017, T. 53, №3, pp. 101-106.

[8] Guzhov V.I., Il'inyh S.P. Opredelenie intensivnosti opornogo i ob"ektnogo puchkov pri ispol'zovanii metoda poshagovogo fazovogo sdviga. NGTU, Novosibirsk, Rossiya. Avtomatika i programmnaya inzheneriya, 2017, № 4 (22), pp. 68–73.

[9] Predstavlenie preobrazovaniya Frenelya v diskretnom vide. Guzhov V.I., Nesin R.B., Emel'yanov V.A. Avtomatika i programmnaya inzheneriya, Novosibirsk, 2016, №1(15), pp. 91–96

[10] Oblast' vozmozhnogo primeneniya diskretnyh preobrazovanij Fur'e i Frenelya. Guzhov V.I., Emel'yanov V.A., Hajdukov D.S. Avtomatika i programmnaya inzheneriya, Novosibirsk , 2016. №1(15), pp. 97–103

Video-based fall detection system in FPGA

Peng Wang[1], Fanning Kong[2], Hui Wang[3]

[1,2,3] *Harbin University of Science and Technology (HUST)*

- *wpkunpeng@hrbust.edu.cn[1], 294316713@qq.com[2], liraaa@163.com[3]*

***Abstract*—As there is a high tendency of falling in the independent living of the elderly and the post-fall injury is very serious. It is necessary to get timely assistance when they fall down. The main objective of this work is to build an FPGA-based hardware implementation of video-based fall detection system. First of all, the moving object model will be extracted through background subtraction based on Gaussian Mixture Models (GMM). Second, we judge whether there is a fall through the aspect ratio, the effective area ratio, and the change in the center of the human body. Finally, the detection system will make sound-light alarm and send messages to the elder's family and the community via GSM when they fall down. The experimental results demonstrate the accuracy of this fall detection system is up to 95% and this system satisfices the requirement of real-time, low rate of false positives and good robustness.**

Keywords—Fall detection, FPGA, Video-based, Background subtraction, GSM

I. INTRODUCTION

With the global aging population grows tremendously, large part of elderly people has to live alone while their children work outside. As reported that 28-35% from age group 65-75 falls at least once a year [1]. Falling exposes the elder to greater chances of suffering fall-related injuries [2]. Therefore, it is essential to put forward an automatically fall detection system for enabling the falling elder get immediate help to avoid any post-fall injuries or deadly cases due to delayed assistance.

While various kinds of fall detection system have been researched in recent years, research in video-based fall detection has gained much attention [3]. Most of video-based fall detection which are implemented on the general purpose CPU or PC with software processing not targeting for real-time [4,5]. FPGA has advantages over CPU and PC because of the large number of processing cores that work in parallel in FPGA. It has proposed a video-based fall detection system, in this work, which FPGA is selected as an accelerator to improve the performance of the system.

The followings are the organization of this paper. The overall concept of the system is described in Chapter 2. In Chapter 3 the fall detection algorithm is explained. Chapter 4 discusses the implementation on FPGA. At the end, results and conclusions are presented.

II. OVERVIEW OF THE SYSTEM

The presented system consists of a digital camera, an automatic detection platform with Cyclone IV FPGA device (EP4CE15F17C8N), LEDs, a Buzzer and a GSM module. All computation of the system should be done inside the FPGA and the alerts will happen together with LEDs, Buzzer and GSM. The idea is described in Figure 1. The system is based on the following elements: Digital camera with OV7725 from OmniVision for capturing the video streaming,

The automatic detection platform with Cyclone IV FPGA device from Altera, which as the main computing platform, carries out all image processing and fall detecting operations,

LEDs and Buzzer for giving an alarm of light and sound to caution the neighbors, the LEDs also could be used as the lighting in daily life,

GSM module for sending the falling messages to the falling elder's family and the community.

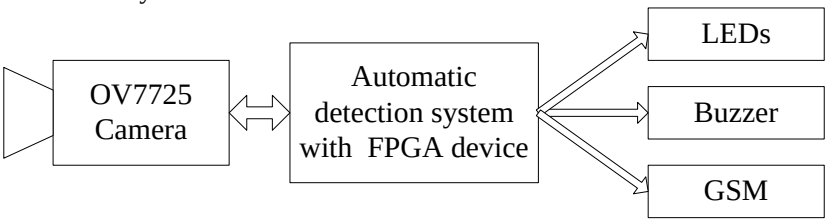

Fig. 1. Overview of the fall detection system

III. FALL DEECTION ALGORITHM

A number of algorithms for object detection have been presented. Object detection algorithms can be classified into Frame subtraction schemes, Optical flow method and Background subtraction. The algorithm of Frame subtraction schemes is easily influenced by the time interval that could not extract the full foreground. The disability of Optical flow method is complex computation which leads bad real-time performance. In this work, we choose the Background subtraction with its simple principle and computation. Figure 2 shows the process of Background subtraction. The behavioral simulation results were completely compliant to software model created in Matlab R2012a.

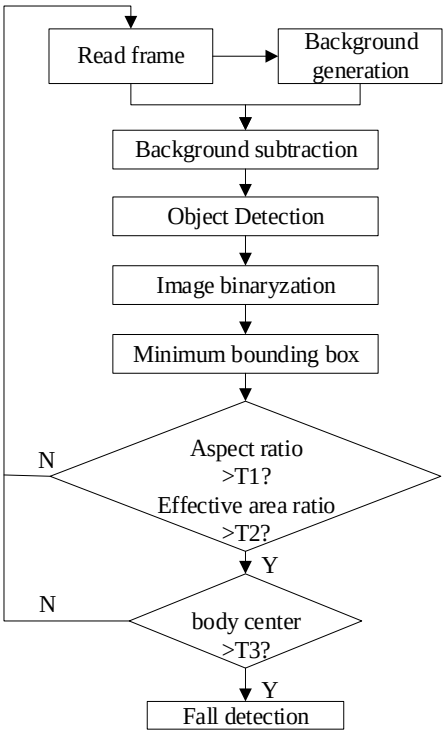

Fig. 2. Flow chart of the fall detection algorithm

A. Background generation

In this work, GMM (Gaussian Mixture Background Modeling) was adopted for background generation. Every single pixel was expressed the feature with Gaussian model according to the following Equation 1:

$$F_i\left(x_t, u_{i,t}, \sum_{i,t}\right) = \frac{1}{(2\pi)^{\frac{n}{2}}\left|\sum_{i,t}\right|^{\frac{1}{2}}} e^{-\frac{1}{2}\left(x_t - u_{i,t}\right)^T \sum^{-1}\left(x_t - u_{i,t}\right)} \quad (1)$$

Then the background model was built with the weighted sum of the K - Gaussian models by the Equation 2:

$$P(x_t) = \sum_{i=1}^{k} w_{i,t} \times F_i\left(x_t, u_{i,t}, \sum_{i,t}\right) \qquad (2)$$

B.Moving object segmentation

After background generation, the next step was classifying the pixels into foreground object as the Equation 3 shows:

$$\left|I_N(x,y) - I_B(x,y)\right| > T \qquad (3)$$

while at coordinate (x, y), $I_N(x, y)$ is the intensity value for the new pixel; $I_B(x, y)$ is the intensity value for the background pixel; T is a difference threshold which is pre-determined. Meanwhile, the pixel will be classified as the background object if the condition in Equation 3 is not fulfilled.

C.Fall detection

The minimum bounding box was generated with its features (height, width and size) for foreground object following the image binarization. As we know, a standing person should have a height (H) greater than width (W). It turns out to a height to width ratio (aspect ratio) > T1, which T1 is the threshold, as shown in Figure 3a. On the contrary, a person who is falling should have an aspect ratio < T1, as illustrated in Figure 3b. In spite of that, this work has proposed the supplementary condition to distinguish the real-fall from the daily exercises by the effective area ratio as shown in Equation 4.

$$R_{effective} = \frac{S_O}{S_B} \qquad (4)$$

Where S_O = the area of the foreground object; S_B = the area of the bounding box. It will be detected as a fall if the $R_{effective}$ greater than T2. T2 is the threshold that predetermined.

Because normal movement is slow and the center changes little when the old man squats, push-ups or walks normally. Fall is a kind of rapid and violent phenomenon. During the fall down, the change of the center will suddenly increase. Finally, in order to further improve the accuracy of the system, the judgment results are corrected according to changes in the body center. After calibrating the minimum external bounding box of the human body, find the center position $O(x, y)$ of the human body, and correct the fall judgment result by using Equation 5:

$$\left.\begin{array}{l} O_{k-1_y} > O_{k_y}, \\ \sqrt{\left(O_{k-1_y} - O_{k_y}\right)^2 + \left(O_{k-1_x} - O_{k_x}\right)^2} > T_3 \circ \end{array}\right\} \quad (5)$$

Compare human body centers $O_k(x,y)$ and $O_{k-1}(x,y)$ of two adjacent images. When the center of the human body in the k-th frame image is lower than the body center in the k-1 frame image. And the distance between the two centers is greater than the threshold T3, the result of the determination is a fall. Otherwise, it is not a fall.

Compare human body centers $O_k(x,y)$ and $O_{k-1}(x,y)$ of two adjacent images. When the center of the human body in the k-th frame image is lower than the body center in the k-1 frame image. And the distance between the two centers is greater than the threshold T3, the result of the determination is a fall. Otherwise, it is not a fall.

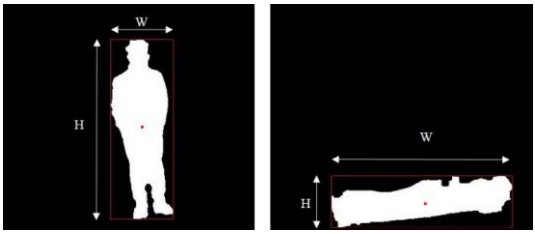

(a) Person standing (b) Person falling down

Fig. 3. Aspect ratio, effective area ratio and body center of bounding box

IV. IMPLEMENTATION ON FPGA

In this work, it has proposed a hardware implementation of fall detection system using FPGA. Figure 4 has shown the functional diagram of the system implemented in FPGA. Most important are：

- CMOS sensor config - block for configuring the COMS sensor,
- Image capture - reading the video streaming received from CMOS sensor,
- RAW2RGB - module for changing the color space from RAW to RGB,
- SDRAM controller - hardware SDRAM memory controller.
- Write FIFO/Read FIFO - write the image frames to SDRAM or read the image frames from SDRAM,
- SRAM controller - registers holding parameters for the fall detection algorithms,

- Algorithms - this part mainly conclude: background generation, background subtraction, mini-mum bounding box and fall detection,
- LED controller - controlling the LEDs with flashing for alarm when a fall happened,
- BUZZER controller - realizing the audible alarming along with the LEDs flashing, so that could alert neighbors when a fall is detected,
- GSM controller - controller for sending falling messages to ensure the victim got timely assistance.

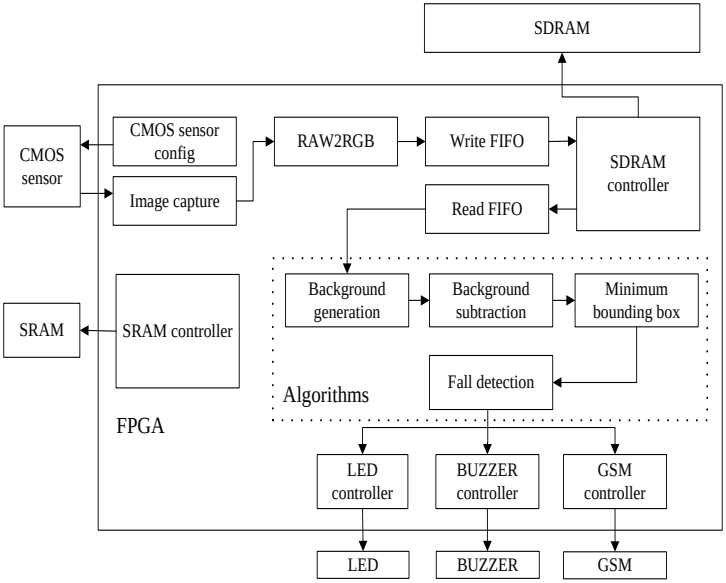

Fig.4 Overview of the fall detection system

Firstly, the CMOS sensor was configured through a configuration block. The FPGA acquired the video streaming through a capturing module from the CMOS sensor. Then, change the raw data from Bayer format to RGB format through a conversion module. The video frames and the generated background models were stored in the SDRAM with the FIFOs. To detect the moving object, the new image frame and background model will be read together in pixels from the SDRAM. The foreground model was generated by setting their absolute difference threshold. Finally, the FPGA will drive the alarm controller after a fall event being determined with the bounding box.

The project was synthesized for an Altera Cyclone IV (EP4CE15F17C8N) FPGA device using Quartus II Design Suite. The behavioral simulations performed

in ModelSim 10.0c verified that the hardware modules are fully compliant with the software described in Matlab R2012a. Table 1 presents the resource usage of the FPGA.

It is worth noting that the data from Table 1, even a small FPGA device from Cyclone IV series can run quite complex video-based fall detection system which resource utilization at about 35% of the available resources.

TABLE I. Project resource utilization

Resource	Used	Available	Percentage
FF	**5457**	**54576**	**10%**
LUT6	**5730**	**27288**	**21%**
LE	**4922**	**15408**	**32%**
DSP48	**54**	**112**	**48%**
BRAM	**22**	**116**	**19%**

V. IMPLEMENTATION ON FPGA

An Altera Cyclone IV (EP4CE15F17C8N) FPGA device is used to implement the presented fall detection system. The implementation was made using Verilog HDL hardware description language. The same fall detection algorithm was implemented in Matlab for benchmarking purposes using C programming language on a PC which contains Intel Core i3-4170 3.70 GHz CPU with 4GB RAM.

(a) standing

(b) squatting

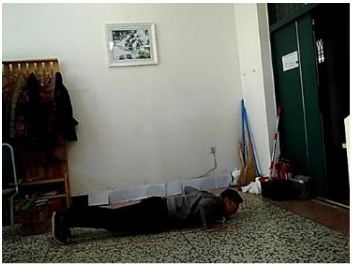

(c) lying down

(d) leg pressing

(e) falling down

(f) doing push-ups

Fig.5. Fall detection with Aspect ratio and Effective ratio

After repeated experiments, we took 1.2 as the aspect ratio threshold. Using 0.45 as the effective area ratio threshold and 6.5 as the body center threshold in this work.

Take the first 1000 image frames of the video stream for the tests. Figure 5b, Figure 5c, Figure 5d, Figure 5e and Figure 5f were detected as fall events just with the aspect ratio, which were shown in Figure 5. Figure 5b, Figure 5d and Figure 5f were misjudgments for doing daily exercises such as squatting, leg pressing, doing push-ups and so on. Therefore, this work introduces effective area ratios and center changes as corrections for falls. This can improve the accuracy of the fall detection.

A. Accuracy of the System

A large number of tests were conducted to assess the accuracy of the fall detection system. Table 2shows the results of the tests. The true positive of the FPGA-based solution is 2% lower than the Matlab-based solution. This result could be simply because of the processing speed of FPGA is much faster compared to Matlab.

TABLE II. Fall detection rate for both FPGA and Matlab implementations

Platform	True Positive	True Negative	False Positive	False Negative
FPGA	**96.00%**	**94.46%**	**5.54%**	**4%**
Matlab	**97.00%**	**93.56%**	**6.44%**	**3%**

1) Ture Positive = correctly detected the number of falls/the actual total number of falls.

2) Ture Negative = number of normal activities detected / total number of normal activities.

3) False Positive = number of falls judged by mistake / total number of normal activities.

4) False Negative = No number of falls detected / Total number of actual falls.

Table 2 shows that the FPGA platform's fall detection accuracy is 1% lower than the Matlab platform. The result may be due to the FPGA processing speed is too fast. Causes the loss of image frames. This is where this article needs to continue to improve

B. Processing Frame Rate

The processing frame rate of the implemented system was evaluated and is shown in Table 3. The results give a value of 56.36 fps with the resolution 640×480. The number of clock cycles required to complete a frame of image processing by the test system algorithm to calculate the frame rate of the video. In the meantime, the time required for Matlab to conduct the same image frames processing was calculated. The results demonstrate that the performance of video based fall detection in FPGA is near to 6X faster than the Matlab-based implementation.

TABLE III. Detection time for a single frame on the FPGA and Matlab

Platform	Max.(s)	Min.(s)	Avg.(s)	Frames per second(fps)
FPGA	**0.017**	**0.017**	**0.017**	**56.36**
Matlab	**0.128**	**0.076**	**0.099**	**10.10**

C. System alarm time

The average time of audible and visual alarm response in Table 4 is 0.51s. The time for sending GSM messages is often influenced by cell phone signals or network operators. the average time of GSM message sending time is 4.97s. The experimental results prove that the real-time nature of the fall detection alarm system based on FPGA can meet the system requirements.

TABLE IV. The response time for falling alarm

Alarm method	Max.(s)	Min.(s)	Avg.(s)
Audible and visual	**0.73**	**0.29**	**0.51**
GSM	**6.85**	**3.36**	**3.36**

Hence, FPGA is an effective instrument in this work to improve the performance of video based fall detection system. Besides that, FPGA is more suitable with its low power consumption and availability to be implemented in image processing.

VI.CONCLUSIONS

In this work, we have presented a video-based fall detection system in FPGA. The experimental results demonstrate that this system is able to process up to 56.36 fps with the resolution of 640×480. At the same time, it could alarm automatically through the configuration with Verilog HDL when a fall happened. This work shows the performance of better stability and low false positives. And it also demonstrates good robustness of FPGA for fall detecting with image processing.

REFERENCES

[1]. Ong, P. S., Ooi, C. P., Chang, Y. C. & Karuppiah, E. K. 2014. An FPGA-based hardware implementation of visual based fall detection. IEEE Region 10 Symposium: 397-402.

[2]. Zhang, D., He, Y., Liu, M., Yang, H. B., Wu, L. & Wang, J. H., et al. 2016. Study on incidence and risk factors of fall in the elderly in a rural community in beijing. Zhonghua liuxingbingxue zazhi, 37(5)：624-628.

[3].Kryjak, T., Komorkiewicz, M. & Gorgon, M. 2011. Real-time moving object detection for video surveillance system in FPGA. Conference on Design and Architectures for Signal and Image Processing, November: 1-8.

[4].Asano, S., Maruyama, T. & Yamaguchi, Y. 2009. Performance comparison of FPGA, GPU and CPU in image processing. International Conference on Field Programmable Logic and Applications: 126-131.

[5].Shuai Che, Jie Li, Sheaffer, J.W., Skadron, K. & Lach, J. 2008 Accelerating Compute-Intensive Applications with GPUs and FPGAs. Symposium On Application Specific Processors: 101-107.

Security of Users in Cyberspace

Ivan L. Reva

Novosibirsk State Technical University(NSTU)

reva@corp.nstu.ru

***Abstract* - Recently, telecasts, video clips and news lines on the Internet include such words as "information wars, hackers, cyber weapons, viruses ...". Ten or fifteen years ago, such phrases could only be heard in fantastic films. In the age of rapidly developing information technologies, WWW (Internet), social networks and information resources, IT-technologies are widespread in all of society's life areas. The virtual world is becoming more realistic, now a modern person, typically, has two lives – so-called "material" and "virtual". And if the material life is governed by laws and society traditions, the virtual one has no legal framework; it creates its own unspoken rules, which affect modern society. The virtual world has no border, that is why countries cannot completely control it with laws. The problem is still up-to-date and many IT-specialists try to find solutions. The need for common rules that would allow finding violators of the behavior standards in this area is obvious, but it is not easy to make the united rules for everyone, because laws in different countries differentiate one from another. However, it is still possible to find a general solution, there are things that unites all - for example, dislike for spam and viruses (except for those who receive money from this harmful activity).**

***Keywords* - user security, cyberspace, information security.**

I. INTRODUCTION

Now almost all international organizations have groups that deal with the development of laws regulating work in cyberspace that are acceptable for most countries. At moments of danger, humanity still knows how to negotiate, so I think that this task is quite feasible. [1]

The scale of influence of Information Technologies industry on the state exceeds only partial effects. Development of Information Technologies is one of the most important tasks of the Russian Federation. According to the online news edition RIA Novosti, the number of Russian Internet audience exponentially growing (Fig. 1 a,b). [1] In Russia, the number of information services has increased significantly, both on a commercial and state level. But with development of information services, the number of cyber-attacks on the servers of Russian companies is also increasing. So according to Kaspersky Lab's (Fig. 2), in 2016

Russia took the fourth place in the World in terms of the number of cyber attacks. [2]

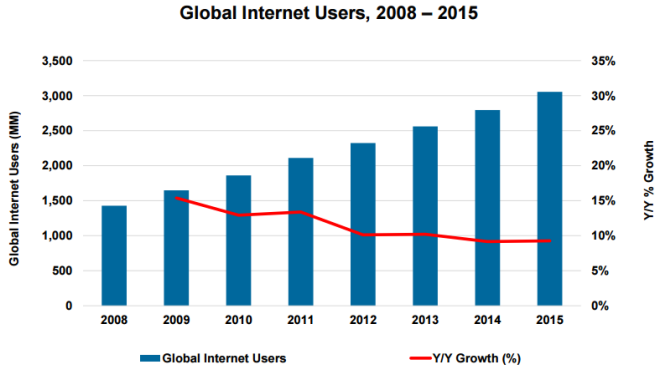

Fig. 1a. The Global Internet users number

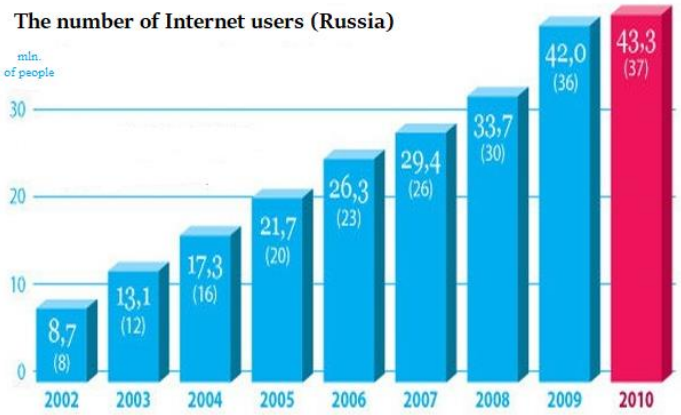

Fig. 1b The Russian Internet users number

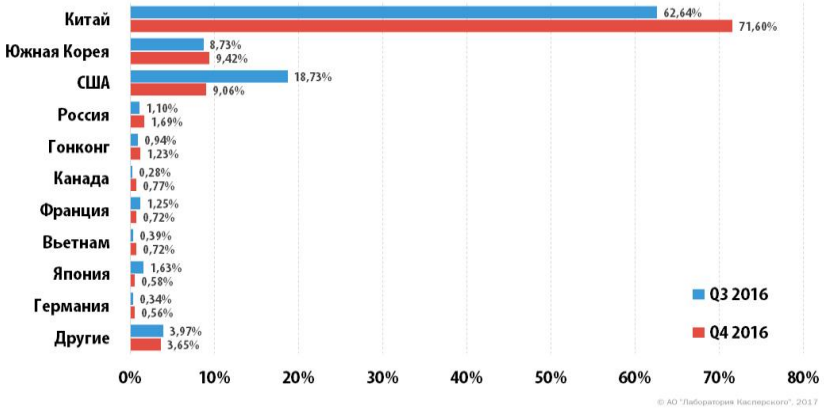

Fig. 2 Cyber-attacks geography

This is not surprising, because by the beginning of 2007 hacking became commercial, what lead to competition in this sphere, which contributed to the rapid growth of the quality of malicious software products and decrease of prices for services in this field. The growing number of hacked machines all over the world makes us talk about an industrial revolution in this sphere. On the one hand, it has become one of the most important types of criminal business, on the other - the level of organization, automation and division of labor in this industry have reached an unprecedented scale.

According to experts, more than 140 countries around the world develop cyber weapons, which are characterized by their secrecy and economic efficiency. Therefore, the number of operations in cyberspace is constantly growing: thousands of attacks are carried out daily throughout the world aimed at disrupting operation of state and commercial infrastructure of different countries.[1]

Obviously, in the pursuit of IT implementing, humanity faced a number of problems. The key problem was the safety of users in cyberspace, only in some social networks there is a huge amount of personal information, such as:

- FULL NAME;
- Date and place of birth;
- Place of residence;
- School number;
- Phone number;
- Names, photos and contacts of family and friends;
- etc.

The users of the Russian Federation public services portal (www.gosuslugi.ru) perfectly know what data is stored in their personal cabinets, use of banking online services and so on. It is not even possible to imagine the consequences of the leakage of this data into the hands of intruders.

Another not less important problem of informatization of the society is its influence on development of the younger generation. Impact of malefactors on children through the worldwide network is well-known, and sometimes the situations end up tragically. Propaganda and false information into the network can affect even the consciousness of an adult. The listed problems are so serious that they need to be solved at the state level.

What can we do? How to protect yourself in the virtual world? Typically, the society is not competent in these matters, and sometimes underestimates the threats. In fact, to protect yourself is not so difficult. Everyone remembers from an early age, what is good and what is bad, how we were taught a healthy lifestyle, so that we would not get sick, everyone remembers these simple rules:

- Brush your teeth when you are woke up;
- Do exercises;
- Wash hands before eating;
- Eat three meals a day;
- Do sport;
- etc.

There is the similar situation in virtual world: you need to remember the simple rules and try to follow them.

II. RULES FOR ENSURING THE SAFETY OF TEENAGERS IN CYBERSPACE

- In order to form and develop the ability to use safe information and communication technologies and use the virtual pace competently, one must adhere to the following rules:
- Stimulate and warn teenagers that they need to place their personal information on the Internet carefully;
- Tell them about a possible threat from strangers, especially in chat rooms and social networks;
- Teach a teenager how to act when unpleasant materials appear and close such Web sites;
- Regularly remind that information on the Internet is not always reliable;
- Do not disclose your passwords and periodically change them.
- To ensure effectiveness of the teenager protection in a network , you need to install security filters on your computer to protect it from viruses and spyware. If necessary, consult with specialists.

III. RULES FOR ENSURING THE PERSONAL SAFETY IN CYBERSPACE

As mentioned earlier, the human life is impossible without IT technologies, almost everyone has a personal computer with Internet access in which a user stores their data, performs any work, purchases goods. We must take steps to protect data. There is a list of actions which can help you to make your Internet activity safer:

- Try to copy all important information to removable media.
- Do not place a lot of information in social networks.
- To make purchases through the Internet use a debit rather than credit cards. (It is advisable not to store large sums of money on plastic cards).
- Do not download software from unknown vendors.
- In mail services, do not start .exe files from unknown recipients.
- The optimum length on passwords is 7 -8 characters.
- Do not click the pop-up windows. It is better to close such resources immediately. (I recommend blocking pop-ups in the browser settings.)
- It is not recommended to insert a personal USB - flash drive in unfamiliar computers.
- Try to use licensed software.

These simple rules would help you to avoid any problems in cyberspace. Please, take care about your personal data.

REFERENCES

[1]. RIA news [Electronic resource] URL: www.ria.ru. – Title from screen.

[2]. DDOS-attacks on networks in contemporary world [Electronic resource] URL:https://securelist.ru/analysis/malware-quarterly/30152/ddos-attacks-in-q4-2016/. – Title from screen.

[3]. Informatics[Electronic resource] URL: http://ppt4web.ru/informa tika. – Title from screen.

Feature-based Image Processing Algorithms for Vehicle Speed Estimation

Reda Harradi [1], Ariane Heller[2], Wolfram Hardt[3]

[1,2,3]TU Chemnitz

[1]reda.harradi@cs.tu-chemnitz.de. [2]ariane.heller@cs.tu-chemnitz.de,[3]wolfram.hardt@cs.tu-chemnitz.de

***Abstract*—The aim of this paper is to implement a filter-based software solution for detecting vehicles from a set of videos and estimating their speeds. The proposed implementation utilizes a set of low-level filters for extracting different regions of interest that depict the initial motion of each detected vehicle. Different approaches are then proposed to extract stable low-level features; either using the Shi-Tomasi algorithm, the Scale Invariant Feature Transform (SIFT) algorithm or the Speeded- Up Robust Features (SURF) algorithm for enabling the further tracking. The tracking of those aforementioned low-level features is then performed using the Kanade-Lucas-Tomasi (KLT) algorithm. The speeds of the vehicles are then calculated by the means of an Inverse Perspective Mapping, and by projecting the traveled displacements of the tracked features to known real world measures, in order to be able to change the measurements' unit system of the calculated vehicles' speeds from pixels per second to kilometers per hour.**

Furthermore, the implementations were done on the Automotive Data and Time-triggered Framework (ADTF) from Elektrobit, which provides the possibility of having a good modularity of algorithmic models for image processing. The testing was based on a dataset of videos provided by the research project done by Luvizon et al. at the Federal University of Technology in Parana, Brazil, on proposing a novel vehicles' plates detector, where almost five hours of videos were captured in different conditions by a single low-cost digital camera, placed at meters from the ground. The provided dataset contains more than 8 thousand vehicles and is associated with a ground truth reference obtained through the use of a state-approved inductive loop detector, that provides the real world speed measures of almost all the vehicles within the dataset.

Keywords—ADTF, Feature Extraction, Feature Tracking, Shi-Tomasi, SIFT, SURF, KLT.

I. INTRODUCTION

Preventing road accidents has always been a major field of research within the automotive industry. Sadly, nearly 25,300 people departed this life and another 135,000 people were seriously injured or left with life-changing injuries on the European roads in 2017, according to the recently published data on Road Safety that is pursued by the European Commission based in Brussels. In fact, the rate of death on European roads has dropped down by 2 % compared to 2016, and has showed the same decreasing trend as in the previous year. The study also showed that of all the road accidents, 8 % occurred on motorways, 37 % in urban areas, and 55 % in rural areas [1].

While these numbers still hide stories of pain and grief, the European roads remain amongst the safest in the world. With 49 road casualties per one million inhabitants, against 174 mortalities per million worldwide, the European Union has made a substantial improvement in reducing the number of road accidents over the past twenty years. A part of this progress was thanks to the establishment in 2010 of the Road Safety Programme 2011-2020, that came up with European and national level orientations with the aim of cutting by half the ratio of traffic deaths in Europe by 2020 [1].

This paper falls within two of the main building pillars of the Road Safety Programme 2011-2020, which are building safer road infrastructures and boosting smart technologies. The program aims at introducing new active safety measures for safety equipment, extending the existing legislations to cover the rural roads as well, and speeding the new technical projects for enabling the data and information exchange between the vehicles and the road infrastructures. As a matter of fact, this paper is motivated by the desire of using normal electro-optical sensors present in modern-day cameras to detect, classify and recognize vehicles present within an urban road traffic. The goal is to tackle the issue of detecting the vehicles' speeds in urban areas at reduced costs; by the means of image processing instead of relying on currently used specialized-sensing technologies, e.g., ultra-sonic sensors, loop detectors, etc.

II. PROPOSED APPROACH

The main methodological approach in this paper is com- posed of a six-stages processing chain, as depicted in Figure 1. The processing chain starts with a pre-processing step, which consists of first applying a set of pre-processing filters on the input video frames, in order to provide a noise-free base that would facilitate the further processing.

The second step is then responsible of deriving the contours and convex hulls shapes of the vehicles present within each frame. Once accomplished, the next step of the processing, which focuses on the multiple separate regions of interests

(ROIs) given by the convex hulls, continues the processing chain thence, where the low-level features extraction mechanisms allow the extraction of the feature keypoints describing the vehicles of interest. Note that in this approach, only one low-level feature extractor is used at a time, i.e., either Shi-Tomasi, SIFT, or SURF. A comparison of the results of using each different extractor is given in section IV. The vehicles are then classified, depending on their sizes and aspect ratios, into either motorbikes, cars, or trucks, to be then tracked throughout the whole sequence of the video frames in which they appear, through the use of the Kanade-Lucas-Tomasi (KLT) algorithm. Finally, the process ends with a scene interpretation, where an Inverse Perspective Mapping (IPM) projection is applied, in order to estimate the detected vehicles' speeds, not only in pixels per second, but also in kilometers per hour.

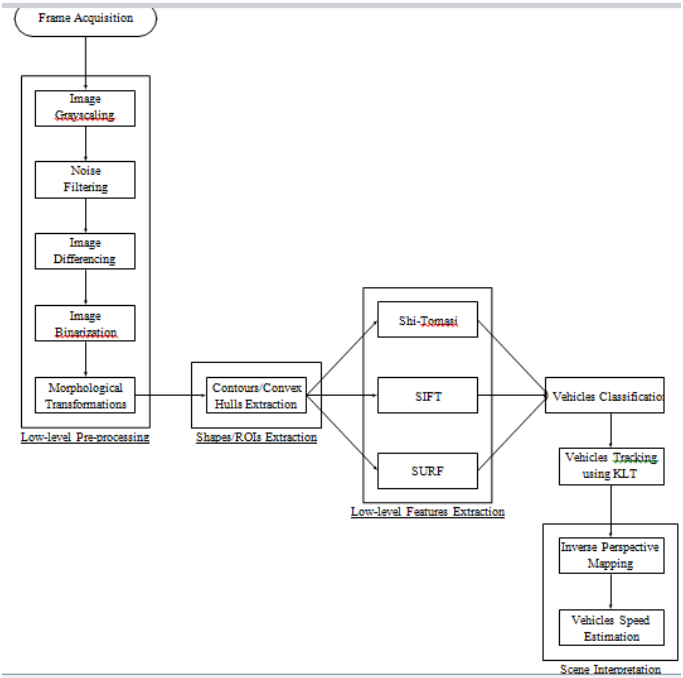

Fig. 1 – Diagram of the processing flow chain of the main methodological approach used in this paper

III. IMPLEMENTATION

The implementation of the system has been done in accordance with the Automotive Data and Time-triggered Frame- work (ADTF) version 2.13.1 from the Elektrobit company. This framework allows several benefits for the evaluation and validation of software algorithms. It consists of a well-defined software development kit (SDK) for the C++ programming language, an organized graphical configuration editor, and a suite of pre-defined toolboxes for various purposes, such as the *Video Compression Toolbox*, that manages the compression and decompression of the video streams used within ADTF, and the *Device Toolbox*, which ensures the connection to several types of external devices, e.g., CAN, LIN, FlexRay, MOST and Ethernet bus systems, and the *Display Toolbox*, that provides pre-defined *Filters* for various displaying and rendering purposes.

Furthermore, the choice of ADTF as a developing frame- work is justified by the fact that it offers the support for implementing new functions in a fast, prototypical and incremental way. Additionally, ADTF offers a layered architecture that enhances the modularity of the implemented software solutions, in such a way that the modules, i.e., filters, are freely changeable and expendable.

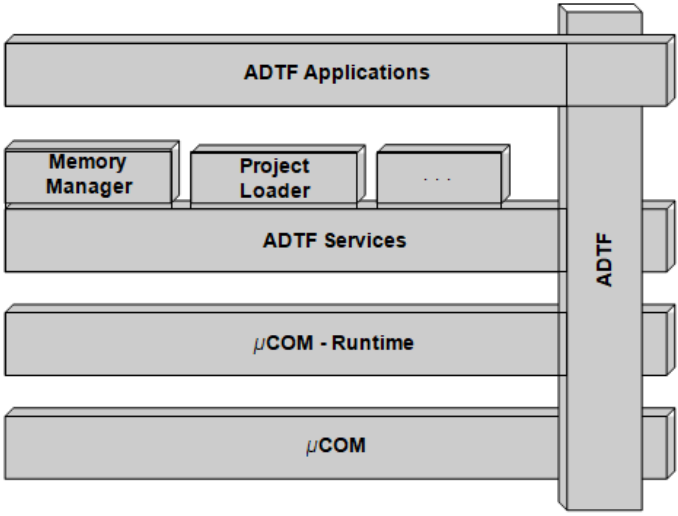

Fig. 2 – Figure showing the overall architecture of ADTF. Figure adapted from [2]

As a matter of fact, ADTF is based on a layered architecture, as depicted in Figure 2. The architecture consists of four main tiers: The *Micro Component*

Object Model (*µCOM*), which is the base layer; based on the Microsoft Component Object Model, and is responsible of defining the components, the basic interfaces and the inter-process communication, as well as the components' interactions. Next comes the *µCOM Runtime* layer, where the plugins that are managing the interactions between the different modules could be loaded, registered, and deregistered. Moreover, the *ADTF Services* layer consists of defining the various system services provided among the functionalities of ADTF itself. Those services, e.g., memory management, project loading and management, etc., remain throughout the whole running cycle of ADTF, i.e., from the start-up of ADTF until its shutdown. Finally, the last layer in ADTF's architecture is the *Application* layer, which represents the highest user module for integrating the software components, i.e., Filters, based on a streaming architecture, as depicted by the following figure. Note also that ADTF offers the ability to modify the configuration of those filters during the runtime, which further strengthens its modularity aspect for image processing implementations.

The filters in ADTF incorporate the algorithms implemented to solve the given task, and provide the pin interfaces for the mutual interaction of the whole configuration. In fact, the data exchanged between the filters is achieved through a filter graph that defines the connections between each respective input and output pins, in such a way that only matching pins, with matching media types, are linked together. Furthermore, the transmitted data through the pins is encapsulated within a set of data containers called *Media Samples*. These media samples hold several metadata properties such as the timing flags, the data size, as well as the data buffers holding the referenced data in memory. Figure 3 is depicting the streaming architecture of ADTF in detail. Note that most of the filters implemented within this paper make also use of the pioneering OpenCV library developed by Intel, which is an open-source cross-platform library that is widely used in the computer vision and image processing fields, and which allows the implementation of several modern state-of-the-art algorithms.

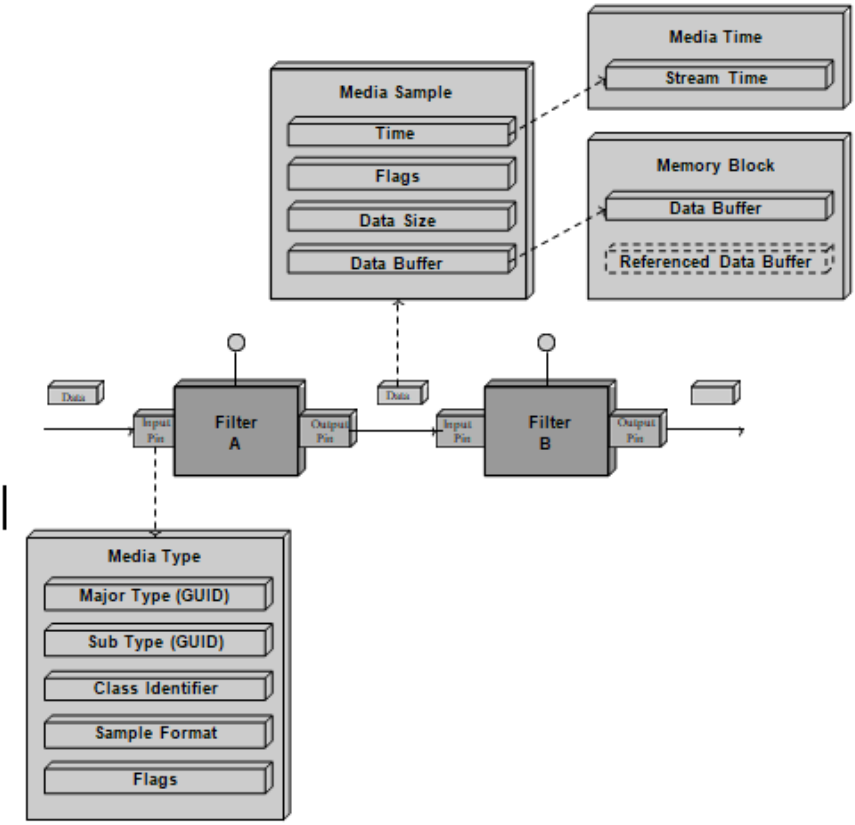

Fig. 3 – Figure showing the streaming architecture that is used within ADTF for the filters communication and data exchange. Figure adapted from [2]

IV. RESULTS

This section focuses on the assessment and the evaluation of this paper's implementation's results. First, the section introduces the dataset used for the testing of the proposed system. Next, a performance analysis of the filters implemented in ADTF is addressed, and the average computational consumptions in terms of required memory and CPU usage are given. Moreover, the detection rate of the vehicles observed by analyzing the system's output while running

several videos from the dataset is presented. Finally, the section also discusses the evaluation of the vehicle speed estimations, with respect to the tolerance interval allowed by both the German and the American authorities.

A. Dataset

The provided dataset covers 20 videos that are split into five parts, depending on the weather conditions, as well as on the recording conditions. The frame resolution of the videos provided by the dataset is equal to 1920 1080 pixels, with a frame rate of 30*x*15 frames per second. Furthermore, additional XML files have been provided by Luvizon et al. [3], containing the ground truth speeds for every video. These ground truth speeds are the result of a well-calibrated speed meter that uses inductive loop detectors, and that has been approved by the Brazilian national metrology agency Inmetro1.

Furthermore, and according to the annotations of the ground truth reference, a differentiation has been done between the appearing vehicles into either motorbikes or normal vehicles, i.e., cars and trucks. It was also possible to notice that the inductive loop detectors were able to record the speeds of 43 % of all motorbikes, and 92 % of all the normal vehicles, appearing in the video sequences of the dataset, where most of the recorded speeds were below 60 km/h, due to the speed limit enforced by law on the road where the data has been gathered.

TABLE I. Table stating the criteria used for analyzing the system's performance

Criterium	Description
Duration	$\Delta t = 15$ seconds
Interval	each 3 seconds
Measurements	M_i *are done* $\times$ 3 times
Number of Measures	$Nbr_{Meas.} = 5$
Measurement Equation	$M_{eq} = \sum(M_{i+1} - M_i)/Nbr_{Meas.} \mid i \in \{3, 6, 9, 12, 15\}$ seconds

B. Performance Analysis

The analyses were performed on a x64 machine running Windows 7, and powered by an Intel 8 Cores i7-4770 processor clocked at 3.40 GHz, and with a 16 GB RAM memory. Furthermore, the machine was ensured to be in a relatively resting state, prior to the beginning of the measurements, where [0, 1] % of the CPU and [1.64, 1.65] GB of the RAM memory were being used by other processes running in the background. As a matter of fact, the analysis on ADTF showed that the overall memory consumption increased with the increase of the number of

inter-linked filters within the active configuration, at the time of the configuration's initialization.

Moreover, in order to ensure the forward compatibility with both the OpenCV library and the ADTF framework, the videos have been decoded, converted to the MP4 format, and downscaled to a resolution of 640 360 pixels, while keeping the same embedded frame rate, in order to allow for faster processing and execution times. In fact, the experiments showed that the downscaling of the videos' resolutions affected the clarity of the images; i.e., the appearing vehicles are more "pixelated", but did not affect the quality of the overall system in successfully detecting and tracking the vehicles present in the video sequences.

As a matter of fact, each performance analysis measurement cycle was lasting for a timespan of 15 seconds, where a raw single image frame was being sent repeatedly each 3 seconds for processing. Moreover, in order to ensure the consistency and accuracy of the results, the were repeated three times in a row for each measured filter, while ensuring the aforementioned resting state of the machine prior to repeating the measurements. In fact, the measures were done for all the implemented filters using both RGB colored and grayscale images. Furthermore, the criteria used for making the measurement are summarized in Table I.

TABLE II. Table summarizing the image-based performance analysis of the implemented algorithms

ADTF Filter	CPU Usage (%)		Physical Memory Usage (MB)		Virtual Memory Usage (MB)	
	RGB Image	Grayscale Image	RGB Image	Grayscale Image	RGB Image	Grayscale Image
Image File Reading	1.046	-	0.203	-	0.59	-
Video File Reading	1.25	-	0.024	-	0.023	-
Overlay Blending	0.28	0.008	0.203	0.015	0.059	0.012
OpenCV Grayscaling	6.305	-	0.892	-	0.934	-
Homogeneous Blur	0.049	0.019	1.123	0.439	0.212	0.025
Gaussian Blur	1.031	0.269	1.105	0.633	0.262	0.249
Median Blur	0.439	0.342	1.309	0.368	0.07	0.062
Binary Thresholding	5.931	5.16	1.108	0.422	0.267	0.069
Morphological Dilation	0.068	0.005	1.251	0.066	0.066	0.015
Morphological Erosion	0.042	0.003	1.302	0.564	0.116	0.096
Contours Extraction	-	0.261	-	1.854	-	0.386
Convex Hulls Extraction	-	0.106	-	1.810	-	0.253
Inverse Perspective Mapping	6.176	6.118	1.278	0.704	0.410	0.056
Shi-Tomasi Detection	0.248	-	2.101	-	1.643	-
SIFT Detection	1.124	-	1.361	-	0.963	-
SURF Detection	0.135	-	1.329	-	1.068	-

The observed measurements for the *Image_File Reader* and the *Video File Reader* filters were deduced from the results of the measurements observed for each analyzed filter, in order to alleviate the overhead caused by the extraction of the image frames. In addition, the overhead caused by the *Performance Analysis* filter has also been taken into account. The results of the analysis are summarized in Table II.

As previously mentioned, the measures were done on single colored and grayscaled image frames, and the values given by Table II represent the average performance values of each respective implemented filter, except for the three detection filters[2]. In fact, the image and video reading filters that were used to extract the RGB colored image frames consumed relatively low physical and virtual memory. Note that the colored RGB image frames were converted to their grayscale equivalents using different grayscale conversion techniques, and that the Single Color Channel conversion filter consumed the least amount of CPU usage, whereas the algorithm behind the OpenCV grayscale conversion function consumed the highest amount of memory, as depicted by Figure 4.

Moreover, the homogeneous blurring algorithm was observed to be the most performant amongst all, which is in fact due to its simplicity of equally weighting the images' pixel intensities.

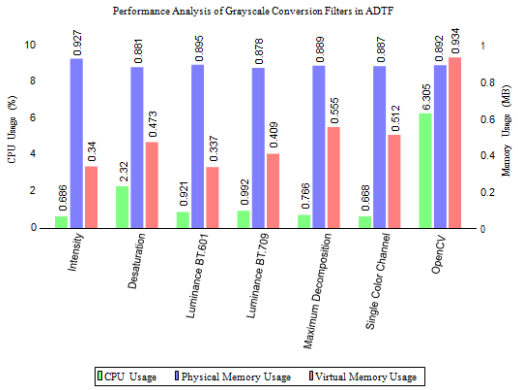

Fig. 4 - Figure showing the performance analysis of the grayscale conversion filters in ADTF

Furthermore, it has been noticed that the binary thresholding using the OpenCV functions requested more CPU usage than most of the other analyzed

filters. Concerning the morphological operations, both the dilation and erosion computational consumptions were negligibly low, where the erosion has been observed to consume a tiny more memory than the dilation. In addition, the Convex Hulls filter has been noticed to perform better than the Contour extraction filter, which is in accordance with the literature findings. Furthermore, it has also been noted that the Inverse Perspective Mapping filter requires the highest number of CPU cycles among all filters, due to its rather complex calculations for changing the perspective view of the image frames.

Last but not least, the three used algorithms for feature detection have also been analyzed, where the Shi-Tomasi algorithm ranked last by having a higher memory consumption but a rather low CPU usage requirement compared to the other algorithms. Following in the rank was the SIFT algorithm that had a relatively improved memory consumption compared to SIFT, but required more CPU usage. Finally, the SURF algorithm ranked first with a slightly higher virtual memory usage, but clearly lower physical memory and CPU consumptions, when compared to the other low-level feature extraction algorithms. It could hence be concluded that the SURF algorithm is the best suitable algorithm when coming to implementing this system in an embedded environment.

C. Vehicles Detection Rate

The following table sums up the performance of the pro- posed implementation, which has shown an accuracy of 0.78, a precision of 0.93 and a recall of 0.83.

TABLE III. Summary of the vehicles detection rate results

Metric	Measured Value
FNR	0.173
Accuracy	0.779
Precision	0.927
Recall	0.827

D. Estimated Vehicle Speed Evaluation

The performance evaluation of the speed estimation was achieved through the comparison of the estimated speed results obtained by the system with the results obtained from the inductive loop detectors, given within the ground truth reference. In fact, the estimation of the speed has to lay within a given error interval. In the USA for example, the error interval ranges from 3 km/h to +2 km/h. According to the German authorities, the tolerance towards the measurements of the vehicles' speeds using video recording methods is about 5%, as applied for the ProViDa measuring device[3]. Since this paper deals with the detection of vehicles within urban areas, and knowing that the speed limitation

within cities is set to 50 km/h, a valid output speed estimate should be within a range of 2.5 km/h. Thus, the adopted standard is the one following the German enforcements, due to its more restrictive measures.

– Furthermore, the minimal and maximal error values recorded by the system for the used dataset are respectively -4.98 and +3.51 km/h, whereas the average absolute error was 1.328 km/h, making 76.322 % of the measured values fall within the German tolerance range. Moreover, the feature tracker; which was set up to select the best 15 features, achieved satisfying results in tracking the vehicles in the different frames. In fact, the feature tracker was able to correctly track; on average, 90.556 % of the vehicles that appeared in the videos.

V.CONCLUSION AND OUTLOOK

The goal of this paper has been to use low-level feature- based image processing algorithms, in combination with a tracking algorithm, in order to be able to detect vehicles in an urban environment, and estimate their corresponding speeds. The work done in solving the aforementioned task consists of a sequential processing chain made of various low-level processing filters implemented within the ADTF framework, three main low-level features extraction algorithms; i.e., Shi-Tomasi, Scale Invariant Feature Transform (SIFT) and Speeded-Up Robust Features (SURF), a tracking mechanism based on the Kanade-Lucas-Tomasi (KLT) algorithm, and an according scene interpretation that utilizes the approach of the Inverse Perspective Mapping (IPM).

Furthermore, although several other modern feature extraction algorithms are available in the literature, the focus of this paper has been directed towards the usage and analysis of three low-level feature extraction algorithms, namely Shi-Tomasi, SIFT and SURF, which are considered as being part of the most widely used algorithms within the image processing research field. The analysis yielded to the results that the Shi-Tomasi algorithm ranked last by having a higher memory consumption but rather low CPU usage requirements when compared to the other algorithms, followed by the SIFT algorithm that had a relatively improved memory consumption compared to SIFT, but required more CPU usage, and finally, the SURF algorithm that ranked first and showed its suitability for an embedded implementation with a slightly higher virtual memory usage, but clearly lower physical memory and CPU consumptions, when compared to the other low-level feature extraction algorithms.

Last but not least, future scopes for further improving the presented system could be proposed. These may consist amongst others of applying data and task parallelization approaches [4], [5] for a better embedded performance suitability, in cases where the handling of a bigger resolution input feed is required.

Furthermore, enhancements of the model could also be achieved by utilizing other techniques useful for solving and consolidating the solution to the problem given by the task. An example would be the addition of the Kalman Filter (KF) that could be used in conjunction with the implemented KLT tracker, in order to alleviate the problems of the tracking misses, by using the predictions of the Kalman filter, and hence improve the overall tracking of vehicles. Furthermore, a 3D pose of the appearing vehicles could also be estimated using the POSIT technique, which would allow the precise localization and encapsulation of the 3D bounding dimensions of the appearing vehicles. This would in fact compensate the lack of the vehicles' heights knowledge, and could be used to further improve the estimation of the vehicles' speeds.

Not to mention that since the implemented system's soft- ware components comply with the MISRA C++ rules, a possible embedded implementation could be envisaged within the YellowCar project [6] undertaken at the Computer Engineering Department of the Computer Science Faculty of the Chemnitz University of Technology. The YellowCar's ability to deal with automotive real-time scenarios could eventually be enhanced by integrating the proposed system into one of its existent ECUs.

REFERENCES

[1] The European Commission, Directorate-General Mobility and Transport, Unit C2 - Road Safety, "Road Safety in the European Union - Trends, statistics and main challenges," European Commission, Tech. Rep., April 2018.

[2] Elektrobit Assist, "ADTF v2.13.1 SDK Documentation," Audi Electronics Venture GmbH, Tech. Rep., July 2015.

[3] D. C. Luvizon, B. T. Nassu, and R. Minetto, "A Video-Based System for Vehicle Speed Measurement in Urban Roadways," in *IEEE Transactions on Intelligent Transportation Systems (ITS)*, September 2016, pp. 1–12.

[4] S. Blokzyl, M. Vodel, and W. Hardt, "A Hardware-accelerated Real-time Image Processing Concept for High-resolution Electro-optical Sensors," *Deutscher Luft- und Raumfahrtkongress*, 2012.

[5] S. Blokzyl, M. Vodel, and W. Hardt, "FPGA-based Approach for Runway Boundary Detection in High-resolution Colour Images," in *Proceedings of the Sensors and Applications Symposium*, 2014.

[6] N.Englisch, O. Khan, R. Mittag, F. Hänchen, W. Hardt, and A. Heller, "YellowCar: Automotive Multi-ECU Demonstrator Platform," in *IN- FORMATIK 2017, 15. GI Workshop Automotive Software Engineering*, ser. Lecture Notes in Informatics (LNI) - Proceedings, Volume P-275, September 2017, pp. 1517–1522.

Face Recognition via Joint Feature Extraction based on Multi-task Learning

Ao Li[1], Deyun Chen[2], Guanglu Sun[3], Kezheng Lin[4]
[1,2,3,4]*Harbin University of Science and Technology (HUST)*
dargonboy@126.com [1], chendeyun@hrbust.edu.cn [2],
sunguanglu@hrbust.edu.cn [3], link@hrbust.edu.cn [4]

***Abstract*—In this paper, we proposed a novel joint feature extraction framework to address the face recognition problem. It is found that different face images have some hidden shared information, which can be used to help to improve the recognition performance. Hence, the proposed framework take face images for each person as a task, and then explored the shared and class-specific structures across different persons simultaneously based on multi-task learning. Meanwhile, an extra subspace projection for each person is also learned to enhance the discrimination. Extensive experimental results demonstrate that our proposed framework is superior among the existing face recognition methods.**

Keywords—Face recognition; Feature extraction; Multi-task learning;

I.INTRODUCTION

Face recognition is a fundamental issue in computer vision, which aims to assign a query face into an known person in the database. Many literatures aboutface recognition are emerged in the past two decades, and several recognition frameworks are formed to address the face recognition problem. J. Wright et al proposed a general classification method for robust face recognition with sparse representation(SRC)[1]. In their method, the query sample was approximated by the linear combination of training samples, and the label for face can be easily assigned with a minimum class-specific local fidelity term. Then, to explore the intrinsic character of SRC, the working mechanism of SRC is discussed in [2], and the collaborative representation-based face recognition is proposed to reveal theory of face recognition problem. A.. Wagner t al found that the face alignment can significantly improve the recognition rate, and put the face alignment and classifier into a unified framework to extend the conventional SRC model[3]. Q.Shi et al analyze the face recognition from the view of sparsity, and talk about its relevant to compressive sensing problem[4]. With the help of robust regression, M. Yang et al

proposed a robust regression coding method, and obtain excellent results in face recognition issue[5]. Some more relevant literatures can be studied in [6-11].

Though the above linear regression-based methods achieved remarkable performance to promote the accuracy recognition rate, they all utilized the training face sample individually. Nevertheless, in practice, face images from different persons have hidden shared features. If these shared features can be well studied, it will improve the recognition performance greatly. Meanwhile, with the successful application in mining shared information, multitask learning-based classification model shows increasing interest in recent computer vision community. So, in this paper, we introduced the multitask learning into the conventional model, and established a joint feature extraction framework to address the face recognition problem. To obtain extra discrimination, a discriminative projection is also learned in our proposed framework. Experiments are tested on several face datasets to verify the effectiveness.

The remainder of this paper is listed as follows. The detail of our proposed model is discussed in Section II. Some experimental results are shown in Section III. Section IV concludes the paper.

II. JOINT FEATURE EXTRACTION FRAMEWORK

A. Joint feature extraction model

For clarity, we first list some notations used in our paper. The training data set is denoted as $\{X_i\}_{i=1}^{C}$, where $X_i \in R^{d\times N_i}$ presents training subset of i-th class with N_i instances , and d denotes the instance dimensionality. For each training instance $x_k \in R^d$, let $y_k \in R^C$ be its label vector, where C denotes the total number of classes in the training set. Furthermore, if x_k is chosen from the c-th class($c = 1,2,3...C$), only the c-th entry of y_k is one and all others are zero. That is, if x_k is chosen from the second class, its label y_k is denoted as $y_k = [0,1,0,...]^T$. Let $W \in R^{C\times d}$ be the regression parameters as $W = \left[w_1^T, w_2^T, ..w_C^T\right]^T$, where each w_c denotes the regression vector for c-th class and can be seen as the classifier for the c-th class in regression-based classification problem. With these notations, the general training model for W with linear regression can be formulated as follows.

$$\min_W \left\{ \|Y - WX\|_F^2 + \lambda\phi(W) \right\} \qquad (1)$$

where $Y=\left[y_1, y_2, ...y_k, ...\right]$ denotes the label matrix for all the instances ($X=\left[X_1, X_2, ..X_C\right]$) in training data set, $\phi(W)$ presents the certain constraint on the parameters, $\|\bullet\|_F$ denotes the Frobinus norm and λ is the positive scalar to balance the two terms.

By enforcing the training data close to their labels, equation (3,1) aims to learn the regression parameters from a mount of instances statistically. And then, the label vector y_q of a test instance x_q can be predicted with the parameters as $\hat{y}_q=\hat{W}x_q$, and the label $\hat{c}_q$ can be decided with $\hat{c}_q=\arg\max_c\left(\hat{y}_q(c)\right)$.

Similar to equation (1), what we want is to introduce the multitask learning to our proposed model. In our model, we take face samples of each person as a task, and explore the shared and class-specific structural components simultaneously across different person, which is believed to help to extract extra joint information hidden in different person to make the feature more effective. Based on this idea, we formulated our proposed model as follows.

$$\min_{W_i,P_i,W_S}\left\{\sum_{i=1}^{C}\begin{pmatrix}\left\|Q(X_i)-(W_S+W_i)P_iX_i\right\|_F^2\\+\alpha\|P_i\|+\beta\|W_i\|_1\end{pmatrix}+\lambda\|W_S\|_F^2\right\} \quad (2)$$

where $Q(X_i)$ is a designed operator to extract the Gabor feature, which is used to transform the data matrix X_i to a low-dimensional vector with respect to its columns. W_S and W_i denote the parameters to explore the shared structural component among the tasks, and the class-specific structural component respectively. P_i represents the discriminative projection matrix for i th person. α , β and λ are the positive constant to balance the terms in model. With our proposed model in equation (2), shared and class-specific feature extraction parameters, and discriminative subspace projections are learned simultaneously in a unified framework. The three variables will benefit each other during the iteration, which will improve the recognition performance progressively.

B.Numerical scheme for proposed model

Now, we will present a numerical scheme to solve the objective function in the proposed model. The alternating direction method of multipliers(ADMM) has

been widely used in the multivariable minimization problems[12]. With ADMM, our proposed model can be divided into three subproblems as follows, which can be solved independently and iteratively.

For each task, fix its projection operator P_i and class-specific structural feature extraction parameter matrix W_i, we can obtain the following subproblem for W_S.

$$\min_{W_i,P_i,W_S}\left\{\sum_{i=1}^{C}\left(\left\|Q(X_i)-(W_S+W_i)P_iX_i\right\|_F^2\right)+\lambda\|W_S\|_F^2\right\} \quad (3)$$

From equation (3), it can be seen that objective function is a convex and differentiable function. By forcing its derivative to be zero, the closed- form solution can be obtained in the k -th iteration as

$$W_S^{k+1}=\left(\sum_{i=1}^{C}\left(Q(X_i)-W_i\Phi_i\right)\Phi_i^T\right)\left(\sum_{i=1}^{C}\Phi_i\Phi_i^T+\lambda_s I\right)^{-1} \quad (4)$$

where, $\Phi_i=P_iX_i$. $(\bullet)^T$ and $(\bullet)^{-1}$ denote the transpose and inverse operation on matrix. I presents the identity matrix.

Fixing the P_i and W_S , the class-specific structural feature extraction parameters W_i can be optimized by the minimization as follows.

$$\min_{W_i}\left\{\left\|Q(X_i)-(W_S+W_i)P_iX_i\right\|_F^2+\lambda\|W_i\|_1\right\} \quad (5)$$

The objective function in (5) is a classical lasso problem, which can be solved with the method in [13].

When the shared and class-specific feature extraction parameters are fixed, we can obtain the minimization problem for projection operator P_i as

$$\min_{P_i}\left\{\left\|Q(X_i)-(W_S+W_i)P_iX_i\right\|_F^2+\beta\|P_i\|_2\right\} \quad (6)$$

Similarly, forcing the objective function in (6) to be zero, we can easily learn the projection operator.

Based on the above equations, the numerical scheme for the proposed model can be summarized as follows:

Numerical Algorithm

Initialization: Shared structural parameters $W_S^{(0)}$, class-specific structural parameters $W_i^{(0)}$ and projection operator $P_i^{(0)}$. Iterative step $k=0$.
While not converged do
1.Compute the shared parameters $W_S^{(k+1)}$ with equation (3);
2. For i =1:C
(1) Compute the class-specific structural parameters $W_i^{(k+1)}$ with equation (5);
(2) Compute the projection operator structural parameters P_i with equation (5);
end for
End while
Output the parameters W_S^*, W_i^*, P_i^*;

with the learned parameters W_S^*, $\{W_i^*, P_i^*\}_{i=1}^C$, a query sample x_q can be classified into a category by the self-regression loss term in our framework as follows.

$$\hat{l}_q = \arg\min_i \left\{ \left\| Q(x_q) - (W_S^* + W_i^*) P_i x_q \right\|_F \right\} \quad (3.19)$$

where $\hat{l}_q$ denotes the estimated label indicator.

III. EXPERIMENTAL RESULTS AND ANALYSIS

In this section, we will conduct extensive experiments on several face datasets. The proposed framework will be compared to existing excellent methods to evaluate the competitive performance. In our experiments, the extended YaleB and ORL face datasets are used test the performance. The comparison method includes SRC, CRC and symmetrical face feature(SFF) proposed in []. The details of dataset are described as follows.

The Extended YaleB face dataset contains a total of 16128 face images, which were shot by 38 people under different lighting conditions. Each person has 64 positive face images under different expressions and lighting conditions. Fig.1 shows a small sample of the images in the data set.

Fig.1 instances of two persons in Extended YaleB

The ORL face dataset contains 400 face images, which were shot by 10 people under different lighting conditions, varying view and expressions. Each person has about 10 face images. Figure 2 shows some face samples of the ORL dataset.

Fig.2 instances of two persons in ORL

We performed simulation experiments on the above two face datasets methods with the comparison methods. We test five time for each method, and take

the average accuracy as the final result, which is shown in Table.1. The number shown in the parentheses denotes the proportion of training samples in the dataset.

TABLE I. Average accuracy of each classification method

	Extended YaleB(50%)	**ORL(50%)**
SRC	**95.21%**	**90.23%**
CRC	**97.03%**	**92.15%**
SSF	**97.79%**	**94.01%**
Proposed Method	**98.06%**	**95.32%**

From the results in Table.1, we can see that our proposed method obtained the highest recognition rate in the comparison method. Due to joint feature extraction in the proposed method, some extra information are explored from different face, and the shared structural information, such as illumination, holistic contour of face, are transferred between each other, which help to construct a more realized face and improve the performance.

IV. CONCLUSIONS

A joint feature extraction model is proposed to focus on the face recognition problem in this paper. The proposed model includes there parameters, which are used to extract the shared structural component, class-specific structural component and projection operator. Also, to facilitate the mentioned parameters , they are put into a unified framework and improve each other iteratively. Some experimental results shows the effectiveness of our proposed model among the comparison ones.

REFERENCES

[1] Wright J, Ganesh A, Zhou Z, et al. Robust face recognition via sparse representation[J]. IEEE Transactions on Pattern Analysis and Machine Intelligence, 2009, 31(2):210-227.

[2] Zhang L, Yang M, Feng XC. Sparse Representation or Collaborative Representation: Which Helps Face Recognition?.[C] IEEE International Conference on Computer Vision, 2011, Barcelona Spain, pp.471-478.

[3] Wagner, J. Wright, A. Ganesh, Z. H. Zhou, H. Mobahi, and Y.Ma, "Toward a practical face recognition system: Robust registration and illumination via sparse representation," IEEE Trans. Pattern Anal. Mach. Intell., vol. 34, no. 2, pp. 372–386, Feb. 2011

[4] Q. Shi, A. Eriksson, A. Hengel, and C. Shen, "Is face recognition

[5] M. Yang, L. Zhang, J. Yang, and D. Zhang, "Regularized robust coding for face recognition," IEEE Trans. Image Process., vol. 22, no. 5, pp. 1753–1766, May 2013.

[6] R. He, W. S. Zheng, B. G. Hu, and X. W. Kong, "A regularized correntropy framework for robust pattern recognition," Neural Comput.,

vol. 23, pp. 2074–2100, 2011.

[7] R. He, W. S. Zheng, and B. G. Hu, "Maximum correntropy criterion for robust face recognition," IEEE Trans. Pattern Anal. Mach. Intell., vol. 33, no. 8, pp. 1561–1576, Aug. 2011.

[8] X.-X. Li, D.-Q. Dai, X.-F. Zhang, and C.-X. Ren, "Structured sparse error coding for face recognition with occlusion," IEEE Trans. Image Process., vol. 22 , no. 5, pp. 1889–1999, May 2013.

[9] R. Rigamonti, M. Brown, and V. Lepetit, "Are sparse representations really relevant for image classification?" in Proc. IEEE Conf. Comput. Vis. Pattern Recog., 2011, pp. 1545–1552.

[10]I. Naseem, R. Togneri, and M. Bennamoun, "Robust regression for face recognition," Pattern Recog., vol. 45, pp. 104–118, 2012.

[11] A.M. Martinez, Recognizing imprecisely localized, partially occluded, and expression variant faces from a single sample per class, IEEE Transactions on Pattern Analysis and Machine Intelligence 25 (6) (2002) 748–763.

[12] S. Boyd, N. Parikh, E. Chu, B. Peleato, and J. Eckstein, "Distributed optimization and statistical learning via the alternating direction method of multipliers," Found. Trends Mach. Learn.,vol. 3, no. 1, p. 1122, 2011.

[13] P. Zhao and B. Yu, "On Model Selection Consistency of Lasso," J. Machine Learning Research, no. 7, pp. 2541-2567, 2006.

[14] Y.Xu, X.Z Zhu, Z.M Li, et al. Using the original and 'symmetrical face' training samples to perform representation based two-step face recognition.[J] Pattern Recognition, 46:1151-1158,2013.

Automated setting Eye Diagram for optimization of optical transceiver manufacturing process

Mikhail E. Pazhetnov
Novosibirsk State Technical University (NSTU)
vanifgen@gmail.com

***Abstract* - This article describes how to set up optical transceivers using the Eye Diagram. Uncover the essence of one of the methods for optimizing the production of optical transceivers. The program part, methods used to implement automated configuration, are described. The basic principles of the Eye Diagrams applying to evaluate the correct data transfer in the optical transceiver are shown.**

Keywords - Eye diagram, optical transceiver, FOCL, automated setting.

I. INTRODUCTION

At the current stage of modern society development and modern means of communication, it is impossible to overestimate the growth and development of the Internet technologies. Where there's demand, there's supply. Because of that the various communication lines are rapidly developing and researched, which must meet future requests for data transmission capacity. One of these methods is fiber-optic technology.

Fiber-optic technology implies a way of transmitting information in which electromagnetic radiation of the optical (near infrared) range is used as the information signal carrier, and cables made of optical fiber serve as guide systems.

FOCL has several advantages. Mainly, the fiber optic link has a high transfer rate and a sufficiently high protection against noise, due to the fact that the fiber is made of a dielectric material. Also, a very significant advantage is the security of data transmission. The fact, is that the cable has practically no radio emission, creating an unfavorable environment for attackers, for theft of transmitted data. Unlike a copper cable, to obtain the transmitted information, without penetrating into the channel, is much more labor-intensive. A monitoring system allows you to notify and stop attempts to "hack" the channel. In this regard, the technology of the fiber optic communication line is actively used wherever a secure transmission of data is required.

When using fiber optic technology and organizing an optical connection, optical transceivers. They appear as an electron-optical converter. The technology

of manufacturing optical transceivers is quite complicated. It consists of a large number of stages that follow one another. And, the final result is affected by the success of each of them. Therefore, there is an urgent issue of optimizing the production of optical transceivers. Each enterprise, regardless of the product being produced, aims at exploring those technological solutions that will increase production rates, reduce the amount of waste and costs. As the proposed method, consider the automation of the process of setting up the correct data transfer. It is based on the construction of the Eye Diagram.

II. THE EYE DIAGRAM

The Eye Diagram is a graphical method for evaluating the quality of a digital output electrical signal, which is the sum of all the bit periods of the measured signal superimposed on each other. It is the result of superimposing all possible pulse sequences over a period of time equal to two clock intervals of the linear signal. With its help, you can understand at what level of accuracy data is transmitted over the communication channel. The use of the Eye Diagram is considered to be a rough but fast method of obtaining a sufficiently good estimate of the quality of the received signal.

To confirm the fact of qualitative data transfer, it is analyzed: opening of the eyes (distance from the upper to the lower boundary), average power (intersection), signal-to-noise ratio, mask margin, upper and lower boundaries of the diagram. When analyzing the mask margin, the following approach is used: if the signal lines on the display remain outside the mask boundaries, then the scheme is considered of acceptable quality. The height from the top to the bottom of the Eye Diagram is a measure of noise in signal. As soon as the lines become thicker and shorter, the circuit turns out to be more susceptible to noise and the signal quality can be expected to deteriorate. The width of the signal in the central part of the Eye Diagram is a measure of the accumulated jitter (phase jitter). If the lines are thin then the level of accumulated jitter is small. The wider the line in the center of the Eye Diagram, the greater the jitter level.

The process of analyzing the correct Eye Diagram can be automated. In order to influence the oscilloscope chart, in the optical transceiver itself, the bias, modulation and phase shift readings are changed, which in turn are written in the form of byte sequences. There is a huge number of processors on which optical transceivers are built. Correspondingly each type has its own algorithm for storing and initialize the service information.

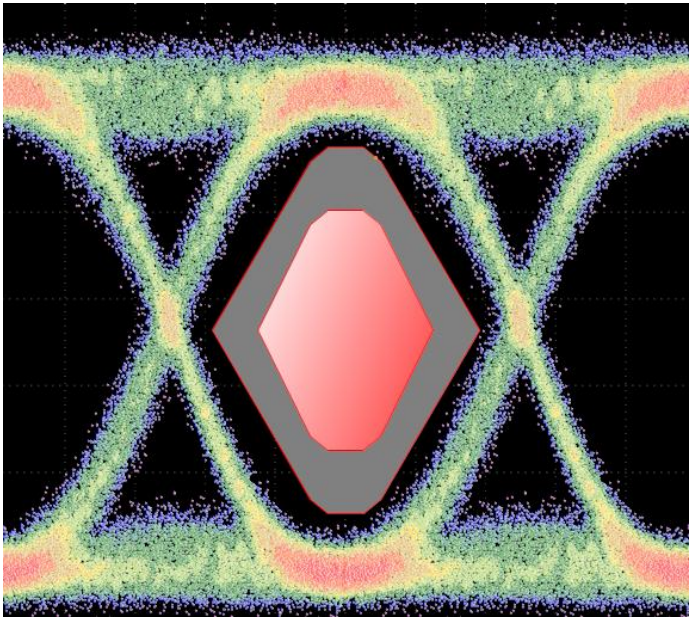

Fig. 1 – Normal Eye diagram

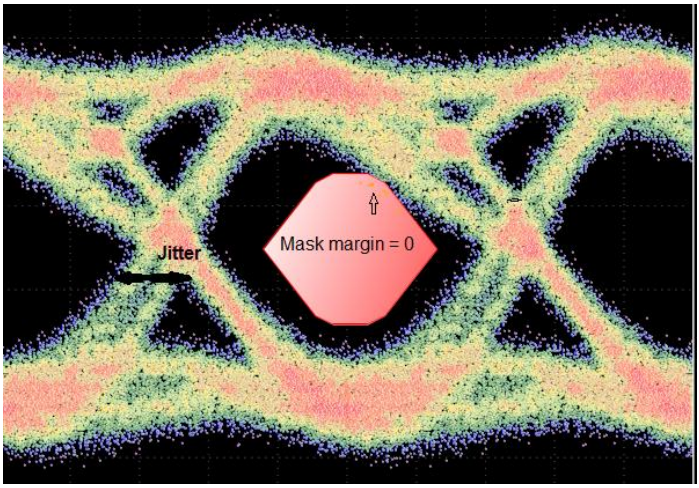

Fig. 2 – Eye Diagram with high level jitter and without mask margin.

III. AUTOMATED SETTINGS OF THE EYE DIAGRAM

The system can be represented as follows: a ready-to-configure optical transceiver is installed in the debug board. The debug board is attached to the oscilloscope, the bit error generator, and to the computer. The developed software part combines:

1) Oscilloscope management.

In the program window, you can configure the oscilloscope operation modes, the frequency of updating the indications, the number of points participating in the drawing of the diagram, and so on.

2) Visual display of the Eye Diagram.

In a separate window, an oscillogram is displayed in the form of a cluster of small dots. The display itself is necessary for visual analysis of the diagram in the case of manual tuning. In addition, the necessary parameters are duplicated in the TextBox. This whole complex helps to prevent accidental program errors.

3) Interface for connecting and setting up the optical transceiver.

Here are the sliders for the visual change of values in the optical transceiver. When the module is initialized on the debug board, the program reads the readings itself, sets the acceptable threshold values and visually displays the Bias and modulation values in the Textbox.

4) Interface of automated mode of eye chart adjustment

To start the automated mode, you only need to enter the desired indications for opening the eye and the level of intersection. By pressing the "Auto" button, the system will start selecting the necessary parameters, which can be observed in the settings panel. Also, to increase the speed of automated setting, the function of changing the error was added. As the error increases, the tuning time increases. With its decrease, the set parameters approach the desired values as much as possible, but the adjustment takes longer.

Adjustment mechanism

In order to use automated setting, enough optimization methods have been considered, such as: PI regulator, PID regulator and so on, but in the course of studying these methods, it was revealed that in order to calculate and predict the necessary parameters for a correct Eye Diagram, it takes time, and also it was not exact but close to the linear dependence of the bios on the level of intersection and modulation to the level of opening of the eye. The most optimal tuning algorithm was the method of binary segments (Bisection method). Firstly, it is easy enough to perform. Secondly, the required speed of adjustment was obtained. Thirdly, almost every optical transceiver, even with the same components, shows a different picture of the Eye Diagrams during the tuning phase, therefore it will not be possible to calculate the coefficients and a priori to specify the parameters.

With reference to this problem, the classical method of bisection looks like this:

Provided that the current value is greater than required:

BL = currentvalue; (1)

X = (RB - currentvalue) / 2 (2)

Provided that the current value is less than required:

BR = currentvalue; (3)

X = (BL - currentvalue) / 2 (4)

Where X is the value:

BL - Left border.

BR - Right border.

The condition for the completion of the algorithm is the comparison of the error and the difference between the actual and the required value.

Error estimation> = | Actual - Required | (5)

IV. EXPERIMENT AND RESULTS

As an experiment, the manual and automated adjustment of eye diagrams was tested. 100 pieces of optical transceivers were selected, 50 of which were manually tuned and 50 were in automated mode. During the experiment it was found, that in manual mode the test time was 45 minutes, and in automated mode, 31 minutes. As a result, productivity increased 1.45 times. This is a significant result, given the production volumes. In addition, automated mode implies only control by the operator, excluding the human factor (tiredness, inattention). The operator just needs to set the correct type of optical transceiver and watch the Eye Diagram change. In the end of the testing phase, the program recalls it with a pop-up window.

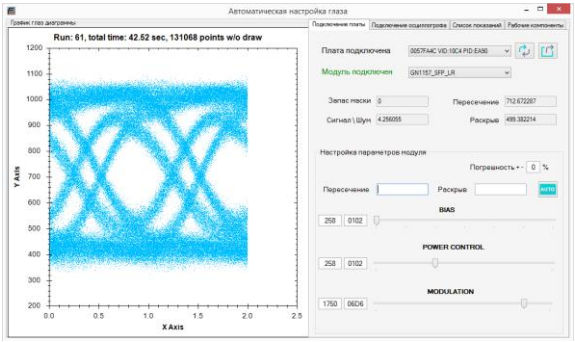

Fig. 3 – Optical transceiver initialization

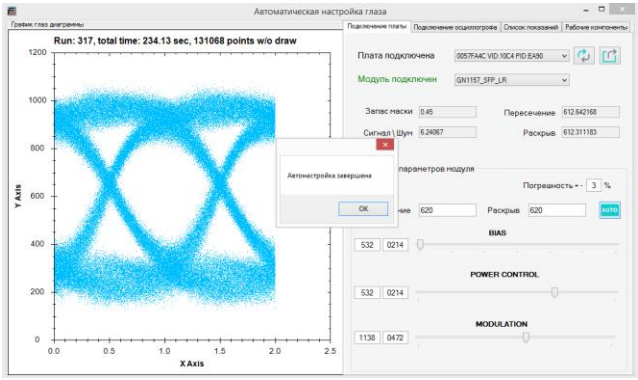

Fig. 4 – Customized Optical transceiver

V. CONCLUSION

Throughout the World, including in Russian Federation, the demand for fiber-optic communication is only increasing. In this connection, the further prospect of development of FOCL technologies in information networks is obvious. Of course, there is a need for research and development of solutions in this area. Accordingly, the topicality of the development of optical systems investigations arises from this.

In order to increase the performance of optical transceivers, the task was to automatize the adjustment of the optical eye. In the course of development, the shell for the oscilloscope API was written and the interface for the initialization and setup of optical transceivers was fully developed. The software part is developed taking into account the addition of new types of optical transceivers and auxiliary devices. In the future, the system will be tested in a longer mode, at the end of which, a verdict will be approved about further refinement or start-up of the system.

REFERENCES

[1] Harbour, Stephen. Soliton Research May Improve Optical Fiber Transmission. – "EuroPhotonics", Oct/Nov, 1998, p. 38-39.

[2] Nakazawa, Masataka. Telecommunications Rides a New Wave. – Photonics Spectra. Feb. 2016, p. 97 104.

[3] Eye diagram analysis. 21.10.2018. / [Electronic resource]. - http://www.mathworks.com/ - Title from screen.

Experience In Implementing Project Training In A Technical University

Alexander.A. Yakimenko

Novosibirsk State Technical University (NSTU)

yakimenko@corp.nstu.ru

Abstract **- The object of research was the technology of project-oriented learning. The aim of the research was to study the experience of project training and evaluate the possibility of introducing technologies of project-oriented learning in the educational process of the NSTU. In conclusion, the features of the organization of project activities in the university are given.**

Keywords **- project training, practice-oriented training, project method, team work**

I. INTRODUCTION

Education systems are called upon to contribute to the realization of the main tasks of the socioeconomic and cultural development of society, for it is the school and the university that prepare the person for active work in various spheres of the economy, culture, and political life of society.

The analysis showed that the problematic situation of modern education is that the teaching technologies have changed little over the past two hundred years. In essence, the teacher of the modern university does the same thing as the university professor of the 19th century: for example, Herbart, who offered a class-lesson system and a specific lesson plan for the lesson.

The Information Society is interested in ensuring that its citizens are able to act independently, take decisions, adapt flexibly to the changing conditions of life:

- Flexibly adapt in changing life situations, independently acquire the necessary knowledge, skillfully applying them in practice to solve a variety of emerging problems, so that throughout life you can find a place in it;
- independently think critically, be able to see the problems arising in real life and seek ways to rationally solve them using modern technologies; clearly understand where and how the knowledge they acquire can be applied in their environment; be able to generate new ideas, think creatively;
- Competently to work with information (be able to collect the facts necessary for solving a certain problem, analyze them, put forward hypotheses for solving problems, make necessary generalizations, compare them with similar or

alternative solutions, establish statistical regularities, draw reasoned conclusions, apply the findings to identify and solve new problems);

- be communicative, contact in various social groups, be able to work together in various fields, in different situations, preventing or skillfully leaving any conflict situations;

- independently work on the development of their own morality, intellect, cultural level.

The above requirements are implemented in the global pedagogical community in the framework of various programs and projects, including the implementation of a competence approach.

II. ITRAINING IN COOPERATION

Training in small groups was used in pedagogy for a long time. It is an important element of the pragmatic approach to education in the philosophy of J. Dewey, his project method, developed principles and methods of problem-based learning [1]. According to him, these methods have undeniable advantages compared to explanatory-illustrative. The problem situations created during the educational process can reveal the inadequacy of the knowledge previously learned by the students, which encourages them to search, promotes the formation of cognitive independence, development of critical thinking and creative abilities.

A. Syndicate method

Provides that a large group of students (usually a whole course) is divided into subgroups of 4-6 people. These groups work during the seminar, performing certain collective tasks. After some time, the course is going together to discuss the results of the subgroup work [2].

B. Grouping

The group can be divided into separate individual tasks. Group work can take part of the seminar, the whole seminar or even several lessons in a row. Each subgroup is then divided with the whole group by the results of its work. Unlike the syndicate method, the main work unit here is the whole seminar group, the subgroups are organized only if necessary. The function of the teacher is to summarize, give necessary explanations, introduce and explain new tasks [3].

C. Division of lessons

The whole seminar group spends half the time with the teacher, half without it. During the meetings with the teacher, the work the group has done on its own is discussed, and the next self-study is planned.

D. Interconnections of participants in project training

In the described approaches, we can distinguish three types of interdependence of participants in joint training:

1. Dependence on a single goal, which is realized by the students and which they can achieve only through joint efforts.

2. Dependence on information sources, when each student of the group owns only a part of the general information or a source of information that is necessary to solve the overall task; everyone must contribute to the solution of the common task. This dependence can be at the level of the division of labor, role functions, training material (tools, equipment), divided between the students of the group (for example, one scissors, one sheet of paper, one paint, etc.).

3. Dependence on the form of encouragement. Each student receives the same grade for the work. Either all are encouraged the same way, or are not encouraged in any way.

III. PROJECT TRAINING (PROJECT METHOD)

• The educational process is built not in the logic of the academic subject, but in the logic of activity that has a personal meaning for the trainee, which increases its motivation in the teaching;

• The solution of a specific problem of the surrounding reality is placed at the center of the process of creating an educational project;

• The teacher is only the guiding link in the activity, the process of creating the educational project is focused on the independent activity of the trainees;

• The trainee becomes the subject of the education process, sets goals and selects information, determines its necessity, based on the design of its project;

• An integrated approach to the development of educational projects promotes the development of general educational, communicative and research skills;

• The individual pace of work on the educational project ensures the exit of each student to their level of development;

• A deep, conscious assimilation of basic knowledge is ensured through the universal use of them in different situations.

The purpose of project training is to create the conditions under which students: 1) independently acquire new knowledge from different sources; 2) learn to use the acquired knowledge to solve cognitive and practical problems; 3) acquire communication skills, working in groups; 4) develop their research skills (the ability to identify problems, collect information, observe, conduct experiments, analyze, construct hypotheses, generalize, etc.) and system thinking.

At the heart of the project method is the development of cognitive skills of students, the ability to independently design their knowledge, skills to navigate in the information space, the development of critical thinking.

The method of projects is always focused on the independent activity of students - individual, pair, group, which students perform for a certain period of time. This approach is organically combined with a cooperative learning approach to learning. The method of projects always involves the solution of a problem that involves, on the one hand, the use of various methods and means of instruction, and on the other, the integration of knowledge and skills from various fields of science, technology, technology, and creative fields. The results of the completed projects should be, as they say, "tangible," ie, if this is a theoretical problem, then its concrete solution, if practical, concrete result, ready for implementation [4].

IV. BASIC REQUIREMENTS FOR USING THE PROJECT METHOD

1. The existence of a significant / research / creative problem / problem requiring an integrated knowledge, research search for its solution.

2. Practical, theoretical, cognitive significance of the expected results (for example, a report, a joint article, product registration or patenting ... etc.)

3. Independent (individual, pair, group) activities of students.

4. Structuring the substantive part of the project (indicating step-by-step results).

Use of research methods:

- the definition of the problem, the research problems arising from it,
- the hypothesis of their solution,
- discussion of research methods,
- formalization of the final results,
- analysis of the data obtained,
- summarizing,
- adjustment,
- Conclusions (use of the method of "brainstorm", "round table", statistical methods, creative reports, views, etc.).

Experience shows that joint projects based on cooperation between students from different faculties, universities, cities and countries are most effective.

TABLE I. Stages of project activities and the interaction of the teacher and student on them [5]

The stage of the project activity	The tasks of the stage	The activity of the teacher	Activity of the student
1. The Trust	Definition of objectives, selection of working groups	Determination of the subject of research, motivation of educational and professional activities, assistance in setting the goals of the training project	Discussion of the subject of the study and obtaining additional information if necessary, setting research objectives
2. Analytical	Analysis of the problem, identification of sources of information, statement of tasks, distribution of roles in the team	Statements about the choice of sources, ways of collecting and analyzing information, correction of tasks assigned to trainees, definition of roles in accordance with the selected components of the initial problem	Formulation of research tasks, identification of information sources
3. Research	Solving individual problems	Submission of specially selected materials to each participant of the project, consultations, coordination of the trainees' work, monitoring of the progress of the performed work, motivation for and stimulation of activities through rewards	Drawing up an action plan, information gathering, practical implementation of selected roles, execution of relevant functions
4. Constructional	Analysis of the degree of achievement of each task, collection, design of the project	Identification of shortcomings, provision of advice on their elimination, consulting on preparation of accompanying project documentation	Analysis of the information received, a combination of ideas, their generalization, the promotion of a common idea
5. Presentation	Presentation of the educational project	Organization of expertise	Public protection of the educational project
6. Reflective-evaluative	Evaluation of the results of the training project and the process of its implementation	Synthesis of reviews and feedback from the expert commission, a prognostic assessment of the organization of the implementation process	Reflection of the project implementation process, self-assessment in the framework of the project activity, prompting to acquire new knowledge

V. LIMITATIONS ON THE USE OF THE PROJECT TRAINING

The project method has its limitations, which must be taken into account when planning its activities in the technology of project-oriented learning:

• low motivation of students to participate in the project;

• Inadequate level of formation in the students of research skills;

• impossibility to acquire professional and training skills in the course of project activities;

• The difficulty in determining the criteria for evaluating the results of the project activity.

VI. CONCLUSIONS

One of the main features of modern educational programs in the areas of engineering education is the need to develop decision-making skills, their rationale and ensure organizational and instrumental support. This is due at least to two factors. First, most engineers sooner or later become managers (linear, middle or senior) and, consequently, are forced to make managerial decisions, and secondly, engineering itself involves the adoption of numerous technical and technological solutions (designing the best engine design, choosing the optimal sequence processing task flows and the optimal mode of operation of power plants and many others).

The logic of modern innovative programs of engineering education predetermines not only the inclusion of a block of courses related to effective management (strategic and operational production management, project management, innovative management, etc.), but also the use of active teaching methods, including problem and project technologies learning.

Educational programs of engineering education are characterized by:

- a large number of laboratory works performed, as a rule, by groups of students, which can be regarded as a prototype of the project,

- a large number of course projects and calculation and graphic works,

- the practical focus of most of the diploma projects being carried out,

- the presence of social partners - organizations interested in the results of research and development projects of the technical university, in which students take an active part,

- a significant "rejuvenation" of some engineering specialties, when there is a situation in which the student often starts on the third year of the labor market more in demand than his teachers [6].

REFERENCES

[1]. Beane W. E., Lemke E. A. Group variables influencing the transfer of conceptual behavior // J. Educat. Psychol. 1971. V. 62(3). P. 215—218.

[2]. Hänsel D. Handbuch Projektunterricht. Weinheim 1997.

[3]. Hudgins B. Effects of group experience on individual problem solving // J. Educat. Psychol. 1960. V. 51(1). P. 37—42.

[4]. Atanov G.A. Activity approach in training. - Donetsk: "EAI-press", 2001. - 160 with.

[5]. Gafurova N.V. Integral model of the intellectual-personal development of students in the education system / Gafurova N. V .. - M .: MAKS Press, 2004.- 219 p.

[6]. Romanov E. L. Teaching software engineering. A look from the code [Electronic resource] / EL Romanov, GV Troshina, AA Yakimenko // Science: Internet magazine: electron. journal. - 2016. - Volume 8, No. 5. - Access mode: http://naukovedenie.ru/PDF/66TVN516.pdf (access is free). Ver. from the screen. - Ver. from the screen.

Challenges of learning analytics and the current situation

Battsetseg Ts[1], Munkhchimeg B[2], Bolor Lkh[3]

[1,2,3]*Mongolian University of Science and Technology (MUST)*

battsetseg_ts@must.edu.mn [1], munkhchimeg@must.edu.mn [2], bolor_lk@must.edu.mn [3]

Abstract **- An essential part of the activities of educational institutions and universities is the selection and development of the learning management system (LMS) thus there is created an experience in developing a variety of methodologies to guide the research work collecting and processing of large amounts of data and and reporting organizational data for decision making. The learning management system data can not be very substantial for decision making, concerned with processing data which is created in the learning environment, evaluating the learning quality and contents, improving study program. Evaluation of the learning system varies greatly depending on each country's growth level, the characteristics of the educational system, and the university's curriculum.**

Keywords **- learning analytics, learning management system data, data mining, WEKA**

I. INTRODUCTION

Since introducing of the learning management system in the university activities, the biggest challenge that universities are facing is the immense and quick growth of the educational data. In many research works were reflected on implementation learning analytics such as to identify the factors which influence the learning quality, to predicate students' performance and analyse its impact parameters, to evaluate study program, contents, quizzes, exams, and educator`s activity through processing data.

Many universities around the world take into account different factors that influence student`s learning performance, but it is not inadequate to make a conclusion using commonly used factors.

It's proved that various factors such as previous learning background, general admission score, governance, age, parents education level, where graduate high school, major and GPA affect to students` learning performance and all of these factors are used to predict students' performance.

It is important to form log data of learning process or traceability for collecting the necessary data evaluating learning activity. Factors, influencing to the student`s learning performance have internal and external characteristics. It is important to define students' learning style and to create effective learning environment by using suitable learning activities for reducing side effect of unsuccessful learning such as drop out, students at risk. There has been used main conclusion in around 600 researches in last 10 years to develop LMS, to process, to mine learning environment data and to analyse learning factors.

II. RESEARCH PURPOSE

[1] To introduce research work Learning Analytics.

[2] To determine required data for development LMS which can provide effective data to make decision, to improve university learning quality.

[3]To introduce learning analytics tool.

III. RELATED WORK

1. To determine appropriate method by comparing data mining methods for processing learning environment data

2. To determine precision evaluation using methodology prediction students learning performance

3. To analyse affecting learning factor

4. Research works of learning analytics, implementation experience of learning analytics, research report of data processing gathered for long time of period

5. Educational data mining, learning factor analyse, role of LMS for EDM, mathematic model and theories of learning analytics are dominant research field for USA researchers

Several core of problems was decided by research work on this field during development of LMS are: usage of LMS function for learning activity, to establish learning enviroment available online learning tools, to implement face to face learning methodology in online learning environment, to accomplish flexible learning such as collaboration, cooperative, interactivity, to built up most suitable way to distribute learning content, to choice and use LMS optimally.

The selection of top learning management systems and introduce of results contributes to the implementation and development of training systems educational institutions and universities. However, the evaluation of the learning management system varies greatly depending on the level of development, nationality, features of education system, and university education policy.

IV. DATA ANALYSIS

In research works of learning analytics were used more than 50 factors such as previous learning background, general admission score, demographic details, social status etc and the impact parameters were different for each country.

A. Types of data

Large amounts of data are gathered in universities for helping improve the learning quality and activities.

Table 1. illustrates the types of available data in the LMS. The first column includes data that is regularly produced by LMS. The second column is an illustration of the types of data that is provided by the educator that can be stored in the LMS.

TABLE I. Types of data available for Learning analytics

Data generated by LMS	**Data generated by Instructor**
Number of times spend	Grades on exchange forum
Date and time of access	Assignment marks
Number of discussion posts generated	Grades on tests
Number of discussion posts read	Final grades
Types of resource accessed	Questions asked in discussion forum
	E-mails notification ot/for instructor attendance

B. Data attributes

The type of data is classified according to the field's properties. It is basically divided into numerical (quantitative) and categorical (qualitative). Numerical data has significance as numbers, and order, distance and equality of two numerical variables. In opposition, categorical data has no meaning as figures only correspondence within two definite variables.

Numeric data is organized as discrete or continuous. Discrete data countably many values, and if the domain is portrayed on the number line, it

consists only of isolated cases. Discrete numbers are not always integers as it can be decimal numbers with a predefined precision. The categorical variables can be further classified as nominal or ordinal. The nominal values are only named for sections and have no other meaning than classifying.The purpose of the research work is to analyze the large unprocessed data generated in the learning environment and to produce effective data.

Learning activity analysis is aimed to gather the data and analyse them. Data mining is concerned with the implementation automation tools identifying of big data trends which is created in learning process and developing its activity.

By implementing the theory and methodology of learning process analysis educators and instructors process data creating in the learning environment and to find more optimal decision, to manage learners successfully, to implement strategy improving quality in this way can be created the free space to reach more efficient result.

The important tool will be created to evaluate the learning process and to make the decision by collecting and processing effective and qualitative data in LMS. Therefore, within the framework of the research work, the type of data is defined and by processing these data it can help to evaluate students` performance and to identify factors affecting learning quality (Figure 1).

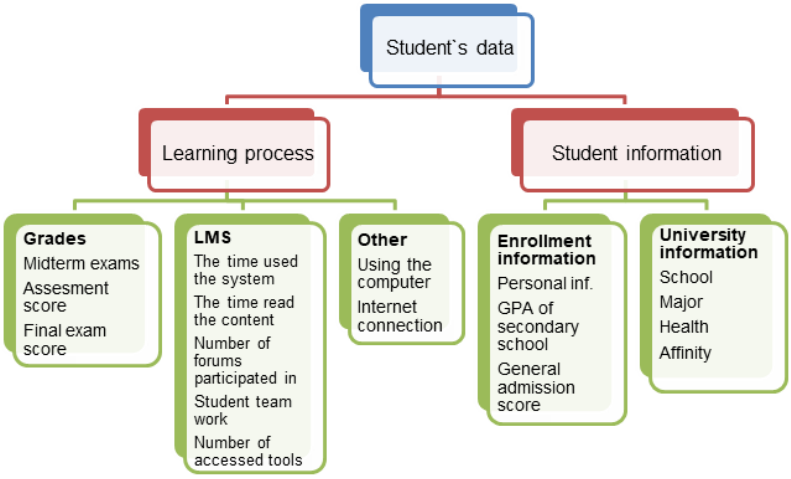

Fig. 1. Data types collecting in LMS

Learning activity analysis and data mining etc essential terms are very common and differ in their use and study and research field. It is the theoretical concept covering the machine learning, artificial intelligence, estimation methods,

recycling data and data visualization techniques. Research works is linked inseparable with methodology data mining, smart system and personalized learning.

There is a growing need for data collection in education and the use of data mining tools. This emerging trend is named as a data mining in the learning environment (educational data mining) and is being developed as a research study to use big data processing techniques. One of the main problem deciding by data mining methods is to create the methodology predicting students' performance.

Educational data mining consider on detecting algorithm of the data style and developing new procedure. Data analysis of the learning environment consider how to adopt above methodology in the learning activity.

It is considered that one of the ratio students' performance and admission operations is the success continue of learners.

The methodology of predicting students' performance is detected unsuccessful learning and it is important to develop a decision-making system to improve the learning quality and data mining is used for this purpose.

V. PREPROCESSING OF DATA

There has compared and analysed in student assessments who has studied Mathematic, Physic and Information technology-1 in the Unimis learning system from 2014 to 2017.

1. The original data was 37044, therefrom after deleted 8177 data which is concerned with 872 duplicated data for change profession or study dual profession, 1109 retrained data, 3538 Withdrawal (W), 2658 Exam incomplete by the student (E) and 2658 Repeating a course (R) 28177 data left (Table 2).

TABLE II. Lesson evaluation data

Lesson	Row data	1	2	3	4	5	6	7	Total (1-5)	NET TOTAL
		Duplicated	Retrained	W	E	no pass exam R	passed exam R	F		
U.IT101	7689	750	77	903	700	115	103	386	2545	5144
S.PH101	13000	122	510	1200	881	107	173	1272	2820	10180
S.MT101	16355	0	522	1435	1077	163	153	1457	3197	13158

2. After deleted all null data which is concerned with mathematics entrance exam, teacher's score, midterm exams etc 17674 data left (Table 3).

TABLE III. Percentage of adequate data

Fields	U.IT101	S.PH101	S.MT101
UNIMIS row data	7689	13000	16355
Midterms, teacher score, exam score, general admission score of mathematics	3591	6430	7653
Data persentage meet the requirements of analysis	47%	49%	47%

3. There are not deleted null data from the Teacher code and Entrance location.

4. It has done first step to analyse for learning evaluation that general admission score, total score, exam score, teacher score, student code, student name, school and profession etc (Figure 2).

Shown by chart which is distribution of students evaluation of performanced students of selected lesson. In research work highlighted about it can concluded that mentioned lessons have standard distribution. But it is impossible to determine factors that evaluation affect, improvement and renewment for details list of teacher's score.

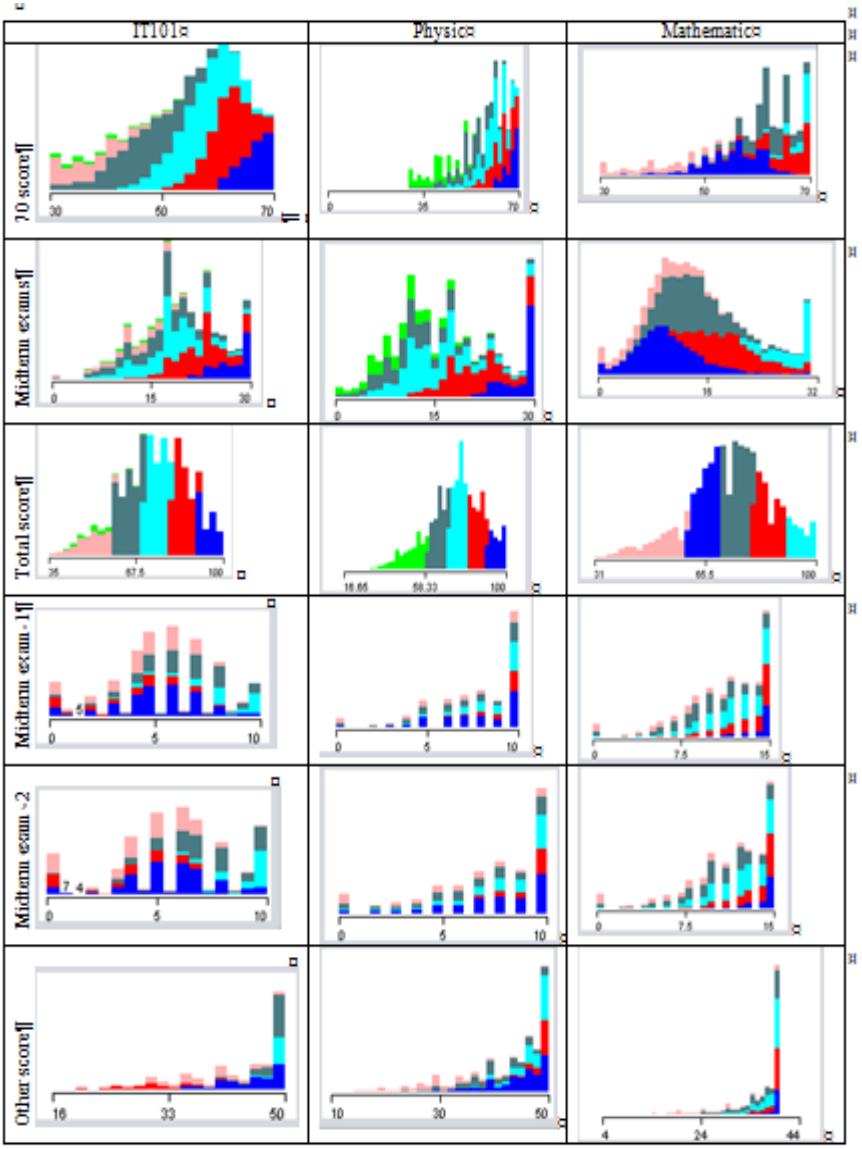

Fig.2. Compared analysis of assesment of 3 subjects from UNIMIS

V. WEKA TOOL

Weka is a graphical user interface tool that includes algorithms for data analysis and predictive modeling, and data visualation methods. It is now used in many different application areas, in particular for educational purposes and research. Weka provides a number of methodologies of extraction of data, such as preprocessing, classification, clustering, associations, and visualization.

There is shown students` assessments who has studied Information technology-1 (Figure 3). In figure 1 was shown type of data generated by data collecting and storing necessary for the decision making and here fewer data types were selected and analyzed. It is a graphical way of preparing data to process the Weka program.

Fig.3. Data visualation of student assesment for IT-1 last 4 years in Weka

VI. CONCLUSION

Analysing learning activity log data which is gathered by using various type of learning content through LMS is making requirement to develop decision support system. This type of data analysis helps to identify students 'learning styles and develop a suitable training strategy to differentiate students' progress so that

flexibility can be followed by the fact that students in one group have different levels of knowledge and skills.

Although the academic result analysis by final exam and course evaluation curve is the first performance in UNIMIS (University Management Information System) of Mongolian University of Science and Technology (MUST), different methodology of teachers' assessment negative impact on the end result of this work.

The following conclusions are being made from experimental work on the disaggregated assessment of students' knowledge assessment.

1. The student`s duplicate data arise when the student changes his or her profession or studies double major.

2. There is a need to monitor the accuracy and reality of the data collected in the system. It was difficult to analyze data which entered into the field of data teacher's score, two mid term exam scores (maximum score is 50 points) are exceeding the limit.

3. 70/30 score analysis is not enough to assess the effectiveness of the lesson, and it is important to decide the data type is inadequate to determine the factors that influence the failure of the W evaluation analysis to do.

4. The differences in the methodology of academic affairs of the various universities (MUST has 8 branch universities) are evident from the R values. Therefore it is necessary to provide training for the employees of academic affairs.

5. There is a need to evaluate same methodology, to unify difference teachers' assessment of W.

6. Evaluation of student knowledge should be different for each subject, but it is necessary to improve the methodology of analyzing the dependency of parameters such as progress tests and other points. Using the learning system to track student learning processes and to collect log data activities, it is best to identify attitudes of teachers and learners, provide accuracy of estimation the learner.

7. Improving the learning quality in universities can be solve by assessment students 'academic performance, teacher and student participation, monitoring progress, gathering data required to evaluate teachers' attendance and development of evaluation methods using of learning management system functions.

REFERENCES

[1]. Claris Kerlyn Ke Yue'e, "Design and Development of a Learning Analytics Toolkit" School of Computing Science University of Glasgow.

[2]. Saurabh Pal Head, "Mining Educational Data to Reduce Dropout Rates of Engineering Students", I.J. Information Engineering and Electronic Business, 2012, 2, 1-7

[3] Ajay Kumar Pal, “Analysis and Mining of Educational Data for Predicting the Performance of Students” International Journal of Electronics Communication and Computer Engineering Volume 4, Issue 5, ISSN (Online): 2249–071X, ISSN (Print): 2278–4209

[4] Billy Tak Ming Wong, “Learning analytics in higher education: an analysis of case studies” Asian Association of Open Universities Journal

[5] С.Байгалтөгс, Б.Мөнхчимэг “Сургалтын удирдлага мэдээллийн систем ашиглан оюутны суралцах явцыг хянах боломж” Цахим засаглал, мэдээллийн технологи. Монголын мэдээллийн технологи ММТ 2013.

[6] B.Munkhchimeg, S.Baigaltugs “Analysis of Developing Proper Design of Learning Management System” Монголын мэдээллийн технологи ММТ 2014

[7] Sunita B Aher , Mr. LOBO L.M.R.J. “Data Mining in Educational System using WEKA” International Conference on Emerging Technology Trends (ICETT) 2011.

Containing Hybrid Worm in Mobile Internet with Feedback Control

Hailu Yang[1], Deyun Chen[2], Guanglu Sun[3]
[1,2,3] *Harbin University of Science and Technology (HUST)*
[1]*yanghailu@qq.com.* [2]*chendeyun@hrbust.edu.cn*,[3]*guanglu_sun@163.com*

***Abstract*—As hybrid worm can be propagated by both personal social interactions and wireless communication services, it has been identified as one of the most serious threats to mobile Internet. This problem is expected to become worse with the boom of social applications and mobile service. In this work, we study the propagation dynamics of hybrid worm, and propose a systematic countermeasure. Our approach utilize the user's social relationship as principal part and the device's interaction history as feedback. Through Extensive real-trace driven simulation results have proved that the method proposed by this paper has feasibility and effectiveness.**

Keywords—mobile Internet, hybrid worm, propagation model, containment system

I. INTRODUCTION

Mobile Internet, one of the core technologies to build smart city, makes urban life more convenient by using Smartphone-based information and communication technology. In mobile network, popular social services such as Facebook, Twitter, and Wechat have attracted billions of users worldwide, many of whom have integrated those services into their work and family life. On the bright side, mobile Internet provides ideal places for people to keep in touch with friends and socialize online. On the other side, however, it also fertile grounds for the rapid propagation of malicious worm.

The spreading of malicious worms in mobile Internet is aided by two dominant communication protocols [1]. First, a short-range worm can infect all Bluetooth or Wi-Fi activated devices within the infection radius resulting in a spatially localized spreading pattern similar to the one observed in the case of contact-based diseases. Such kinds of infection rely on peer-to-peer communication between proximity individuals in Geographical Information Network (short for GIN). Second, a long-range worm can send a copy of itself to all mobile phones whose numbers are found in the infected phone's contact book, a delocalized

spreading pattern based on social relations in Social Information Network (short for SIN).

GIN worm can exploit hardware vulnerabilities of the mobile device to crash them. Defending against this kind of worm will be challenging due to the lack of centralized regulation. On this account, most of the existing methods utilize a distributed coping scheme which allows nodes to limit communications towards vulnerable devices to insulate the proximity worm [2, 3]. SIN worm is similar to the one observed in Multimedia Messaging Service (MMS), both of which exhibited the characteristics of slow start and exponential propagation [4]. Recent works mostly utilize a partitioning strategy to insulate SIN worm in several disjoint islands [5, 6], while these partitions do not always reflect the natural network community structure, and the worm still have chance to propagate widely.

With the increasing number of mobile devices and services, the worm propagation is not confined to a single way. The hybrid worm propagates by using social services as well as device's interface. The first variant worm that utilizes hybrid propagation mechanism is Commwarrior which spreads from one phone to another via Bluetooth and MMS. Such synergetic infection mechanism will promote the infection speed of worm and bring huge challenge to worm containment. Obviously, the communication patterns of SIN and GIN needs to be tracked simultaneously so as to prevent hybrid worm from spreading out to a large population.

In this paper, we present a novel coping scheme to tackle the problem of hybrid worm containment. To summarize, our contributions are as follows:

- We model and analyze the propagation dynamics of hybrid worm in mobile Internet.
- we exploit a new granularity of security, which is based on the community structure, to guide the design of the scheme.
- we develop a trust evaluation scheme to link node's contact histories with future predictions.

Due to space limitations, we will only give a brief description of the system components in the text.

II. SPREADING MODEL OF HYBRID WORM

The model is originated from the susceptible infected recovered (SIR) model in epidemic theory [7] to measure propagation of infections within a population under risk. In the general deterministic SIR model, $S(t)$, $I(t)$, and $R(t)$ denote the number of susceptible, infected, and recovered (or immunized) individuals at time *t*, respectively. Denote function $J(t) = I(t) + R(t)$ as the number

of infected individuals includes immune. If β denotes the infection rate and γ denotes the recover rate of infected individuals, N denotes the total number of individuals, then the basic differential equations of SIR model are given by

$$\begin{cases} \dfrac{\mathrm{d}J(t)}{\mathrm{d}t} = \beta J(t)[N - J(t)]; \\ J(t) = N - S(t); \\ \dfrac{\mathrm{d}R(t)}{\mathrm{d}t} = \gamma I(t). \end{cases} \tag{1}$$

For mobile network, we assume that all of the interactions between devices stem from SIN and GIN. Denote function $I(t) = I_{\mathrm{SIN}}(t) + I_{\mathrm{GIN}}(t)$ as the total number of infected devices at time t, where $I_{\mathrm{SIN}}(t)$ and $I_{\mathrm{GIN}}(t)$ are those that have been infected via SIN and GIN at time t, respectively. Then, we have

$$\frac{\mathrm{d}I(t)}{\mathrm{d}t} = \frac{\mathrm{d}I_{\mathrm{SIN}}(t)}{\mathrm{d}t} + \frac{\mathrm{d}I_{\mathrm{GIN}}(t)}{\mathrm{d}t} \tag{2}$$

Fig.1 demonstrates the hybrid spreading behavior of mobile internet worm.

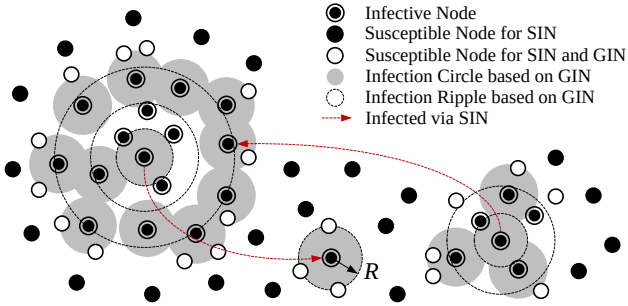

Fig.1. Propagation dynamics of mobile Internet worm.

A.Spreading Dynamics of SIN Worm

When an infected node tries to spread worm via SIN, it behaves like traditional SMS virus seen in the Instance Messaging. To IM worms, an online address book

provides an instant *hit-list* – a list of users vulnerable to the worm from an infected host.

If β_{SIN} represents the probability that a susceptible node becomes infected in SIN after receiving a worm (i.e. worm being activate), η_{SIN} represents the average degree of nodes in SIN, the total number of susceptible nodes is thus given by

$$S'(t) = S(t)\frac{\eta_{\text{SIN}}\beta_{\text{SIN}}}{N} I(t) \tag{3}$$

and the dynamics of infected nodes by SIN with time is

$$\frac{\mathrm{d}I_{\text{SIN}}(t)}{\mathrm{d}t} = \beta^2{}_{\text{SIN}}\frac{\eta_{\text{SIN}}S(t)}{N} I^2(t) - \gamma' I(t) \tag{4}$$

Where γ' represent the recovery rate of mobile device by means of sending patches.

B.Spreading Dynamics of GIN Worm

When an infected node intends to spread worm via GIN, it first scans to search the nearby nodes within its transmission range *R*. We assume that the mobile devices is distributed uniformly and stationary with node density ρ. Let $F'(t)$ and $F(t)$ respectively represent the number of nodes lie on and lie within the periphery of the ripple, then the infected dynamics of the periphery nodes with the incremental infected radius $r(t)$ is given by

$$F'(t) = F(t) - \rho\pi(r(t) - R)^2 \tag{5}$$

$F(t) = \rho\pi r^2(t)$ based on the fact that the number of nodes inside infection ripple is the sum of neighbors of each center node. Thus, equation 5 can be simplified into the following.

$$F'(t) = 2R\sqrt{\rho\pi}\sqrt{F(t)} - \eta_{\text{GIN}} \tag{6}$$

Without loss of generality, we assume that a single infection ripple is generated at time *a* by a point source infected through SIN, and kept stretching for *b*

time units to achieve the current infection status $F(a+b)$. Then the incremental spatial infection at time $a+b$ is:

$$F'(a,b)=\frac{\left(2R\sqrt{\rho\pi}\sqrt{F(a,b)}-\eta_{\mathrm{GIN}}\right)^2}{2N/\beta_{\mathrm{GIN}}\eta_{\mathrm{GIN}}}S(a+b) \quad (7)$$

The incremental infection at time *t* of all infection ripples is thus given by:

$$\frac{\mathrm{d}I_{\mathrm{GIN}}(t)}{\mathrm{d}t}=\int_0^t I'_{\mathrm{SIN}}(\tau)F'(\tau,t-\tau)\mathrm{d}\tau \quad (8)$$

It means that the spatial infection of worm are, in fact, dominated by I_{SIN}. In other words, there are $I'_{\mathrm{SIN}}(\tau)$ infected individuals emerged at time τ, and each approximately contributes $F'(\tau,t-\tau)$ incremental spatial infection at time *t*.

Fig. 2 illustrates the propagation dynamics of a hybrid worm spreading via only SIN and only GIN. We consider the node density $\rho_{\mathrm{GIN}}=0.75$, the activated probability of worm $\beta_{\mathrm{SIN}}=\beta_{\mathrm{GIN}}=0.1$, average node degree $\eta_{\mathrm{GIN}}=\eta_{\mathrm{SIN}}=6$.

It shows that, the propagation via only GIN is relatively slow compared with that via only SIN due to spatial spreading phenomenon, while hybrid worm with fastest propagation speed thanks to the synergetic spreading characteristics.

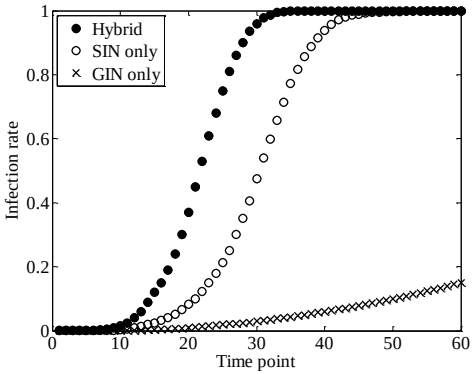

Fig.2. Propagation dynamics of mobile Internet worm

III. CONTAINMENT SCHEME

The problem of detecting worm on mobile internet is extremely challenging, since the propagation dynamics of mobile internet worm behaves like user's habits (these worms search through a user's local address book and recent call records for phone numbers). This requires the containment system is automatically and online since the worm spread so fast that overcome people's response time.

A closer look to the differential equations of hybrid worm reveals that some key parameter dominates the spreading speed of worm. More specifically, we analyze the point of penetration of SIN and GIN worm as following.

A.Containing scheme of SIN worm

Due to the information from an acquaintance has higher possibility to be opened and further activated, the infection rate β_{SIN} in equation 5 is approximately equals 1. We don't expect recover rate γ' to be increased, as the mobile operator will consume much time in detecting worm and coding patches. Thus, in such a situation, a proper scheme to reduce the speed of SIN worm is to decrease the average degree η_{SIN}.

We propose a novel method for worm containment basing on community detection [8] in SIN. The reasons are threefold:

- People tend to trust messages from their friends, which implies that worms propagate within a single community would be much faster than between communities.
- Community is used to represent a group of nodes in a network where nodes inside the community have more internal connections than external connections. As a result, there is a low probability for a worm to spread across two communities.
- Closer nodes are more likely to infect each other quickly as soon as the worm outbreaks. We cannot do too much about it as the infection may have already happened before patching so we prefer leaving them in the same partition.

Therefore, an appropriate reaction should first contain worms into only infected communities, and then prevent them from getting outside. Once the community structure is identified, a worm signature distribution procedure will select the most influential nodes from different communities for sending signatures. These nodes, as soon as they receive signatures, will apply them immune to the worm and then redistribute them to all friends in their communities. These actions will restrict worm propagation to only some communities of the network and prevent it from spreading out to a larger population.

B. Containing scheme of GIN worm

The key parameter that dominates the propagation speed of GIN worm in equation 7 and 8 is β_{GIN} and η_{GIN}. Compared with the delocalized pattern of SIN, η_{GIN} denotes the average number of mobile devices within the infection circle. This parameter is hard to change, as the mobility of people in a certain area is often limited in reality when worm outbreaks. Therefore, we intend to reduce the activated probability β_{GIN}.

Our proposal is to evaluate the credibility of nodes in GIN, based on which rejects communication with low credible ones. Three key factors dominate the trust level of GIN nodes.

Geographical location. Susceptible nodes that far away from the infected host (i.e. beyond the range of localized propagation) propagate worm only by SIN.

History security performances. This feature reflects the security awareness of users. Some mobile device frequently infected by virus and consequently unsafely. It implies that communication comes from such devices has a bigger treat level.

Equipment interaction frequency. Users frequently transfer files by using interface such as Bluetooth has higher threat when worm outbreaks. Worm can spread easily to mobile device pairing with the infection equipment since such devices possess a long accessible communication mode.

A Bayesian-based credibility evaluation method is proposed by synthesizes these three factors. The results will guide the nodes in making future communication decisions. On this basis the infection speed will reduce when worm outbreaks in the network.

C.Hybrid worm containment

Previous discussions separately analyze some feasible scheme of containing SIN and GIN worm. In reality, however, worm outbreaks based on the two routes of propagation at the same time. To solve this, we design a bidirectional feedback system for hybrid worm containment in mobile internet.

As shown in Fig. 3, on the bottom, the system starts with identifying online communities in SIN. Next, a set of guard nodes from each community of the network is selected in order to achieve community quarantine. The guard nodes of a community are ones interact actively not only within their communities but also with people outside, thus, they can easily infect (or be infected by) people both inside and outside of their communities. Obviously, if a guard node receives the worm signature before it being infected, it will become immune to the worm. As a result, the worm propagation can be blocked since an infected node inside its

community has to go through guard nodes to reach other community. The guard nodes, on the other point of view, are the best candidates for the network defender to distribute patches since they can easily forward patches to other members of the network when worm outbreaks. On this account, the forwarding (i.e. delivering worm signature and patches) through guard nodes are collectively called patching in what follows.

Once the worm has detection, the system starts generating the worm signature and delivers it to the guard nodes through Worm Signature Propagation Unit. These guard nodes could be responsible for forwarding the patches to other nodes in the same community so that the uninfected devices can be protected.

The input parameter of Trust Assessment Unit comes from Information Collection Unit. In this unit, GPS information and link frequency are provided by mobile operator, and the history security record is committed by SIN Containment Unit. More specifically, we use a to represents the total number of observed normal communications, and b to represents the total number of observed infections from worm. These parameters are integrated in Trust Assessment Unit to evaluate the credibility of nodes comprehensively.

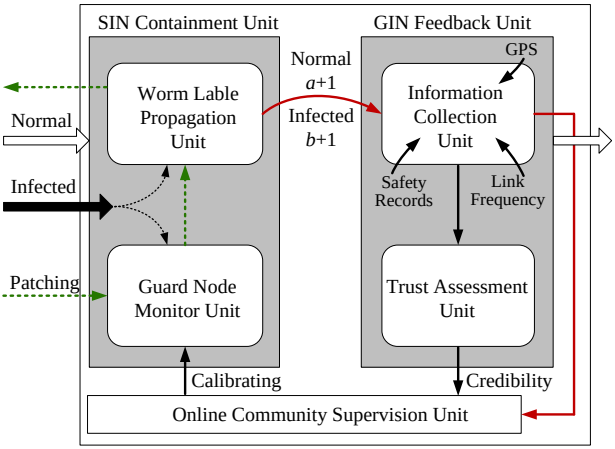

Fig. 3. Hybrid worm containment system

IV. EXPERIMENTAL RESULTS

In this section, we present the experimental results of our method on two different kinds of real-world traces including the MIT Reality [9] and the Haggle

Project [10]. We evaluate and compare our method with other worm coping scheme including:

- A distribute local detection based scheme *[3]*.
- A proximity signature forwarding based scheme *[3]*.
- A community-based proximity malware coping scheme *[6] (*Centralized for short*)*.
- A social network based patching scheme *[11] (*Socializing for short*)*.

The first two methods major focus on GIN worm containment, while the latter two with the purpose of containing the propagation of worm on SIN. We keep the relevant parameters as well as the original literature setting for comparison convenience.

A.Simulation Setup

We primarily focus on two parameters: 1) *Infection ratio*: this parameter is reflected in the proportion of nodes infected by worm; and 2) *Percentage of patched nodes*: the patch contains the worm signature, and the parameter is defined as the average number of signature forwarded in the mobile network.

The worm propagation model in our experiments was proposed in section II. In our model, SIN worms are able to explore their friend list and then send out fake messages containing worm for propagating. In GIN, the worm scans the proximity devices and tries to setup a connection and propagate with the highest priority to the nearest one. The probability of an infected individual's friend activating the worm is proportional to interaction frequency between the individual and his friends. At the very beginning, we randomly choose 0.05% of nodes as the seed set of worm sources to initiate the infection.

B.Performance Evaluation

1) Examine the effectiveness of the five schemes in two different mobility scenarios: The worm infection rates under different coping schemes are compared in Fig. 4 with accumulated simulation time.

In both datasets, the worm will infect most of nodes in network quickly if we don't take any containment scheme (as depicted in diamond curve). We also observe that the effectiveness of SIN worm coping scheme is batter than GIN ones. In comparison, our HWCS scheme successfully controls the spreading of worm in mobile internet and shows an improvement (8%~27%) in terms of worm infection rate over single SIN and GIN based worm coping scheme, since it integrated into account the inherent short-range and long-range communication pattern of hybrid worm.

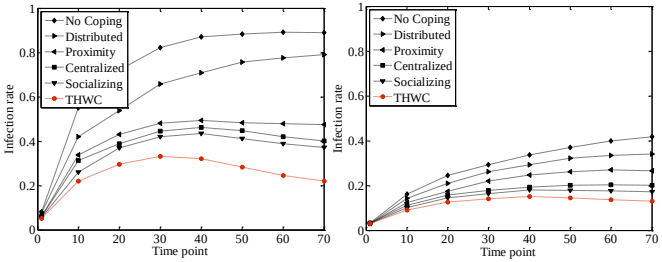

(a) Haggle (b) MIT Reality

Fig.4 Performance comparison on worm infection rate.

2) *Examine the cost of the five containment schemes*: Fig. 5 depicts how the number of patched nodes changes over time under different patching strategies.

The Distributed scheme incurs no cost, it also loses the opportunity to exchange the signatures in the networks. That leads to its poor performance illustrated in Test 1. The Proximity scheme floods the signatures in the network in order to control the spreading of the worm, which incurs huge forwarding costs. Centralized scheme is competitive, but it may require 1~2 times more patches compared to the THWC scheme. In Socializing schemes, a tighter set of separator nodes are used to forward patches as well. However, its clustered partitioning does not necessarily reflect the natural network community structure, and thereby lower the containment efficiency. On this account, it requires more patches to terminate the spreading of worm.

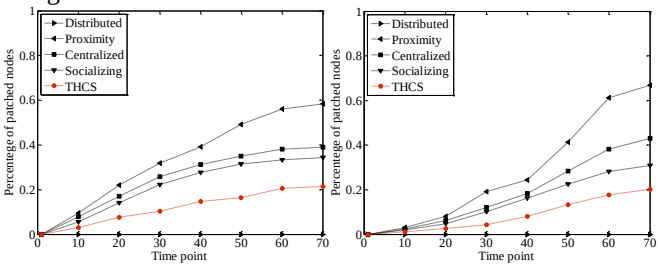

(a) Haggle (b) MIT Reality

Fig. 5. Performance comparison on total number of patching nodes.

3) Performance of different containment scheme: The time when to start the patching procedure depends on the strength of the worm detection system. Obviously, later detection could significantly delay worm containment. In this test, we use a patching threshold μ to simulate the time delay for worm detection. When the infection rate (the fraction of infected nodes over all nodes) reaches the

threshold, the patching process will be initiated. The experiments are conducted with $\mu = 5\%$, 10% and 20%.

We first examine how infection rate changes under different percentage of patched nodes. We observe the performance of THWC in reference to Centralized and Socializing which shows competitive performance in former test. We also choose Blondel and A3CS as a replacement of our trust propagation algorithm to test the practicability of the detected community structure. The results are presented in Fig. 6.

As expect, the longer we wait to begin patching, the more number of nodes we need to be patched. THWC achieves the lowest infection rates in all cases and shows remarkably advantage. The reason behind this is due to the nature of connmunity struture, which veritably simulates the spreading dynamics of worm.

Next, we fix the number of patched nodes (30% of the network data) and examine how infection rate changes over time under different patching strategies. For this test, we use the random patching strategy (randomly select nodes to forward signatures) as a baseline method. Random patching completely ignore the correlations between nodes, as a result, the infection rate does not change fundamentally irrespective of when to start the patching procedure. As shown in Fig. 7, THWC achieves the best performance as it limits the infection rate within a certain bound much faster than the other two schemes.

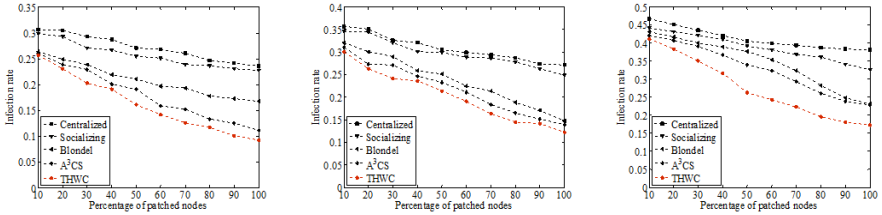

(a) μ = 5% (b) μ = 10% (c) μ = 20%

Fig.6 Performance of node patching strategy

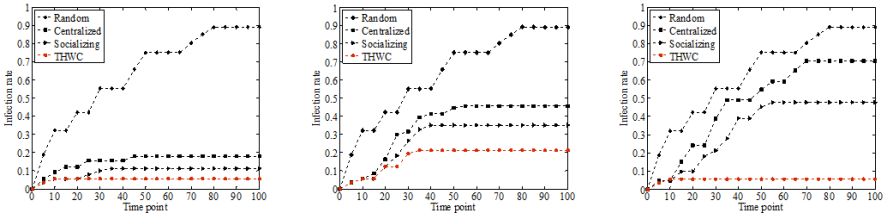

(a) μ = 5% (b) μ = 10% (c) μ = 20%

Fig.7 Infection rate under fixed patching number.

ACKNOWLEDGEMENT

We thank the anonymous reviewers for valuable feedback. This work is sponsored by National Natural Science Foundation of China (61402126), Nature Science Foundation of Heilongjiang province of China (F2016024), Heilongjiang Postdoctoral Science Foundation (LBH-Z15095), University Nursing Program for Young Scholars with Creative Talents in Heilongjiang Province (UNPYSCT-2017094).

REFERENCES

[1] Yan G, Eidenbenz S. Modeling propagation dynamics of bluetooth worms [J]. IEEE Trans on Mobile Computing, 2009, 8(3): 353-368

[2] Mickens J W, Noble B D. Modeling epidemic spreading in mobile environments [C] //Proc of the 4th ACM Workshop on Wireless Security. New York: ACM, 2005: 77-86.

[3] Zyba G, Voelker G M, Liljenstam M, et al. Defending mobile phones from proximity malware [C] //Proc of the 28th IEEE Int Conf on Computer Communications（INFOCOM）. Piscataway, NJ: IEEE, 2009: 1503-1511.

[4] Yang Y, Zhu S, Cao G. Improving sensor network immunity under worm attacks: A software d iversity approach [C] //Proc of the 9th ACM Int Symp on Mobile Ad Hoc Networking and Computing（MobiHoc）. New York: ACM, 2008: 149-158.

[5] Miklas A G, Gollu K K, Chan K K W, et al. Exploiting social interactions in mobile systems [C] //Proc of 9th Int Conf on Ubiquitous Computing (UbiComp). Heidelberg, Germany: Springer, 2007: 409-428.

[6] Li F, Yang Y, Wu J. CPMC: An efficient proximity malware coping scheme in smartphone-based mobile networks [C] // Proc of the 29th IEEE Int Conf on Computer Communications（INFOCOM）. Piscataway, NJ: IEEE, 2010: 1-9.

[7] Daley D J, Gani J, Gani J M. Epidemic modelling: an introduction [M]. Cambridge University Press, 2001.

[8] Xie J, Kelley S, Szymanski B K. Overlapping community detection in networks: The state-of-the-art and comparative study [J]. ACM Computing Surveys, 2013, 45(4): 43.

[9] N. Eagle and A. Pentland. CRAWDAD data set MIT/reality (v. 2005-07-01). Download form http://crawdad.org/mit/reality/, July 2005.

[10] J. Scott, R. Gass, J. Crowcroft, P. Hui, C. Diot, and A. Chaintreau. CRAWDAD data set cambridge/haggle (v. 2006-01-31). Download form http://crawdad. org/cambridge/haggle/, January 2006

[10] Zhu Z, Cao G, Zhu S, et al. A social network based patching scheme for worm containment in cellular networks [C] //Proc of the 28th IEEE Int Conf on Computer Communications（INFOCOM）. Piscataway, NJ: IEEE, 2009: 1476-1484.

No-Wait Integrated Scheduling Algorithm Based on the Earliest Start Time

Zhiqiang Xie[1], Yilong Gao[2], Jun Cai[3], Yu Xin[4]

[1,2,3,4] *Harbin University of Science and Technology (HUST)*

[1]*xiezhiqiang@hrbust.edu.cn,* [2]*gaoyilong91@163.com,*[3]*864023781@qq.com,*
[4]*3864023781@qq.com*

***Abstract*—Aiming at the integrated scheduling problem with no-wait constraints, the no-wait integrated scheduling algorithm based on the earliest start time is proposed. In order to determine the scheduling order of the predecessors and successors of the no-wait operation groups, the allied critical path method (ACPM), shortest processing time strategy (SPTS) and the layer-priority strategy (LPS) are used in turn, and then we use the long-path strategy to determine the scheduling order of the no-wait operation groups. Finally the earliest start time strategy is proposed to determine the start time of the ordinary operations and the no-wait operations. The examples show that the proposed algorithm can solve the no-wait integrated scheduling problem better, and can get better results compared with the previous algorithms.**

Keywords—earliest start time, no-wait constraint, integrated scheduling algorithm

I.INTRODUCTION

With the progress of society, the demand for product diversification has drove the production of products to tend to multi-variety and small-batch, which makes the research on production scheduling shift from the original scheduling of pure processing problems [1] or pure assembly problems [2] to the integrated scheduling problem [3, 4] which deals with the processing and assembly of tree-structured products simultaneously. The integrated scheduling problem is more complex than the traditional job shop scheduling problem, but it has important theoretical significance and practical engineering application value in shortening the product manufacturing cycle and improving the production efficiency. In this paper, we consider the integrated scheduling problem of a special product, that is, there are no-wait constraints among some certain operations of the product. This situation widely exists in the real production environment, such as iron and steel production, pharmaceutical manufacturing, etc.

At present, there are many literatures [5, 6] on ordinary integrated scheduling problem, but the literatures on no-wait integrated scheduling problem are relatively few. For this problem, literature [7] proposed an integrated scheduling algorithm with no-wait constraint operations, this approach avoids the complexity

increase problem caused by the secondary adjustment. However, when determining the relevant operations' scheduling order of the operation group, it neglects the influence of the long-path operations on the scheduling result. Literature [8] proposed a no-wait integrated scheduling algorithm based on reversed order signal-driven, this method fully considers the long-path operations' influence on the scheduling result, which makes the parallel effect of the operations better than that of literature [7]. However, this algorithm does not effectively use the idle period generated by the machine. For this reason, a no-wait integrated scheduling algorithm based on the earliest start time is proposed in this paper, the algorithm first determines the scheduling order of each operation, and then determines its start time. Example verification shows that the algorithm proposed in this paper can generate a better result than the previous algorithm.

II.PROBLEM MODEL DESCRIPTION

Assume that the complex tree-structured product with no-wait constraints is composed of *n* operations, and it will be processed on *m* machines. Let C_i be the completion time of operation *i*, and S_{ik}, T_{ik}, F_{ik} respectively represent the start time, the processing time, and the completion time of operation *i* on machine *k*. So, the mathematical model of this problem can be expressed as follows:

$$\min(\max C_i), i = 1, 2, ..., n \quad (1)$$

$$s.t. \min(S_{ik}) \quad (2)$$

$$S_{ik} - F_{xy} \geq 0 \quad (3)$$

$$S_{ik} - F_{(i-1)k} \geq 0 \quad (4)$$

$$S_{ak} - F_{bk'} = 0 \quad (5)$$

In the formulas, *i* = 1, 2, ..., *n*; *k*, *k*' = 1, 2, ..., *m*; *x* is the immediate predecessor of operation *i*. Formula (1) is the objective function of this problem; Formula (2) indicates that the operations need to be processed as early as possible; Formula (3) indicates that the process *i* cannot start before all its predecessors have been finished; Formula (4) represents that, on machine *k*, the operation *i* must start after the completion of operation *i*-1. Formula (5) shows that there is a no-wait constraint between operation *a* and *b*.

For the convenience of the subsequent description, the following concepts are defined.

1. **Ordinary operation** operations that do not have no-wait constraint relationship with other operations.

2. **No-wait operation group** a set of operations in which one operation have no-wait constraint with another operation.

3. **Relevant operation** A collection of predecessors for each operation in a no-wait operation group.

III.STRATEGY AND ALGORITHM DESIGN

In the no-wait integrated scheduling problem, the no-wait operation group is composed of multiple operations. Therefore, if the start time of the no-wait operation group cannot be reasonably determined, it will cause a series of chain reactions and eventually lead to a longer product completion time. So in our paper, we propose a no-wait integrated scheduling algorithm based on the earliest start time, first determines the scheduling order of each operation, and then determines its start time.

A.Determination of the operations' scheduling order

In order to make the processing of the no-wait operation groups undisturbed by other operations, we prioritize the scheduling of the relevant operations, then consider the no-wait operation groups, and finally we schedule the subsequent operations of the no-wait operation groups.

For a no-wait operation group, its relevant operation is a constraint for the start of processing. Considering that the operations on the dynamic critical path have a great influence on the completion time of the product, this paper firstly use the ACPM to choose an operation whose path length is biggest; When there are multiple operations with the same path length, giving priority to the operation with shorter processing time can release the machine as soon as possible, and can also make the process of its subsequent operations as early as possible, so, we use the SPTS to determine its scheduling order; If some of the operations' processing time are the same, we continually use the LPS to determine its scheduling order, that's because the process from the node which has a large layer number to the root node maybe more complicated, and its subsequent operations may require higher machine, so, giving priority to the operation which have larger layer number can make its subsequent operations process as early as possible under limited machine resources. If we still cannot determine the scheduling order of some certain operations, then we randomly choose one operation to process.

Therefore, the specific method for determining the scheduling order of each operation is as follows: First, the relevant operations of the no-wait operation groups are scheduled according to the ACPM, SPTS and LPS; Then after all the relevant operations are scheduled, the Long-Path strategy is used to determine the scheduling order of the no-wait operation groups based on the first operation of

each no-wait operation group, for other operations within the operation group, the operations are successively scheduled according to the no-wait constraints; Finally, for the subsequent operations of the no-wait operation groups, its scheduling order is also determined according to the ACPM, SPTS and LPS.

B. Determination of the operations' start time

The first fit strategy has been proved to have a good scheduling effect for determining the start time of the operations, but this method does not consider the effective use of the idle period generated in the scheduling process. Therefore, the earliest start time strategy is proposed to determine the operations' start time in this paper, the specific description is as follows:

For the ordinary operations, when the machine is not idle at the earliest time that the operation can be processed, the first idle period is sought forward. When the size of the idle period is larger than or equal to the processing time of the operation, then the operation is put into this idle period for processing; when the size of the idle period is smaller than the processing time of the operation, then the operations after the idle period on the machine is entirely moved forward until the size of the idle period is equal to the processing time of the operation, and then the operation is scheduled in this idle period.

For the operations with no-wait constraints, it is necessary to judge whether the machine idle periods needed of all no-wait operations can meet the constraints of no-wait process because its schedule must be unified and coordinated. The specific method for determining the start time for the no-wait operations is: Firstly, visit the machine required by the first operation in the no-wait operation group, find the first idle period that can be used for processing, and then judge the next operation whether there is a corresponding idle period under the condition of no-wait constraint, If it exists, then determine the other remaining operations in the operation group until all the no-wait operations are scheduled; otherwise, the next machine idle period of the first no-wait operation is find and the above determination process is continued.

C. Algorithm description

According to the above description, the specific flow of this algorithm is as follows:

Step 1: Enter the relevant information of product and machine;

Step 2: Calculate the auxiliary data such as the path length and the layer number for each operation of the product;

Step 3: Determine the scheduling order of the relevant operations according to the ACPM, SPTS and LPS.

Step 4: Use the LPS to determine the scheduling order of the no-wait operation groups.

Step 5: Determine the scheduling order of the subsequent operations of the no-wait operation groups according to the ACPM, SPTS and LPS.

Step 6: Use the earliest start time strategy to determine the start time of the operations.

Step 7: Output the Gantt chart of the product and the algorithm ends.

III.INSTANCE ANALYSIS

Product A is a complex product with no-wait constraints consisting of 27 operations, and there are 4 machines available for use. The extended processing operation tree of product A is shown in Fig. 1. The dashed box in Figure 1 indicates that this group of operations has no-wait constraints.

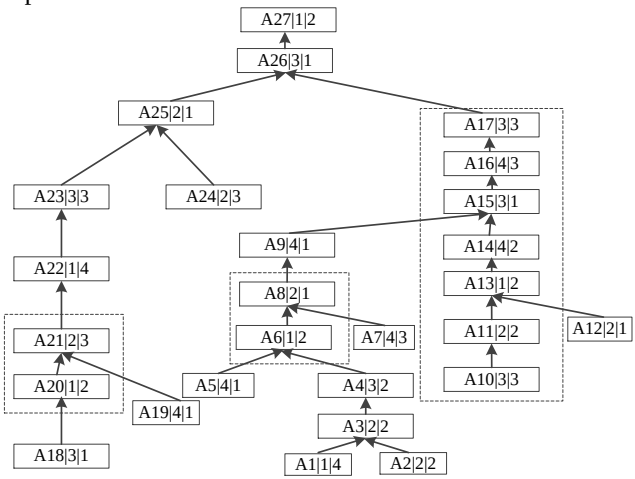

Fig.1. Processing operation tree of product A

As can be seen from Figure 1, the three no-wait operation groups are {A20, A21}, {A6, A8} and {A10, A11, A13, A14, A15, A16, A17}, respectively. The relevant operations are {A18, A19}, {A1, A2, A3, A4, A5, A7}, {A12} and the sub-tree {A1 ~ A9}. According to the ACPM, SPTS and LPS, the scheduling order of the relevant operations is {A1, A2, A3, A18, A4, A5, A7, A19}. Then according to the long-path strategy, the scheduling order of no-wait operation group {A20, A21} and {A6, A8} is {A20, A21, A6, A8}. After the above analysis, the final order of operations is determined as {A1, A2, A3, A18, A4, A5, A7, A19, A20, A21, A6, A8, A9, A22, A10, A13, A14, A15, A16, A17, A23, A24, A25, A26, A27}.

According to the earliest start time strategy, operations A1, A2, A18, A5 can be processed directly without waiting, but operations A7 and A19 need to look forward for the next idle period for processing due to the machine conflict

constraints, so operation A7 is processed on the time interval (1, 4) and A19 is processed on interval (4, 5). For the no-wait operation group {A20, A21}, the first available idle period for operation A20 is the interval (4, 6) and at the same time A21 can be processed on period (6, 9), so the A20 is processed form 4 to 6 and the A21 is processed from 6 9. After determining the start time for all operations according to the above strategy, the Final Gantt chart of product A is shown in Figure 2.

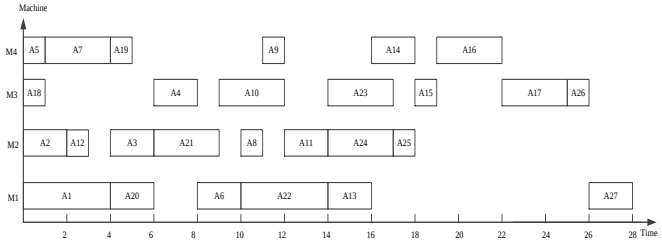

Fig. 2 Gantt chart produced by our algorithm

In order to illustrate the superiority of the proposed algorithm, we have added two comparison algorithms, in which algorithm 1 adopts the algorithm proposed in literature [7] and algorithm 2 adopts the algorithm mentioned in literature [8]. Algorithm 1 and 2 are performed on product A respectively and the Gantt charts produced are shown in Figure 3 and Figure 4. By comparison, we can see that the scheduling result generated by the proposed algorithm is better than the results produced by Algorithm 1 and Algorithm 2. The reason why our algorithm is better than Algorithm 1 is that the operation A22 is arranged according to the earliest start time strategy to a time interval of (10, 14), which is fully parallel with the operations A10 and A11, which make the successor's start time of A22 advance, resulting in shortening the product completion time.

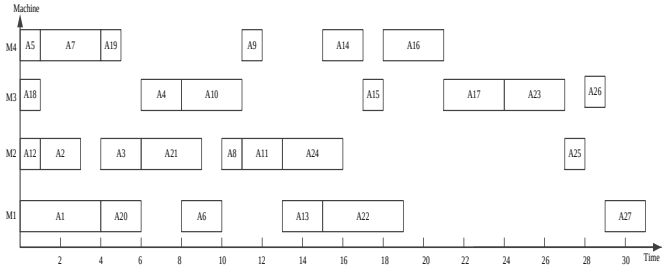

Fig. 3. Gantt chart of product A generated by algorithm 1 in [7]

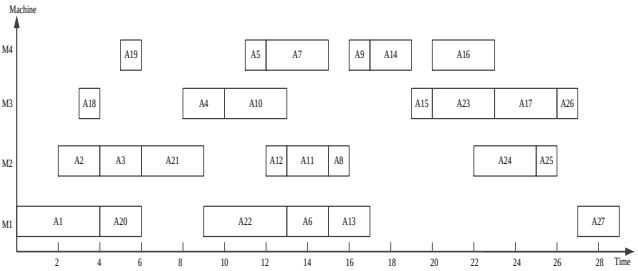

Fig. 4. Gantt chart of product A generated by algorithm 2 in [8]

Also the reason why this algorithm performs better than algorithm 2 is that the operation A4 is arranged at t = 6 for processing according to the earliest start time strategy proposed in our paper. Compared with algorithm 2, this strategy takes 2 hours earlier, so that the no-wait operations A6 and A8 can be assigned to the idle periods (8, 10) and (10, 11), which in turn affects the process of the subsequent operations, and thus the completion time is shorten.

IV.CONCLUSIONS

Aiming at the integrated scheduling problem with no-wait constraints, we proposed a no-wait integrated scheduling algorithm based on the earliest start time, which considers the scheduling order first and then determine the operation's start time. The long-path strategy is used to determine the scheduling order of the no-wait operation groups, and the ACPM, SPTS and LPS are used for the other operations, finally we proposed the earliest start time strategy to determine the operation's start time. The comparative analysis of examples shows that the proposed algorithm is superior to the existing algorithms.

ACKNOWLEDGMENT

We acknowledge the support of National Natural Science Foundation of China (No.61772160, No.61602133, and No.61370086), Postdoctoral Scientific Research Start Fund Project in Heilongjiang Province (No.LBH-Q13092), National University of Computer Education Research Association (No.ER2014018), the Heilongjiang Postdoctoral Science Foundation (No.LBH-Z15096), China Postdoctoral Science Foundation (No. 2016M591541).

REFERENCES

[1] A. Agnetis, M. A. Aloulou, L. L. Fu. “Coordination of production and interstage batch delivery with outsourced distribution,” European Journal of Operational Research, vol.238, no.1, pp.130-142, 2014.

[2] D. N. Li, L. Zhou, J. Q. Zhao, and Q. Q. Liang. “Aggregate Scheduling of Machining and Assembly Systems Based on Bidirectional Negotiation,” Transactions of Beijing Institute of Technology, vol.24, no.4, pp.376-381, 2014.

[3] F. J. Wang, G. K Zhao, Z. Y. Jia, X. H. Lu, and L. P. Wang. “Assembly Job Shop Scheduling Based on Feasible Solution Space Genetic Algorithm,” Computer Integrated Manufacturing Systems, vol.16, no.1, pp.115-120. 2010.

[4] Z. Q. Xie, J. Yu, D. Y. Cheng, and J. Yang, “Integrated Scheduling Algorithm of Two Workshops Based on the Principle of the Neighborhood Rendering,” Journal of Mechanical Engineering, vol.52, no.01, pp.149-159, 2016.

[5] Z. Q. Xie, F. P. Zheng, and Y. C. Xie, “An Algorithm of Asymmetric Three Workshops Integrated Scheduling with Bath Equalization Processing,” Transactions of Beijing Institue of Technology, vol.37, no.3, pp.274-280, 2017.

[6] Z. Q. Xie, X. H. Zhang, Y. L. Gao, and Y. Xin, “Time-selective Ingegrated Scheduling Algorithm Considering the Compactness of Serial Processes,” Journal of Mechanical Engineering, vol.54, no.6, pp.191-202, 2018.

[7] Z. Q. Xie, Y. Z. Teng, and J. Yang, “Integrated Scheduling Algorithm with No-wait Constraint Operation Group,” ACTA AUTOMATICA SINICA, vol.37, no.3, pp. 371-379, 2011.

[8] Z. Q. Xie, Y. Xin, and J. Yang, “No-wait Integrated Scheduling Algorithm Based on Reversed Order Signal-Driven,” Journal of Computer Research and Development, vol.50, no.8, pp.1710-1721, 2013.

Design Techiques for Human-Machine Systems

Mikhail G. Grif [1], Natalie D. Ganelina [2]

[1,2]*Novosibirsk State Technical University (NSTU)*

grifmg@mail.ru

***Abstract* – The paper considers models, methods and techniques for automation of designing human-machine systems functioning processes (HMS FP) based on functional-structural theory (FST) and generalized structural method suggested by prof. A.I. Gubinsky. Top-down, down-top as well as combination of these strategies for HMS design are described. Operation sequence is formed by basic functional units, which can be integrated into basic functional structures. A functional net represents a functioning process of HMS and consists of functional structures. All alternative processes in HMS can be defined in alternative graph. A HMS FP notation based on binary relations between elements included in a functional net is presented. General scheme for optimal solution considers all alternative parts of functioning process. The algorithm suggested includes repeated parametric alternatives without double calculations. Optimal solution can be found by the modified directed search technique with partial solutions designed at each step. Optimization problem takes into account several parameters, including efficiency index, reliability and quality of HMS. These indexes can be calculated for the entire system or any part of functional net. The hybrid expert system developed with extended functionality allows building all isomorphic representations of an alternative graph, and generating specific directed search algorithm automatically and manually.**

Keywords – Functional-structural theory, human-machine system, set of alternatives, design automation, top-down design, down-top design.

I.INTRODUCTION

Information technologies are indispensable in all human ac-tivities. Information systems that allow to design and to assess functioning processes (FP) in complex human-machine systems (HMS) become of special importance.

In HMS it is necessary to analyze a huge dataset, take into account expert assessments from different groups of profes-sionals, and to explore all possible alternatives of functioning process. It is also important to predict the results, obtain grounds for defining parameters.

All these factors make information systems which allow ex-ploring and designing HMS with a big number of alternatives for different process subsystems functioning develop rapidly. One of the models often used for HMS FP designing is a func-tional-structural theory (FST) and a generalized structural method (GSM), suggested by A.I. Gubinsky [1].

In [2-4] models, methods and technologies for serial optimi-zation of HMS FP with effectiveness, quality and reliability (EQR) indexes based on FST were developed. A well-explored top-down strategy for designing functional nets (FN) is pre-sented in [4]. This article considers flaws of the top-dawn strategy and suggests down-top and hybrid strategies for HMS FP design.

II. PROBLEM DEFINITION

A HMS functioning process is a logical and time sequence of actions and operations performed by ergatic and non-ergatic system elements that is steady to disturbances, and results in achieving a goal (-s) of functioning [2-3]. A HMS FP proceeds in interrelated dimensions: HMS elements E, functions performed F, HMS states S, events W and HMS indexes Q.

Using FST and GSM for complex HMS FP design implies each of separate processes to be considered as an independent segment of FN. The process should be represented as a combination of formalized units - basic functional units (BFU). Combinations of BFU applied frequently and having mathematical models evaluated in advance are called basic functional structures (BFS).

Optimization problem (generalized problem of dynamic programming) is stated as follows:

$$\begin{aligned} &K_{EQR}(A) \to extr, \\ &A \in M_d \subseteq M_a \end{aligned} \qquad (1)$$

where $K_{EQR}(A)$ — the optimal criterion for the combination of EQR criteria; M_d — a set of feasible alternatives, alternative variants for the process — M_a [4].

A certain functioning process of HMS (functional net) is presented as a superposition of BFS:

$$O_z = SFS_i\left(O_{i_1}, O_{i_2}, ..., O_{i_k}\right) \qquad (2)$$

where $SFS_i \in M_{SFS}$, O_{i_j} — single or compound operation. Two operations with the same concurrent function F — $O(F, E_1, Q_1)$ and $O(F, E_2, Q_2)$ are alternative ("parametric") variants for execution of operation O, as well as compound operations $O_{=}SFS_i\left(O_{i_1}, O_{i_2}, ...\right)$ and $O_{=}SFS_s\left(O_{s_1}, O_{s_2}, ...\right)$, $i \neq s$ are "structural" alternatives.

Several strategies can be applied to build a functional net and to find optimal solution for HMS.

III. FUNCTIONAL NETS AND STRATEGIES FOR DEFINING A SET OF ALTERNATIVES

A top-down design strategy is one of possible design strategies for HMS FP. When applying this strategy a FN at the highest level of hierarchy is considered as a combined operation and a superposition of a set of alternative realizations. So a user describes a set of alternative HMS processes by an alternative graph (AG) as at Fig.1.

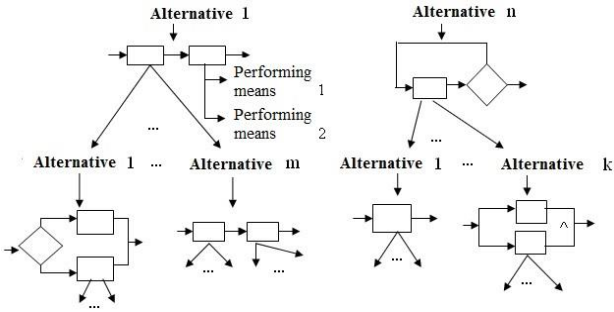

Fig. 1. Alternative graph for HMS FP.

"INTELLECT-3" is a hybrid expert system (HES) implementing the strategy described [4-6]. HES has an option to present FP in series of running operations without preliminary BFS superposition (Fig. 2).

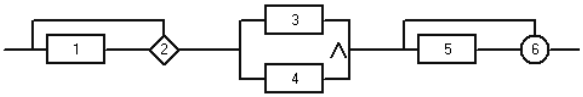

Fig. 2. HMS FP as an operations sequence.

In order to calculate EQR indexes and to determine optimal algorithm for the process functioning a FN should be defined as a superposition of BFSs included. HES"INTELLECT-3" automatically transforms a FN into equivalent superposition of BFSs while building an optimal solution (Fig. 3).

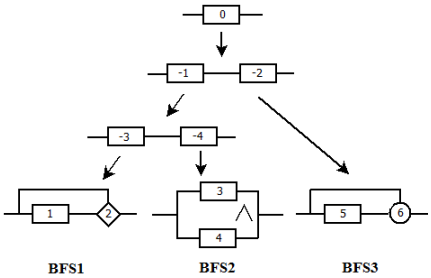

Fig. 3. HMS FP as a superposition and alternative graph.

Those operations in a superposition on the FN that are equivalent (enlarged) are given negative numbers.

A functioning process can be defined as a set of binary relations $\{(O_1, O_2), ..., (O_{n-1}, O_n)\}$ between FN elements, where O_n follows O_{n-1}.

Composition transit "AND" marks the beginning point and the end for every BFU. If one transit denotes the end of the previous BFU and the second starts the next one, two of them are merged and replaced by one. The FN start and end are also denoted by composition elements H and K. An example of HMS FP (Fig. 4) definition as a set of binary relations is illustrated by (3).

$$\begin{aligned} R_{BS} = \{&(H, T_1), (T_1, A_1), (A_1, T_2), (T_2, A_2), \\ &(A_1, T_3), (T_3, \beta_f), (\beta_f, T_4), (\beta_f, A_2), \\ &(T_4, \beta_d), (\beta_d, T_5), (\beta_d, A_1), (T_5, A_3), \\ &(A_3, T_6), (T_6, K)\} \end{aligned} \quad (3)$$

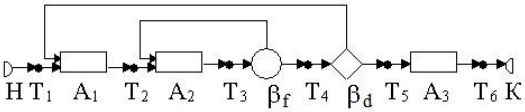

Fig. 4. Example of FH.

A HMS FP representation as a set of binary relations between elements of the net didn't guarantee a definition of the net as a superposition of BFSs. In [7] an algorithm to determine a set of transits points, which form a segment of the net that results in a superposition of BFS, was suggested. As a result a FN will be replaced by one equal operation. If the algorithm results with no isomorphic set found, this functional net doesn't define functioning process within the FS theory.

A directed search algorithm (DSA) is applied to finding optimal decisions in HES "INTELLECT-3". It's used within the general technique of consecutive analysis of alternatives with stepwise designing of partial solutions [4]. The specific stepwise design algorithm is defined by the rule for selecting partial solutions (subnets) ϑ, which should be developed at each step, and a set of tests ξ, that eliminates the subnets which can not be completed to the optimal ones. Requirements for optimality (OR) and feasibility of partial solutions (FR) are used as a set of tests ξ. The general scheme of DSA for FN within the technique of consecutive analysis of alternatives is the following:

$$DSA = \hat{\xi}_1(y_1), \vartheta_1(x_1), \xi_2(y_2), \vartheta_2(x_2), ..., \xi_r(y_r), \vartheta_r(x_r), \hat{\xi}_{r+1}(O_z) \quad (4)$$

where $y_j = O_k$ is a chosen operation O_k.

FN designing in HES "INTELLEKT-3" can result in common (coinciding) segments (Fig. 6), if alternative segments of functioning (Fig. 5) were defined.

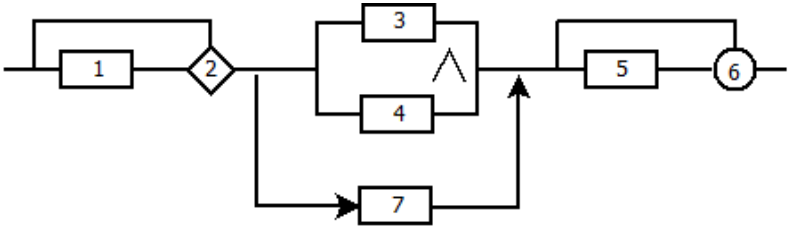

Fig. 5. FN with an alternative segment.

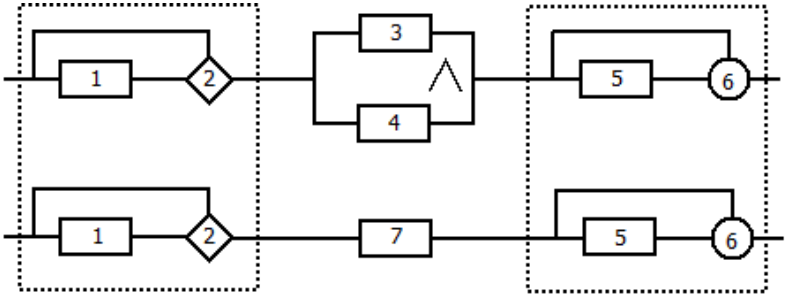

Fig.6. Common segments in FN.

The general scheme for finding optimal solution includes building AG, which considers all alternative segments of functioning. A FN can consist of numerous nodes with the same operation alternatives, i.e. the same set of parametric

alternatives. Fig. 7 shows AG for the FN presented in Fig. 5. In HES "INTELLEKT-3" before building AG a FN is preliminary analyzed if its alternative segments have common parts. And AG later is formed considering these common parts (Fig. 8). Common parts in AG result in DSA modification. If EQR indexes are evaluated in a node that is defined as common, the partial solution found in this node, is retained. This solution will be taken if needed, avoiding double calculations.

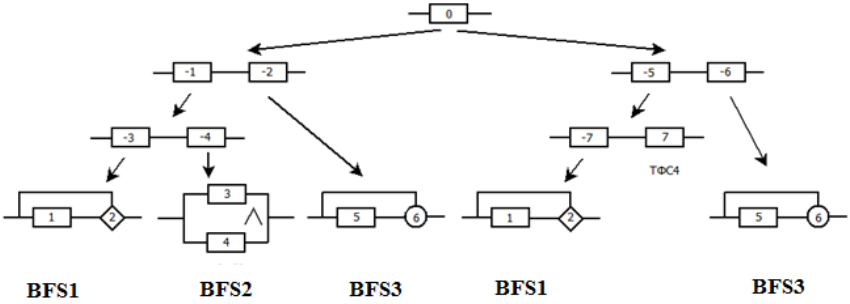

Fig. 7. Alternative graph for a FN with an alternative segment.

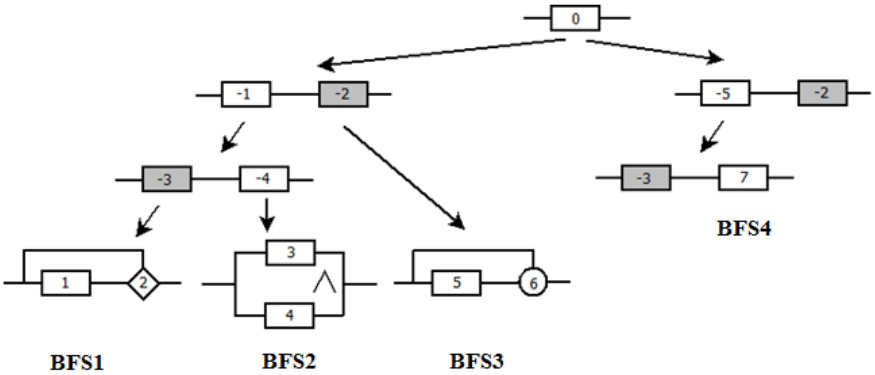

Fig. 8. AG for a FN with common parts

HES "INTELLEKT-3" allows to control DSA bypass in both manual and automatic mode. In automatic mode a rough estimation of complexity is made in case this sequence is chosen by DSA [4, 8].

Default bypass for the example shown in fig. 5 is illustrated in (5), an alternative is in (6).

$$V = \{BFS_1, BFS_2, BFS_3\}, \quad (5)$$

$$V = \{BFS_1, BFS_4, BFS_3\} \quad (6)$$

For the example considered there is a bypass (7) and (8):

$$V = \{BFS_1, BFS_3, BFS_2\}, \quad (7)$$

$$V = \{BFS_1, BFS_3, BFS_4\} \quad (8)$$

An AG which considers coinciding segments for such enumeration alternative will have a minimal number of nodes (Fig. 9).

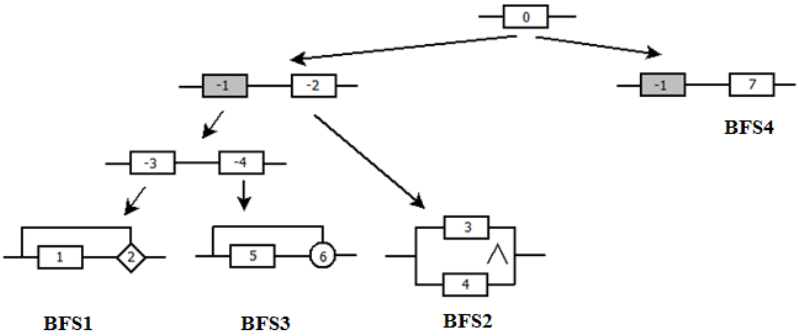

Fig. 9. Alternative graph with minimal number of nodes

IV. CONCLUSION

The paper considers techniques for automation of designing human-machine systems functioning processes based on functional-structural theory and generalized structural method suggested by prof. A.I. Gubinsky. Isomorphic methods for HMS FP defining based on binary relations between elements included in a functional net and superposition of BFS were discussed. An algorithm determining segments of functional net that could be represented as a superposition of BFS was described. A hybrid expert system implementing the techniques described was presented.

REFERENCES

[1] A.I. Gubinsky. Nadezhnost` i kachestvo funktsionirovaniya ergaticheskikh system [Reliability and quality of ergatic system functioning]. Leningrad, Nauka, 1982. - 270 p. (In Russian).

[2] A.I. Gubinskiy, V.G Evgrafov. Informatsionno-upravlyauschie cheloveko-mashinnie sistemy: Issledovaniye, proektirovaniye, ispytaniya. Spravochnik [Control and information human-machine systems. Research, design, testing. Guide]. Moscow, Mashinostroeniye, 1993. - 528 p. (In Russian).

[3] A.I. Gubinskiy, V.G Evgrafov. Ergonomicheskoye proektirovaniye sudovyh system upravleniya [Ergonomic design for ship control systems]. Leningrad, Sudostroeniye, 1977. - 224 p. (In Russian).

[4] M.G. Grif, E.B. Tsoy. Avtomatizatsiya proektirovaniya processov funktsinirovaniya cheloveko-mashinnyh system na osnove metoda posledovatelnoy optimizatsii [CAD technique for human-machine systems based on sequential optimization method]. Novosibirsk, NGTU, 2005. - 264 p. (In Russian).

[5] A.V. Zaykov, S.A. Kochetov, M.G. Grif. Metody i sredstva proektirovaniya processov funktsionirovaniya cheloveko-mashinnyh system na osnove fumktsionalno-strukturnoy teorii [Algorithms and techniques for optimal design of Human-machine systems functioning processes based on functional-strucural theory] // Nauchniy vestnik NGTU [NSTU Science Bulletin] , 2008. № 3(32). Novosibirsk, NSTU, pp. 95-110. (In Russian).

[6] E.V. Geniatulina. Metody proektirovaniya i modelirovaniya v zadachah optimizatsii processov funktsionirovaniya cheloveko-mashinnyh system [Design and modeling methods for optimization of HMS functioning]. E. V. Geniatulina, M. G. Grif, Trudy SPIIRAN [SPIIRAS Proc.] , 2014. № 5(36), pp.151-167. (In Russian).

[1] M.G. Grif, S.A. Kochetov, E.B. Tsoy. Strategii proektirovaniya mnozhesyva alternativ v zadachah optimizatsii na osnove funktsionalno-strukturnoy teorii [Functional-structural theory based strategies for designing a set of alternatives in human-machine systems optimization problems] // Doklady Akademii nauk vishey shkoly Rossiyskoy Federatsii [Reports of the Academy of Sciences of the Higher School, Russian Federation] , 2015. № 4(29), pp. 44-51. (In Russian).

[2] M.G. Grif, S.A. Kochetov S.A., N.D .Ganelina. Functional -Structural Theory Based Techniques for Human-Machine Systems Optimal Design//13 International Scientific -Technical Conference on Actual Problems of Electronic Instrument Engineering (APEIE) – 39281: proc. Russia, Novosibirsk, 3–6 October 2016. - Novosibirsk, 2016. - Vol. 1. Part 2. – pp. 494-497.

Learner Centered Learning: Development of Supportive Environment and Its Evaluation

Uranchimeg Tudevdagva[1], Wolfram Hardt[2]

[1,2]TU Chemnitz

[1]uranchimeg.tudevdagva@informatik.tu-chemnitz.de,[2]hardt@cs.tu-chemnitz.de

***Abstract*—this paper discusses on supportive learning environment for learner centered learning approach. The approach is not new term in education systems, but with technological rapid development and with new generation of learners we have to review this approach with added values. Learner centered learning has many factors for practical cases. One the important factor is learning environment. If we cannot provide corresponding environment for this approach implementation of this idea will not run in practice successfully. Here we describe our idea about "supportive" learning environment for learner centered learning. Learner should be able to design and plan personalized study plan during own study. Because each learner has personal skill and individual methods to learn. Pre-defined study plan and static designed linked courses cannot support learner centered learning approach. We tried to wake up this problem in light and establish supportive learning environment where learner really can plan personalized study plan and can finish study in own time successfully.**

Keywords—study plan; credit point; student centered learning; learner oriented learning; learning environment;

I. INTRODUCTION

Learner Centered Learning (LCL) is by definition not new approach in teaching and learning. Nevertheless, with development of technologies, with change of learners' attitude and behaviors this approach facing to update.

Existing various similar approaches for LCL. For example, student centered learning, student oriented learning, personalized learning, learner centered training, learner centered education, learner centered pedagogy etc.

Researchers are published many works relating to above listed approaches, and discussing about different accepts of LCL [1-6]. For example, Debec studied effectiveness of LCL approach for Teaching an Introductory Digital Systems Course [1-2], Matukhin and Bolgova used LCL approach to teach foreign language [3], Randall and Jane discussed on learner centered pedagogy issues [4]. This list can be continuing longer. Reading confirmed that all researchers are summarizing that LCL is important approach for modern and further education system.

Here we would like to discuss about supportive learning environment for LCL. Our solution for supportive learning environment came from planning of

teaching and design of curricula for offering academic program. Usually universities designing their academic semesters quite early before to start academic year. Schedule of offering courses depend on teaching hours for professors and learning hours for students in curricula. Learner should follow schedule from university and have to select courses, which are offering in that academic semester. Each course has pre-condition to select that course. This can be some knowledge, practical hours or other course. That means learner simply cannot select any course, which he/she want to listen in coming academic semester. To select course learner, have to fulfil pre-defined condition of course.

We see here just some most visible conditions and way to design study plan of learner. There are many other conditions and situations, which are influencing to selection and designing of learners' study plan.

Focus of this paper is to discuss curricula and credit points of courses and planning of offering courses for academic year. These two factors are part of many factors, which are important to develop "supportive" learning environment for LCL.

II. CREDIT POINTS

A. Curricula and credit points

First, let us look into credit points (CP). This is very important element of any level of higher education. To fill requirement for degree learner, have to collect credit points. No expected credit points, no chance to get degree!

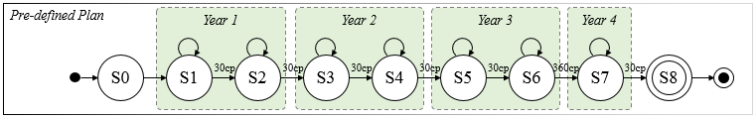

Fig.1. shows us way from enroll to graduation.

As usually, every university has traditional plan for academic degrees. Fig.1 shows, study plan for "Bachelor" degree as finite state machines. If any person enrolled to university this means learner has limited time to finish it. Moreover, we visualized it via states of finite state machine. Learner have to go through of all these states to get degree.

S0 state denoted for freshman. Freshman is any person who received acceptance to enroll university. By pre-defined plan (Fig.1) learner, have to collect at least 60 CPs in each academic year. If learner could collect needed CP in each year by predefined plan (traditional expectation of administration), he/she can reach in planned time state S7. S7 state defines as diploma work or final exam for graduation. Between S0 and S7 we have six more states. These states are defining academic semesters where learner have to collect according CPs. S1 and S2 states are defines first academic year. If learner can collect, 60 CPs in states S1 and S2

then can move to state of next year. If not enough CPs then have to stay in states of first year. S3 and S4 states are defines second academic year. S5 and S6 states are defines third academic year. After completion of credits learner will receive, right to select diploma subject. This state is state S7. Main condition to fit traditional plan of study (Fig.1) is to collect corresponding credits in giving time. Else, this picture will change very much.

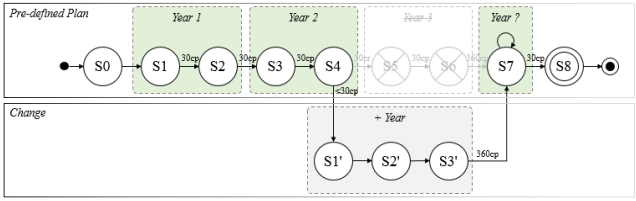

Fig.2. Change in pre-defined plan

For example, learner could not collect necessary CPs in second year of study. In that situation, states of study plan can be change dramatically. Will appear new states (S1', S2' and S3') with new way and no body cannot estimate time to finish study successful (Fig.2). These views (Fig.1-2) could be helpful to learners to follow their study plan. If learner wants to finish study in good time should keep in mind these states and try fit pre-defined time. Our target of research is design flexible environment for individual planning but in expected time to graduation.

As usually, courses has different hours in curricula definition and relating to this CPs for such us courses are different.

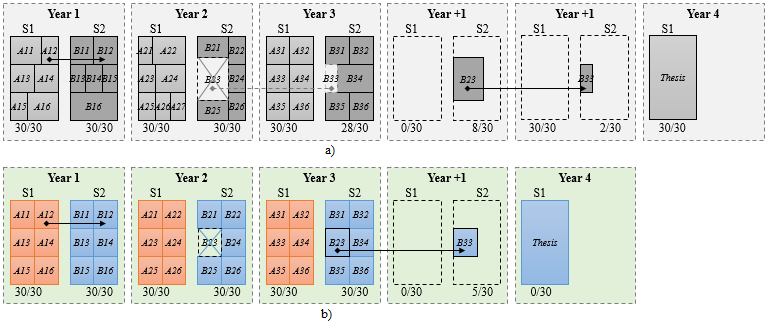

Fig.3. Credit points and study planning

Let us see to pre-defined study plan from different view. In Fig. 3 shows pre-defined plan as boxes. Each box consists of 2 academic semesters (S1 and S2). Here we can see one basic problem for learners. Administration defined total CPs, which have to collect learner during one academic year. For example, here total

summary should be 60 CPs, but offering courses has different CPs. Main challenge of student (learner) is have to look total CPs and decide which course want to learn. Fig. 3 shows how not easy to puzzle courses together to fit expecting CPs. Sometime have to do decision about CPs or course! If learner will collect, less than requested then box will have leer spaces. By means cannot move to next box. Opposite, if learner collected credits more than requested then again it is not fitting to pre-defined box.

TABLE I. Study plan by credit points

Academic Year	Academic Semester	Selected courses	Credit Points	Total Credit Points
First Year	S1	A11	8	30/30
		A13	4	
		A15	3	
		A12	3	
		A14	4	
		A16	8	
	S2	B11	2	30/30
		B12	2	
		B13	6	
		B14	5	
		B15	5	
		B16	10	

In Table 1 visualized above discussed problem. Different CPs of courses are influencing to design of individual study plan a lot. Main reason is total CPs should fit to pre-defined sum and student have to look to not only content of course always have to keep in mind how much credit will get from this course. By means, this type of planning is not enough flexible for LCL. If universities will not illuminate this difference between courses, we cannot provide “supportive” learning environment for LCL.

Some universities already started to solve this problem. For example, TU Chemnitz since 2010 worked on this issue and Faulty of Computer Science reached some agreement between professors. Now all offering course from this faculty has same credit points = 5. This made a lot of progress for individual planning for

students. It gave to students more freedom to select course by own interest and for future target. How solved different hours of courses, how could fit all courses into 5 CPs? Smart solution come with e-learning. E-learning part included to courses, which had, less than PCs in previous curricula.

But here we still have some administration problem, even CPs are same for all courses. In TU Chemnitz for bachelor study student have to collect 60 credits per year. Offering courses has different curricula and following this each course has different CP! Here coming in light problem. What is the problem? Problem is student have to plan own study plan with balance. What means balance? Should collect 30 PCs in each semester and totally 60 PCs can be collected by an academic year. If learner collected 45 PCs in first academic semester and 15 points in next academic semester, then administration issue not accepting it (Fig.4.) [7].

Fig.4. Imbalance: Not accepting

This problem can solve if we can make more flexible study plan for learners. Pre-defined study plan like in Fig.1 should be more flexible and student could have freedom to finish early his study or a bit later than planned in this manner.

B. Personal planung of courses

Every university defining teaching hours plan and publishing it before to start academic semester. Idea is to support learner to design their study plan as personal case.

Fig.5 shows online study planner for students of TU Chemnitz. This is view of Master students for Automotive Software Engineering program.

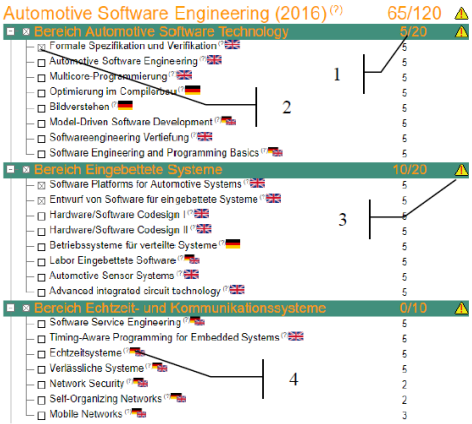

Fig.5. Study planner

Let us explain important points of figures.

1. Number one shows to 5/20. This is credit points which have to collect learner in giving semester. 20 means total number of CPs and 5 of them pre-defined requested course which learner “have to” include to selection. Remaining 15 CPs learner can select from offered list.

2. Here we can see crossed box, that means this course is already in selection. This is the required pre-defined course. Learner cannot change this state.

3. Yellow triangle with red ! shows planning is not finished. If learner selected less or more credits, then us needed this symbol will stay visible. If plan is fitting to expectation, then this symbol will vanish.

4. Flag of countries shows language of offering course. Some course is only in German or English. Some of them is possible to learn in both languages.

In Fig.5 some course: Network security, Self-Organizing network and Mobile networks has not 5 CPs. Because these courses are courses which offering from other faculties. That means not all faculties in TU Chemnitz updated curricula. There are still existing many courses which have different CPs.

III. SUPPORTIVE LEARNING ENVIRONMENT

As we mentioned in Introduction section many researchers agreed that LCL is one of correct way for teaching and learning. The successful implementation of LCL approaches need corresponding environment. In second section, we discussed about case of TU Chemnitz. In this section, we will discuss about need of evaluation and evaluation method.

A. Need of evaluation

Why we need evaluation? Establishment of supportive environment for LCL is costly and long process. No one university cannot manage it in short time. For long-term project, we need corresponding evaluation. Evaluation process will help to us to recognize pluses and limitations, via evaluation we can define early our weak points and can improve in early.

B. Evaluation method

For evaluation existing various type of methods. We will apply structure oriented evaluation model for this evaluation. Originally, this method developed for evaluation of e-learning [8-9].

The quantitative models for the assessment of e-learning quality considered usually are additive models. That means, depending on the considered aspects, which are measured based on a defined scale, a linear function containing corresponding weight factors is used like, e.g.,

$$Q = \Sigma\, a_i\, x_i$$

Here denote ai , $ai > 0$, given weight factors for the obtained measure values xi , $i = 1, \dots , k$, for the considered aspects. The advantage of this formula is, it is very easy. The disadvantage is that the choice of proper weight factors is subjective. Moreover, positive evaluation values can be obtained even in such cases if the targets of certain quality aspects have been failed. A possible logical inner structure of target structures remains out of consideration.

In contrast to linear approaches, we develop here a measure theoretical model for the assessment of an e-learning program. We consider an e-learning program whose quality is determined by k, $k \geq 1$, several aspects or characteristics $M1, \dots , Mk$. We assume that the quality of the single aspects can be measured by means of a given scale where the corresponding observation variables are ordinal or metrical ordered variables. Our aim is to develop an evaluation model for e-learning programs whose quality characterized as above by k several aspects $M_1, \dots , M_k$. For it we will construct a corresponding measure in sense of general measure theory. This requires in the context considered here two steps. First we will construct k corresponding efficiency measure spaces for description of quality of single aspects $M_1, \dots , M_k$. After that we will combine these spaces to a corresponding product space. This space will describe the considered aspect structure as a whole. The via the obtained product space defined product measure will be then our quality measure for evaluation of an e-learning program. For the implementation and application of our assessment approach, the paper rounded off by a statistical procedure for the estimation of scoring values for target structures based on adapted assessment checklists.

The advantage of the model considered here in comparison with linear models is that by the multidimensional consideration via the product measure the logical structure of a target structure evaluated as a whole [9].

C. Design of goal structure for evaluation

Based on structure oriented evaluation model we have to define main and sub goals of evaluation.

Main goal of evaluation is establishing supportive learning environment for LCL. How we can reach this main goal? There is some fact which we have can use to reach our main goal.

- Courses should have same credits.
- A course should be possible to select in every academic semester.
- Learner able to finish study early than defined date.

Main goal reached if each of this defined facts fulfilled. Therefore, we can define these facts like our sub goals. Each sub goal should be successful implemented to reach our main goal. That means by structure oriented evaluation model idea this structure we can define like serial structure (Fig.6).

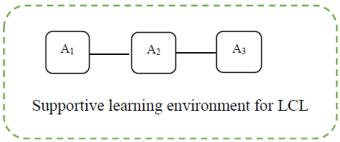

Fig.6. Goal structure of evaluation

By calculation rule of structure-oriented evaluation model if any of these sub goals cannot reach own target main goal of evaluation will evaluate as failed.

IV. CONCLUSION AND DISCUSSION

In conclusion we can summarize that learner centered learning is one of main approach of modern and future education. Relating to dynamic change of technology and behavior of young generation educators and universities have to support more individual and personalized study plan of learners'. As case study, showed universities try to synchronize credit pints of offering courses. Then this will be open new opportunities not only for learners this can be useful for universities to develop joint or flipped study programs together.

For discussion, we are highlighting several questions: How we can manage better our administration issues to support learner centered learning? How we can recognize problems relating to culture different behavior of our learners? How we

can use artificial intelligence and other well developing research results into learner centered learning?

We are looking to your valuable feedback and comments to our on-going work.

REFERENCES

[1] Piote Debies, “Effective Learner-Centered Approach for Teaching an Introductory Digital Systems Course”, IEEE Transactions on Education, Vol. 61, Iss.1, pp.38-45, 2018. DOI: 10.1109/TE.2017.2729498

[2] E. Cetin, C. Wijenayake, V. Sethu, E. Ambikairajah, "A flipped mode approach to teaching an electronic system design course", Teaching Assessment and Learning for Engineering (TALE) 2017 IEEE 6th International Conference, pp. 223-228, 2017.

[3] D.Matukhin, D.Bolgova, “Learner-centered Approach in Teaching Foreign Language: Psychological and Pedagogical Conditions”, XVth International Conference on Linguistic and Cultural Studies: Traditions and Innovations, Journal of Procedia - Social and Behavioral Sciences, Vol. 206, pp.148-155, 2015.

[4] Randall M. Moate, jane A.Cox, “Learner-Centered Pedagogy: Considerations for Application in a Didactic Course”, The Professional Counselor, Vol. 5, Issue 3, pp. 379–389, 2015.

[5] A. Reinert, N. Vollmann, M. Heyder, and W. Krautschneider, “New teaching approaches and student motivation lead to documented gains in engineering education,” in Proc. IEEE Front. Educ. Conf., Madrid, Spain, 2014, pp. 1–4.

[6] A. Lukkarinena, P. Koivukangasa, and T. Seppälä, “Relationship between class attendance and student performance,” Proc. Soc. Behav. Sci., vol. 228, pp. 341–347, Jul. 2016.

[7] W.Hardt, U.Tudevdagva, “Adaptivity and Digitalisation Enables Learner Centred Learning”, Journal Open Access Government. - pagesuite, November 2017, pp. 176-177, ISSN: 2055-7612, 2017.

[8] Source for figure: www.itnews.com.au

[9] U.Tudevdagva, W.Hardt, A new evaluation model for eLearning programs, Dezember 2011, Chemnitz.

[10] U.Tudevdagva, “Structure oriented evaluation model for E-Learning”, Chemnitz, Univ.-Verl., Vol.14, 2014

Based on the improved RNN-CRF named entity recognition method

Jinbao Xie[1], Baiwei Li [2], Yajie Wang[3], Yongjin Hou[4], Kelan Yuan[5], Youbin Yao[6]

[1,2,3]*Harbin University of Science and Technology (HUST)*

[4]*China Telecom*

[5,6]*Harbin International Technology Transfer Service Center*

[1]*jbxpost@163.com,* [2]*779552790@qq.com,* [3]*hyj1516@163.com,* [4]*38822009@qq.com,* [5]*6303454@qq.com*

***Abstract*—This paper proposes a method based on the improved RNN-CRF for the problem of Chinese named entity identification. It uses the Gated Recurrent Unit (GRU) network to extract the sentence features of the marked part of the corpus, and then integrates the conditional random fields (CRF) for entity tagging to complete the named entity recognition. The network performs feature extraction. The GRU network has the characteristics of less parameters, strong fitting ability, and high training speed. It reduces the time spent on training large-scale data, and is used in combination with CRF to mark a location in the CRF. Can use the marked information to get better Chinese entity recognition effect.**

Keywords- GRU, named entity recognition, CRF

I. INTRODUCTION

With the rapid development of Internet technology, humans have become accustomed to acquiring a large amount of knowledge from the Internet. However, with the continuous growth of network resources and the diversity of resources, methods for acquiring knowledge from the Internet have stagnated, so how to obtain information efficiently from the Internet And the discovery of new knowledge becomes more urgent. Named entity recognition has become essential as a basic task in the field of natural language processing. In recent years, computer performance has been continuously improved, and artificial intelligence has developed rapidly. The method of named entity recognition based on machine learning has become the focus of research on named entity recognition. Deep learning has also made some progress in research on named entity recognition. Named entity recognition is a fundamental part of many natural language processing applications. Named entity recognition is a sub-task of information extraction in the field of natural language processing. From the text data, the position of the entity is found and the entity category is correctly divided. For

example, question answering systems, automatic machine translations, etc. are all based on the further research of named entity recognition.

Named entity recognition is a research hotspot in the field of natural language processing. From the early methods based on lexicon and rules, to the traditional machine learning methods, and deep learning methods in recent years, the recognition effect is constantly improving. The neural network-based entity recognition model can process natural language processing of network resources from the perspective of algorithm knowledge more effectively by using natural language grammar, semantics, and other information, what's more it can open up neural network for the mining and representation of algorithm knowledge.

In this paper, we use the improved neural network RNN-CRF method to study the method of Chinese named entity recognition. Recurrent neural networks (RNNs) have been widely used in many natural language processing applications. An improved RNN network is proposed, which uses GRU (Gated Recurrent Unit) instead of RNN. Its purpose is to solve the deficiencies of RNN in the study of named entity recognition, and to capture long-distance impact in the sequence. To better achieve the effect of named entity recognition.

II. NEURAL NETWORK MODEL STRUCTURE

A.GRU Structure

This article uses the GRU (Recursive Recurrent Unit) of a recursive network recursive neural network. The GRU is an improved recurrent neural network (RNN). The state and output of a GRU (Gated Recurrent Unit) network are calculated as follows:

$$z = \sigma(U^z x_t + W^z s_{t-1}) \quad (1)$$

$$r = \sigma(U^r x_t + W^r s_{t-1}) \quad (2)$$

$$h = \tanh(U^h x_t + W^h (s_{t-1} * r)) \quad (3)$$

$$s_t = (1-z) * h + z * s_{t-1} \quad (4)$$

Where t is the sequence length, z is the update gate of the GRU, r is the reset gate of the GRU, and h is the hidden state at time t. * denotes multiplying by elements and multiplying the elements one by one to get a new vector.

z and r have the same form, but the parameters are different. The parameters U and W need to be learned during the training of the sample. r and z together control the new hidden state (s_t)from the previous hidden state (s_{t-1}) calculation. z is used to control the extent to which the state information at the previous time was brought into the current state. The value of z is greater. Explain that the status information from the previous moment brings in more. r is used to control the degree of

ignoring the status information at the previous moment, and the smaller the value of *r*, the more ignoring it is. Its structure is shown in Figure 1:

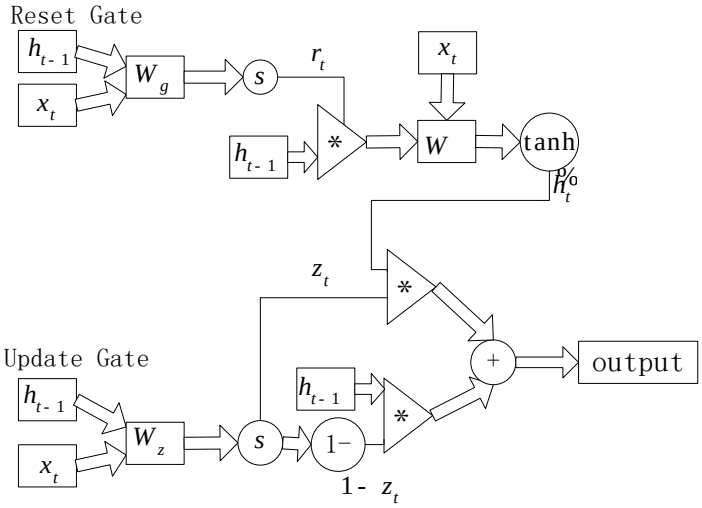

Fig. 1. The Gated Recurrent Unit model structure diagram

x_t denotes the input of model time *t*. The output of GRU at time *t* is defined as h_t. This expression also contains the above information and the following information. It is applicable to the task of named entity identification with many types of labels.

Conditional Random Field (CRF) is an algorithm commonly used in the field of natural language processing in recent years for named entity recognition. Some feature functions with artificial definitions are used as feature templates for name entity recognition research. For sentence given in the sentence In terms of location, different feature templates can be combined to form a new feature template. Using feature templates for sentence tagging, CRF has limitations on named entity recognition and the overall effect is not ideal. This paper proposes an improved model which combine the RNN and CRF together CRF. Its purpose is to solve the

limitations of CRF in the study of named entity recognition, which helps to achieve a better effect of named entity recognition of named entity recognition.

B.Named Entity Recognition Model

The output of the GRU at time t is denoted as h_t.The labeling result at time t is directly predicted and a named entity recognition model is established. The structure of the model is shown in Figure 2:

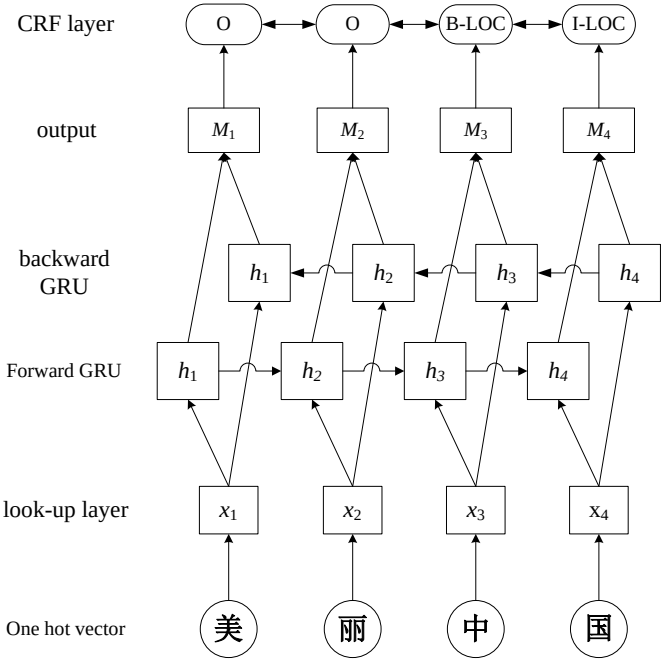

Figure 2 Overall model diagram

As shown in Figure 2, this paper first pre-processes the corpus and marks part of the corpus. In the pre-processing process, it first uses jieba firstly to cut words, segment words, and then use Word2vec to pre-train some of the segmented corpora. Then each word is divided into one line for labeling. This article uses the BIO tagging set in the labeling process, ie B-PER represents the first name of the person's name, I-PER represents the first name of the person's name, B-LOC represents the first name of the place name, I-LOC On behalf of non-first place names, B-ORG represents the first name of the organization, I-ORG represents the

non-headword of the organization, and O represents the word is not part of the named entity.

Then each word in the sentence is represented as a one-hot vector; in natural language processing, because machine learning cannot receive the corpora as input directly, it is usually necessary To digitize the linguistic number firstly, and the word vector is used to carry out the words in the language. In way of mathematics. In this paper, the one-hot vector is used to represent the word vector, and the character is transformed into the corpora with the unit of the sentence, and each word in the sentence is mapped from the one-hot vector to the low-dimensional dense word vector using the randomly initialized embedding matrix. As a neural network input.

Then the word vector is input into the GRU network for feature extraction and the matrix *M* for extracting sentence features is obtained through GRU network training.

Finally, the matrix *M* access conditions obtained through neural network GRU training are tagged with the sentence level of the airport CRF layer. The training process of the CRF model is divided into two parts. The first part is the establishment of the feature function set, and the second part is the estimation of model's parameter, which is the weight of the calculation function. The process of annotating a location by the CRF can use the labeled information and use Viterbi decoding to obtain the optimal sequence. Denote the tagged sequence of sentence length n with $y = (y_1, y_2, y_3, ..., y_n)$, and the score of $x = (x_1, x_2, x_3, ..., x_n)$ for length n is:

$$score(x, y) = \sum_{i=1}^{n} M_i, y_i + \sum_{i=1}^{n+1} Ay_{i-1}, y_i \quad (5)$$

Among them, *M* is the characteristic matrix *M* obtained through the GRU network, and *A* is the transition matrix *A* of the CRF. By performing exponentiation and normalization on this score, the probability value $p(x|y)$ of the annotation sequence can be obtained as follows:

$$p(x|y) = \frac{\exp(score(x, y))}{\sum_{y'} \exp(score(x, y'))} \quad (6)$$

In the model training, the likelihood ratio is selected by the maximum likelihood function. The log likelihood for the training sample (x, y) is as follows:

$$\log p(y|x) = score(x, y) - \log(\sum_{y'} \exp(score(x, y'))) \quad (7)$$

In the model prediction process, a dynamic programming Viterbi algorithm is used to solve the optimal decoding path. The highest probability *y* is shown in formula:

$$y = \arg\max_{y'} score(x, y) \quad (8)$$

III. EXPERIMENTS AND RESULTS

In the experiment, In order to measure the entity recognition's effect in the model objectively, the test corpora were annotated and the results were statistically calculated under the same environment. Through the analysis and comparison of a large number of test results, the results show that the improved neural network can be well applied to the named entity recognition tasks. The marked effect of the model is better than the RNN model.

This article uses the news corpus marked in January 1998 by the People's Daily as an experimental corpus. Because in the named entity Recognition mission , this article takes the recognition effect of the Chinese name, place name and organization name as the main evaluation objects in the experiment. At the same time, precision, P, Recall, R, and F1 measure values (F1-score, F) are used for statistical evaluation of names, place names, and institution names. The calculation method is shown in formula:

$$P = \frac{TP}{TP + FP} \quad (9)$$

$$R = \frac{TP}{TP + FN} \quad (10)$$

$$F = \frac{2TP}{2TP + FP + FN} \quad (11)$$

Among them, *TP* indicates that the positive class is predicted to be positive (True Positive), *FN* indicates that the positive class is predicted to be negative (False Negative), *FP* indicates that the negative class is predicted to be positive, and *TN* indicates that the negative class is predicted to be negative The number of classes, *F*, is the comprehensive evaluation index of precision rate and recall rate.

Through analysis and comparison of a large number of test results, the results show that the modified GRU-CRF model can be well applied to named entity recognition tasks, and the model's labeling effect has better recognition effect. Long Short-Term Memory (LSTM) is a neural network with good effect on named entity recognition. This paper compares the GRU-CRF model with LSTM-CRF model.

TABLE I. Comparison of test results of GRU-CRF model and LSTM-CRF model %

Model name		GRU-CRF	LSTM-CRF
LOC	*P*	92.00	93.31
	R	90.68	89.16
	F	91.34	91.18
PER	*P*	89.42	88.17
	R	81.80	85.64
	F	85.44	86.88
ORG	*P*	84.91	83.57
	R	84.15	86.78
	F	84.53	85.15

From the experimental data in Table 1, it can be concluded that in the GRU-CRF model, the recognition effect of the two types of entities in the names of persons and institutions is better than the LSTM-CRF model. The reason is that most of the name entities in the data set are Chinese names. Generally only consists of surnames and names. Such entities are simple in structure and require less long-distance mem ory information. The LSTM-CRF model has less impact on the recognition effect. In terms of entity recognition such as geographical names, the recognition effect of the LSTM-CRF model is slight. The recognition effect of LSTM-CRF model is slightly higher than that of GRU-CRF model in terms of entity recognition such as geographical names,the analysis is due to the fact that geographical and institutional names are generally longer and the long-range information captured by the LSTM plays an active role. Comparison of experimental data can be seen, The overall recognition effect of the GRU-CRF model is slightly better than the LSTM-CRF model. Recognition effect.

IV.CONCLUSION

This paper proposes a method of improving neural network GRU-CRF combination to study named entity recognition. This method proposes a new solution for named entity recognition. This method uses GRU instead of RNN to solve the problem that RNN is insufficient in naming recognition entity. In addition, the GRU can be preserved through various keeper features, and the characteristics will not be lost during the long-term propagation process, and when an error occurs,

only the weights that cause the error items need to be modified. The GRU has fewer parameters and the training speed is faster. The characteristics of the training time are shortened. The number of samples required during the training process is small. This solves the problem of insufficient corpora in the named entity recognition. The GRU has efficient and rapid training characteristics for the training corpora, and then combines CRF with sentence sequence annotation. Named entity recognition has a good effect.

REFERENCES

[1] Huang Z, Xu W, Yu K. Bidirectional LSTM-CRF models for sequence tagging[J]. arXiv preprint arXiv:1508.01991, 2015.

[2] Dong C, Zhang J, Zong C, et al. Character-Based LSTM-CRF with Radical-Level Features for Chinese Named Entity Recognition[C]//International Conference on Computer Processing of Oriental Languages. Springer International Publishing, 2016: 239-250.

[3] Ma X, Hovy E. End-to-end sequence labeling via bi-directional lstm-cnns-crf. arXiv preprint arXiv:1603.01354, 2016.

[4] Chiu J P C, Nichols E. Named entity recognition with bidirectional LSTM-CNNs. arXiv preprint arXiv:1511.08308, 2015.

[5] Matthew E. Peters, Waleed Ammar, Chandra Bhagavatula, Russell Power. Semi-supervised sequence tagging with bidirectional language models. ACL, 2017.

[6] WANG G Y. Research of Chinese Named Entity Recognition.Based on Deep Learning[D]. Beijing:Beijing University of Technology,2015:33-38. (in Chinese)

[7] FENG Y H, YU H, SUN G, et al. Domain-specific Terminology.Recognition Method Based on Word Embedding and CRF[J].Journal of Computer Applications, 2016, 36(11): 3146-3151. (in Chinese)

[8] Cho K, Van Merrienboer B, Gulcehre C, et al. Learning Phrase Representations using RNN Encoder-Decoder for Statistical Machine Translation. Computer Science, 2014

Numerical Optimization of Automatic Control System

Vadim A. Zhmud[1], Lubomir V. Dimitrov[2], Jaroslav Nosek[3], Hubert Roth[4]

[1]*Novosibirsk State Technical University (NSTU)*

[2] *Technical University of Sofia*

[3] *Technical University of Liberec*

[4]*University of Siegen*

[1]*zhmud@corp.nstu.ru,* [2]*lubomir_dimitrov@tu-sofia.bg,*
[3]*jaroslav.nosek@tul.cz,* [5]*hubert.roth@uni-siegen.de*

***Abstract* – The problem of control object with the use of feedback loop is extremely relevant, because only this method provides for the accurate control. The most difficult part of the task is design of regulators. Mathematical methods cannot be used for object containing delay link or nonlinear elements. For such complex objects the most effective method is numerical optimization. Due to the exixtanse of the smart software, sach as VisSim, this problem can be easily resolved without deep knowledges in the field of theory of feedback control. This paper gives most impotrant information about the numerical optimization of regulators by means of software VisSim.**

Keywords—control, regulator, PID, numerical optimization, modeling

I. INTRODUCTION

Object control with the help of feedback is one of the key methods of robotics. It is also used in all automation devices. Modern engineering is inconceivable without such systems [1–10].

The main difficulty in designing such systems is the calculation of the regulator. This paper gives an automatic method for calculating regulators, which does not require deep special mathematical skills and deep knowledge in the theory of automatic control. The designer only needs to get acquainted with the very foundations of this theory and the methods of numerical optimization in practice.

A typical block diagram of the automatic control system is shown in *Fig.* 1. For the most common case of $W_3(s)=1$ and without considering the noise of the sensor, the loop is simplified to the structure shown in *Fig*.2.

Fig.1. Structure for calculation of ACS

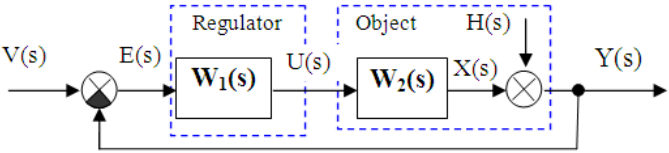

Fig.2. The Simplified Structure of ACS

The most commonly used regulator contains proportional, integrating and derivative links. The transfer function of such a regulator, called the PID-regulator, is given by the ratio (1):

$$W_P(s) = K_P + \frac{K_I}{s} + K_D s. \qquad (1)$$

Here, K_P, K_I, K_D are constant coefficients which are required to determine with the procedures as a result of numerical optimization.

Another form of regulator (1) is:

$$W_P(s) = \frac{K_{П} s + K_{И} + K_{Д} s^2}{s}. \qquad (2)$$

More sophisticated regulators may include additional derivative and (or) integration. For example, if the regulator contains both these additional channel, its transfer function might look like this:

$$W_P(s) = K_{П} + \frac{K_{И}}{s} + \frac{K_{И2}}{s^2} + K_{Д} s + K_{Д2} s^2. \quad (3)$$

Such regulator is named PI^2D^2 or PIIDD-regulator.

II. METHOD FOR THE DESIGNING OF REGULATORS

Among the methods of solving these problems, the following ones can be specified:

1. **Analytical** (mathematical) **methods**.
2. **Tabular methods**.
3. **Empirical tuning**.
4. **Mathematical modeling** for the study of properties of the system.
5. **Numerical methods for optimization** of the locked loop model or a real system with the object based on built-in routines of modern software packages for modeling and mathematical calculations, such as *VisSim*.

Numerical optimization is the most effective method of regulators tuning, if the object model is stationary and known with sufficient accuracy. It uses a mathematical modeling (simulation) of the system that contains the object and the regulator.

III. PROCEDURE FOR THE AUTOMATIC OPTIMIZATION OF REGULATORS

To run optimization in *VisSim*, a developer should do the following things.

1. Setting of one or more optimized parameters using the "parameter unknown" blocks.

2. Setting the initial (starting) values to each of these parameters, giving a constant to the input of these blocks

3. Ensuring of the use of these parameters as regulator coefficients to be optimized. For this purpose, it is useful to give them the names of functional variables (for example, *P, I* and *D* are the coefficients of the proportional, integral and derivative links). Assigned names should be used to call these functions as appropriate gains. A developer can use multiplier blocks or directly blocks of gain factors.

4. Ensuring of calculation of the cost function and sending of the result to the "cost" block, which should be the only one in the project. For this goal, a calculator is formed, the output of which is connected to the input of this block.

5. Providing of an indication of the optimization result, for which it is advisable to use the value indicator block at the output of each of the "parameter unknown" blocks.

In addition, it is possible, but not necessary, to reflect the value of the resulting transient process on the oscilloscope block and the value of the cost function on such a unit and (or) on the numeric value indicator unit.

IV. STRUCTURE FOR THE REGULATOR OPTIMIZATION

To optimize the regulator, it is required to apply a structure containing the system model and a number of auxiliary modules. The model of the system includes a regulator and an object, and other specific blocks can also be included.

In addition to the system model, the structure should contain:

1. Means of formation of test signals.
2. Means of indicating the results of optimization.
3. Means for calculating the value function.
4. Means of formation of initial values of parameters.

5. Optimization tool (performing the analysis of cost function, calculating new parameters, analyzing new costs and deciding on further steps - continuing the search or stopping it).

A possible structure for optimization is shown in *Fig*. 3.

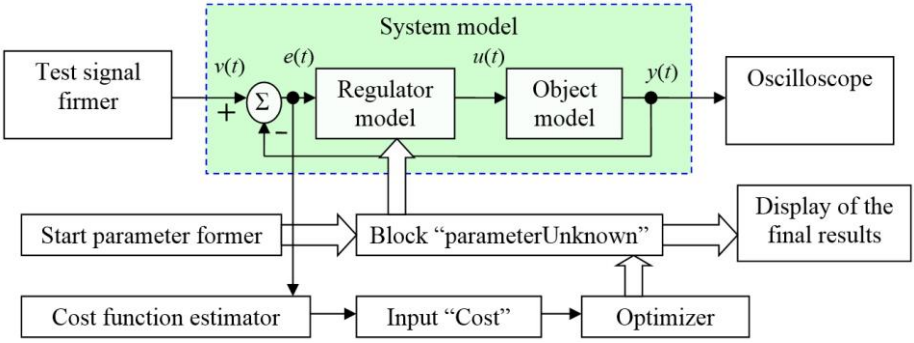

Fig. 3. A typical structure for optimizing of regulator of loocked system with feedback

This structure works as follows. The model of the object and the regulator model together form a model of the locked system. The means for generating test signals is a step jump generator, sine wave oscillator or something similar. For linear systems step is the most convenient and indicative kind of the input signal. The cost function evaluation mean calculates the value of the cost function based on the results of each test. The starting values are fed through the optimization unit to the regulator, specifying the values of its parameters at the very first test of the system from the series of model tests. The indicator means contains an oscilloscope showing the final transient process in the system, and displays the final values of the optimized parameters (regulator coefficients).

The optimization unit performs the following functions:

1. During the first test, it sets in the regulator those coefficients that are entered by the operator into the former of the start values, and also displays these values on the displays.

2. It started every next test.

3. Based on the results of the previous test, it takes in its input and analyzes the value of the calculated cost function in comparison with its previously obtained values.

4. It analyzes the stopping criteria.

5. If the stopping criteria are not met, then according to one of the selected algorithms, it calculates the new value of the set of regulator coefficients, and then

returns to the repetition of all operations starting from step 2. If the stopping criteria are fulfilled, proceeds to step 6.

6. It selects the regulator coefficients corresponding to the lowest value of the cost function.

The stopping criterion can be one of the following:

a) the number of iterations has exceeded the specified value;

b) it is established that further implementation of this algorithm will not lead to a decrease in the value function by an amount exceeding the specified permissible optimization error;

c) an error occurred that makes it impossible to continue the procedure, for example, exceeding one of the parameters or one of the calculated values of the largest permissible value (for different versions of the program this is $10^{28} – 10^{30}$, etc.).

The cost function calculated in the structure implicitly depends on the regulator parameters and on the test actions generating the transient process, since the error function of the system $e(t)$ depends on these parameters. When solving the problem of numerical optimization, it is required to find such values of the regulator coefficients for which the cost function reaches a minimum value. Since the error in the system depends on the regulator coefficients, the entire cost function will depend on these coefficients. The solution of this problem is called the optimum, in our case the minimum. It is necessary to distinguish between local and global minima. Local minima are solutions in which small changes in any parameter cause an increase in the cost function; however, this does not apply to big changes in these parameters. The global minimum can be the only. This is the solution that ensures the least value of the cost function for all parameters from the range of their allowed values.

Various algorithms for finding the minimum can be applied. The correctness of the choice of the optimization method depends on the properties of the problem: the best method for one task may be the worst or completely inapplicable for another task.After rounding of the obtained coefficients, it is necessary to verify the admissibility of such rounding and the preservation of the achieved type of transient processes (minor changes are allowed) and approximate preservation of the value of the cost function. To do this, it is necessary to fill the blocks of preset values by “copy-paste” method with the received parameters values and round these parameters, then in the “optimization” menu one should uncheck the “optimize” window, select the “remember graphs” checkbox in the oscilloscope configuration menu and start the simulation again.

This method of verification is necessary to exclude a non-rough solution, i.e., a solution that ensures a given quality only if the values of the parameters are extremely accurately matched to their values.

The presence of a non-rough solution can arise in the case, for example, when an object contains an unstable oscillatory link, for the stabilization of which mathematical modeling suggests the introduction of a blocking filter tuned to the same frequency in the regulator. Such a decision has no practical value, since its implementation is impossible, and also because a sufficiently accurate identification of such an object is also impossible, that is, an object with such properties is most likely not exactly in accordance with the model used, but the implementation of the regulator, most likely, does not coincide with the calculated regulator.

Example 1. *Fig*. 4 shows an example of a PID-regulator optimization project for some linear object.

The most important principles of application of automatic optimization are the following.

1. Not only the step of sampling in time, but also the simulation time (duration) should be chosen reasonably. We should strive to ensure that the transient process ends in approximately 70–80% of the simulation time. If the transient process is not yet finished, the optimization results should be questioned. If, however, the transient process ends too quickly with respect to the simulation time, hence, the cost function includes the result of the signal processing, which is weakly related to the quality of the transient process.

2. It is advisable to strive to ensure that the cost function at the end of the transient process would reach a stable level and completed its growth by some steady-state value. If this is not the case, then, the choice of simulation duration makes a significant contribution to the cost function and, therefore, to the optimization result, too. The growth of the objective function at the end of the simulation time may also indicate some errors or incorrectness of using the optimization mode, for example, inadequate consideration of factors such as noise or the ADC sampling error that performs the measurement conversion of the output signal.

3. If optimization is carried out using a real object or using the most detailed model, up to the ADC or noise, it should be noted that the control error cannot be strictly zero in practice. In this case, it is necessary to use the maximum permissible error as the boundary value. In any real system, one can specify a sufficiently small value of the error, which can be considered negligibly small, that is, the absolute error value falling into the interval between zero and this value can be equated to zero error value. In this case, such a situation can be considered an achievement by error of zero level. It is necessary to use this in the objective function, that is, to introduce non-linearity of the “dead zone” type. Then the integral of such an error will be zero, which corresponds to the natural acceptance of such an error inessential for the operation of the system.

4. As a result of optimization, a structurally unstable system can result. It should be ensured that the resulting system is sufficiently rough so that it can be used in practice. To do this, it is sufficient to round off the coefficients obtained, leaving only 2–3 significant digits in each of them, and repeat the simulation. The optimization procedure should not be repeated. The resulting transient processes should not differ too much from the processes obtained with the exact values of the regulator parameters calculated as a result of the optimization procedure. If this is not the case, then the system is not rough, and its results are not reliable, that is, the resulting regulator can not provide the required quality of functioning of a real system.

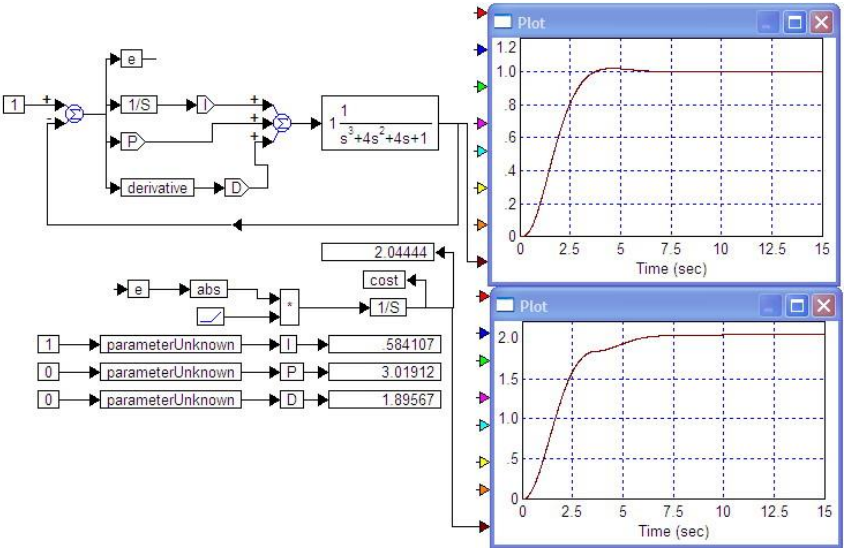

Fig. 4. The project of automatic optimization of the PID regulator

Example 2. Consider the problem of optimizing a PID regulator for an object with the following transfer function:

$$W(s) = \frac{\exp(-10s)}{(20s+1)(s^2+2s+1)}. \qquad (4)$$

The corresponding structure of the object is shown in *Fig*. 5. The structure of PID regulator is shown in *Fig*. 6. The structure for optimizing of PID-regulator

as a whole is shown in *Fig*. 7. In this case, the object and the PID-regulator are assembled into composite blocks in order of clearer picture.

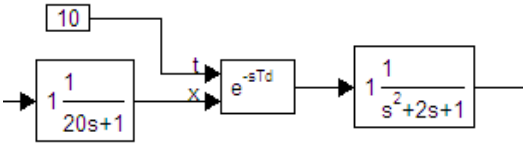

Fig. 5. The structure of the object of automatic optimization of PID-regulator from Example 1

After the optimization procedure is started, the values of the required PID-regulator coefficients are obtained in the windows of the optimization unit's display, as shown in *Fig*.8. The resulting transient process is shown in *Fig*. 9. The transient process ends in about 70*s*. The overshoot is negligible (about 2%), the static error is zero (which is natural when using the PID-regulator).

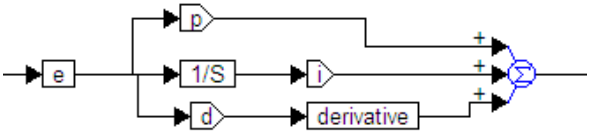

Fig. 6. Structure of the PID-regulator (for all cases)

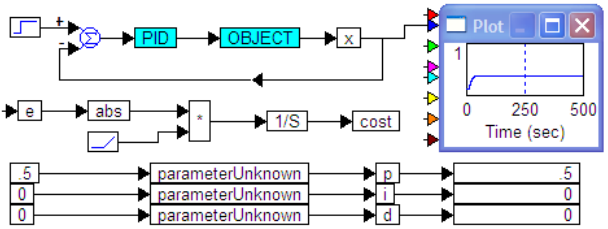

Fig. 7. The structure of the system for automatically optimizing the PID-regulator from Example 1

The next step is to check the result for roughness. For this goal, we round off the results. We set k_p=1.5; k_i=0.052; k_d=6.5. The resulting transient process almost completely coincides with the process shown in *Fig*.10, from which it follows that the system is rather rough.

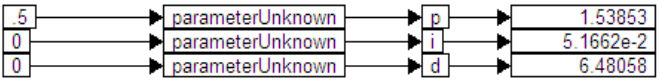

Fig. 8. The result of optimizing the PID-regulator from Example 1

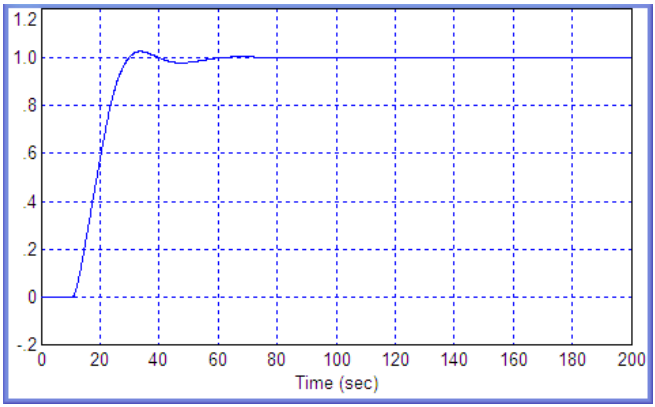

Fig. 9. The transient process resulting from the optimization of the PID-regulator from Example 1

It is also possible to demonstrate (but not prove) the optimality of the obtained solution. To do this, it is sufficient to add an indicator of the value of the cost function to the structure, after which to change the individual coefficients in the direction of increasing and decreasing. If the system is optimal, then any change in any coefficient will give an increase in the cost function. With the obtained coefficients, the value of the cost function is 231.5.

We can set the increment to the proportional coefficient by 0.2. When this coefficient is increased by this value, the value function becomes 292.0, and with a decrease it is equal to 371.8. The graphs of the corresponding transient processes are shown in *Fig*. 10.

Similarly, we set the increment to the coefficient of the integrating path by a value of 0.04. With an increase in this coefficient, the value function becomes 285.5, and with a decrease of 277.5. The corresponding transient processes are shown in *Fig*. 11.

Let us change the coefficient of the derivative path by 0.4. With the increase of this coefficient, the value function becomes 244.3, and with a decrease it is equal to 222.7. The corresponding transient processes are shown in *Fig*. 12.

The latter actions, seemingly, refute the assertion that the obtained values of the PID-regulator coefficients are optimal. However, the conclusions should not be rushed. The point is that we rounded out the optimization results. If we take more precise results, namely, k_p=1.538; k_i=0.0516; k_d=6.4, then the value function takes the value 217.0. Therefore, it nevertheless should be recognized that the tests carried out have confirmed the optimality of the result obtained (although this acknowledgment refers to the result with an accuracy of four significant digits). The changes in the graphs of transient processes during rounding are not significant, so the rounded value of the regulator parameters can be considered optimal in some approximation.

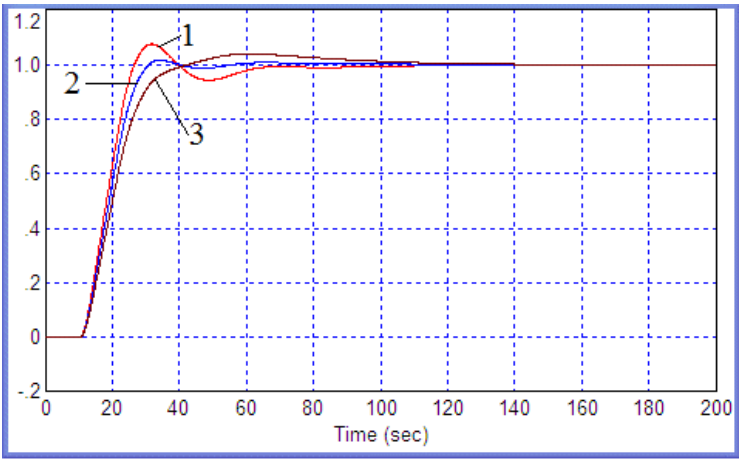

Fig. 10. Transients from Example 1 with proportional link coefficient changes: 1 – increase, 3 – decrease, 2 – initial value

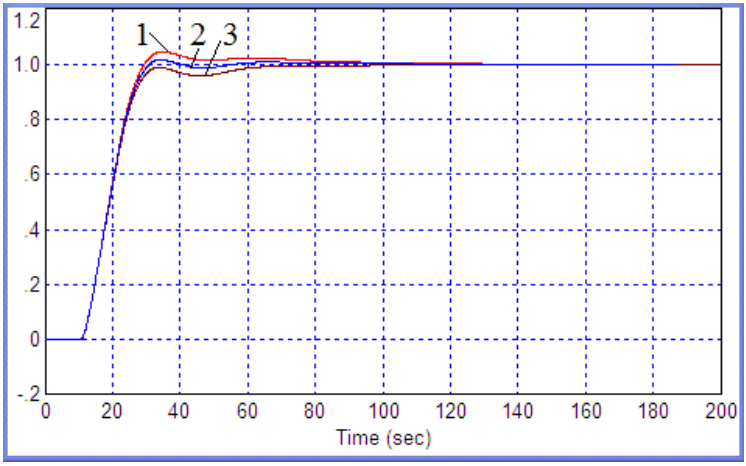

Fig. 11. Transients from Example 1 with changes in the coefficient of the integrating link: 1 – increase, 3 – decrease, 2 – initial value

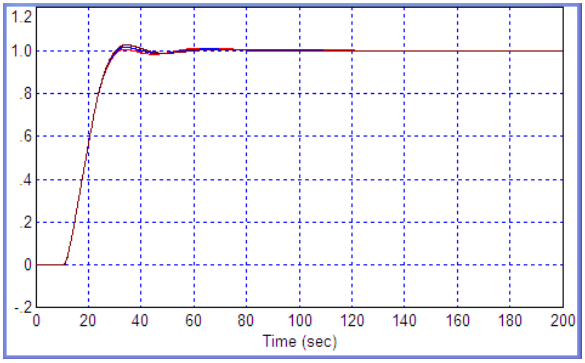

Fig. 12. Transient processes from Example 1 with changes in the coefficient of the derivation link: all lines merge

V. FORCED LIMITATION OF THE FREQUENCY RANGE OF THE MODEL USED IN OPTIMIZING OF THE REGULATOR

A developer can forcefully limit the frequency range obtained as a result of optimization of the system due to the fact that an additional inertial link, filter or delay link is introduced into the existing model of the object, which begins to affect only at those frequencies, at which he has not reliable data on the phase shift in the

real object model. This method is based on the assumption of the worst situation. Optimization of the regulator for such a deliberately degraded version of the model of the object will give such a regulator, which with a high degree of probability will successfully work in a system with a real object. Fig. 13 shows a modified structure for this purpose to optimize the regulator. This method is patented and its effectiveness is proved by modeling.

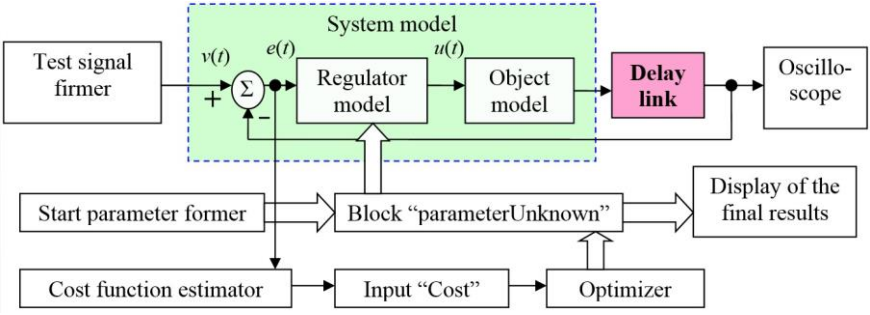

Fig. 13. Modified structure for optimizing the feedback loop regulator

Example 2. Let us solve the problem, which consists in optimizing the PID-regulator for some object. We use the structure of *Fig*.14. We specify the delay in the element that limits the speed of the object, at the level of 0.05 *s*. *Fig*. 15 shows the obtained transient process, and the resulting coefficients, according to *Fig*. 14, are equal to k_p=1380; k_i=11.2; k_d=23.19. The resulting transition process is shown in *Fig*. 15 (line 1).

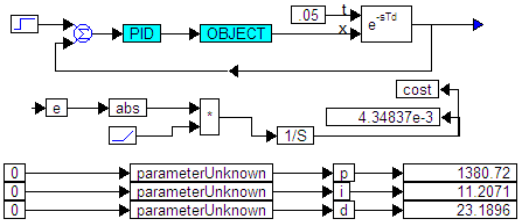

Fig. 14. A modified block diagram for optimizing the regulator in Example 2

Based on this example, we can conclude that the artificial limitation of object model speed is effective for designing a regulator by the method of numerical optimization. This method allows solving even such problems that are formally incorrect for this method.

In addition, this method allows us to supplement the model, which is not well known, in such a way that the result of the simulation is in sufficient agreement with the result of the practical use of this regulator. Indeed, if the model of the object is known in a limited frequency band, the hypothesis that beyond the limits of this frequency band there is a decisive action of the delay link, therefore, when optimizing the regulator, a model supplemented with such a delay is used.

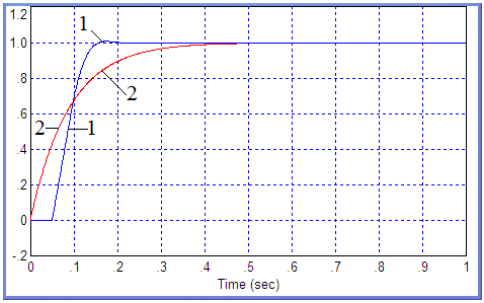

Fig. 15. The transient process in a system optimized according to the structure of Fig. 14 with an integration step of 0.01 s (line 1), as well as a process with no delay (line 2)

For comparison, we can consider the process in the absence of delay (*Fig*. 15, line 2). It is also possible to consider a family of transient processes when the delay is varied from 0.2 *s* to 0.6 *s*, as *Fig*. 16 shows.

If the actual object has such a delay, the system will be stable, if the object does not have a delay, or it is less, the system will also be stable. Finally, if the frequency band in the object is limited not so much by delay, as by a higher-order filter (affecting this frequency band), then in this case the received regulator will provide stable control with a sufficiently high quality (i.e., with a slight overshoot).

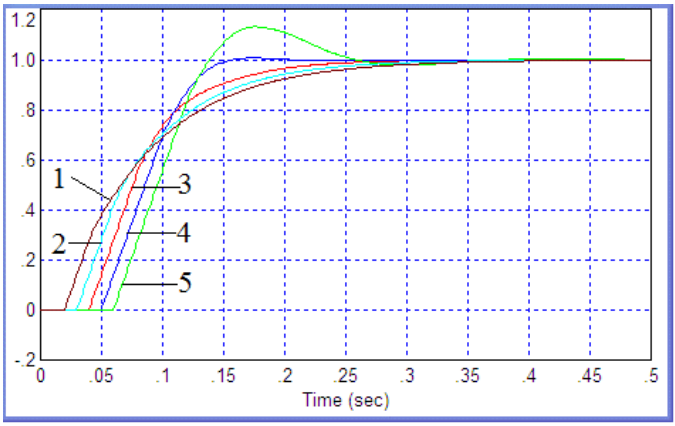

Fig. 16. Transient processes in a system optimized according to the structure of Fig. 14 with different delay values, the delay value can be determined from the beginning of the graphs: the line 1 is 0.2 s; line 3 is 0.4 s; line 3 is 0.5 s and so on

VI. MODIFICATION OF THE COST FUNCTIONS

6.1. Providing of the power saving

To optimize a feedback system, the structure shown in *Fig*. 3 can be used. This structure can be generalized and simplified by the structure shown in *Fig*. 17. Here the cost function calculator can be generally called the "signal analyzer".

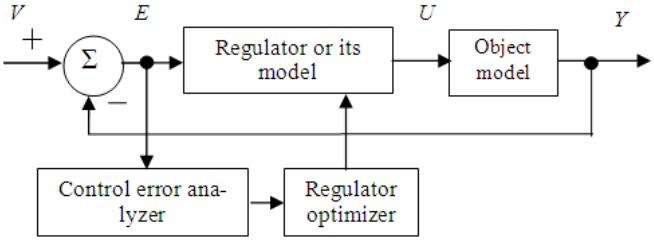

Fig. 17. Generalized and simplified structure for system optimization

In this case, signal analyzer is connected only to the output of the subtractor, which calculates the control error. If a composite cost function is used, additional inputs of this analyzer can be used, connected to other points in the system model.

For example, to provide energy savings in the cost function, an integral of the square of the control action can be introduced, which represents the generalized control energy. The corresponding structure is shown in *Fig*.18. In fact, the role of the signal analyzer is played by two blocks: a control error analyzer and an energy cost analyzer. The signals from the outputs of these blocks are fed to the optimizer, where they are added together with the weight coefficients. The adder can be selected from the optimizer structure and shown in an explicit form, which will formally form a new structure, but the essence of it will remain the same.

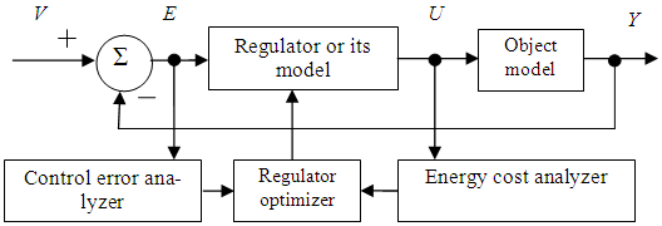

Fig. 18. Generalized and simplified structure for system optimization

This structure of the model for optimizing the feedback system works as follows. The simulation software *VisSim* performs a multiple simulation of the action of the specified structure. At the input of the structure, which is the positive input of the subtractor, the input signal *V* is fed in the form, for example, of stepwise action. The negative input of this subtractor receives the output signal of the model of the object *Y*, which is also the output signal of the structure. The subtractor calculates the difference of these signals, called error *E*. The error is converted by the regulator into the control signal *U*, which is input to the object model input. If the error is positive, the control signal affects the model of the object so that the output signal of the object model increases, and the error thereby decreases. If the error is negative, then the control signal affects the model of the object so that the output of the object model decreases, and the error for the account of this increased.

If the error is zero, the control signal affects the model of the object so that the output signal of the object model does not change, and the error remains zero. The regulator optimizer generates the starting values of the regulator coefficients according to the given algorithm, analyzes the outputs of the analyzer of achievement of the control goal and the energy cost analyzer, calculates the cost function and forms on this basis new values of the regulator coefficients. Using any of the methods of multidimensional optimization (for example, the *Powell* method) the optimizer searches for such values of the regulator coefficients that provide the minimum value of the cost function. These coefficients are the result of applying

the structure of the model to optimize the feedback system. They are extracted from the optimizer's memory and used in the production of the feedback system. If the model of the object is determined quite accurately, then the system works with the same quality and accuracy indicators that were achieved in modeling using the described structure of the model. Thus, the task is solved. If the model of the object is determined only in a limited frequency range, an element with a limited speed, for example, a delay link, as suggested earlier, can be used, see *Fig*. 13.

Energy-saving regulators are particularly effective in saving energy costs for control if the integrator is included in the object model. Indeed, in this case, energy is consumed only in the process of transferring an object from one state to another, and the stay of an object in some equilibrium state does not require the expenditure of control energy. An example of such systems is the transition of a satellite from one stationary orbit to another, and so on.

6.2. The detector of the error growth

In the objective function, we can also add the integral of the positive part of the product of the error to its derivative as a term. A developer should also use a weighting factor.

$$\Psi_2(T) = \int_0^T \{R[e(t)de(t)/dt] + |e(t)|t\}dt \,. \quad (5)$$

$$R[f] = \begin{cases} f, f > 0; \\ 0, f < 0. \end{cases} \quad (6)$$

Here *R* is the lower limiter that passes only the positive signal, and if the input signal is negative, but zero is output at its output.

The logic of this modification is this: if the error and its derivative coincide in sign, this means the wrong development of the transient process, the error increases when it should decrease or decrease when it should increase. The presence of such sections of the transient process is undesirable, such areas arise when the process has overshooting and (or) oscillations.

Example 3. Let us consider an object whose transfer function contains a second-order link and a delay link:

$$W(s) = \frac{\exp(-2st)}{10s^2 + 0{,}1s + 1} \,. \quad (7)$$

The model of this object is shown in *Fig*. 18. The structure of the system for optimization with the result obtained is shown in *Fig*. 19. The resulting transient processes are shown in *Fig*. 20. We introduce the error growth detector in the cost function. In this case, only a weight function of at least 100,000 functions efficiently, as shown in *Fig*. 21. The resulting transient processes are shown in *Fig*. 22.

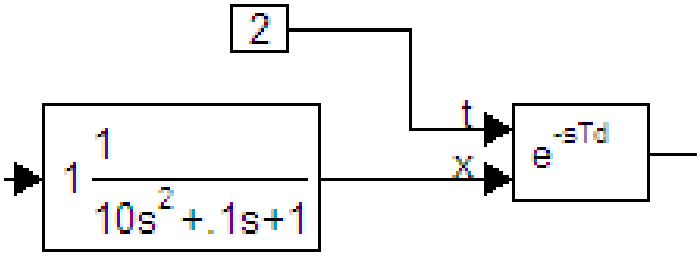

Fig. 18. Structure of the object for modeling from Example 30

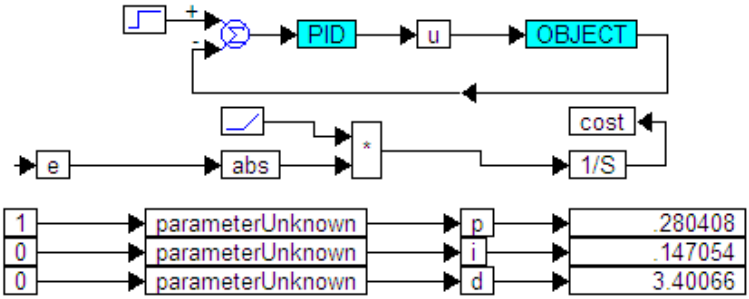

Fig. 19. The structure of the entire system from Example 3

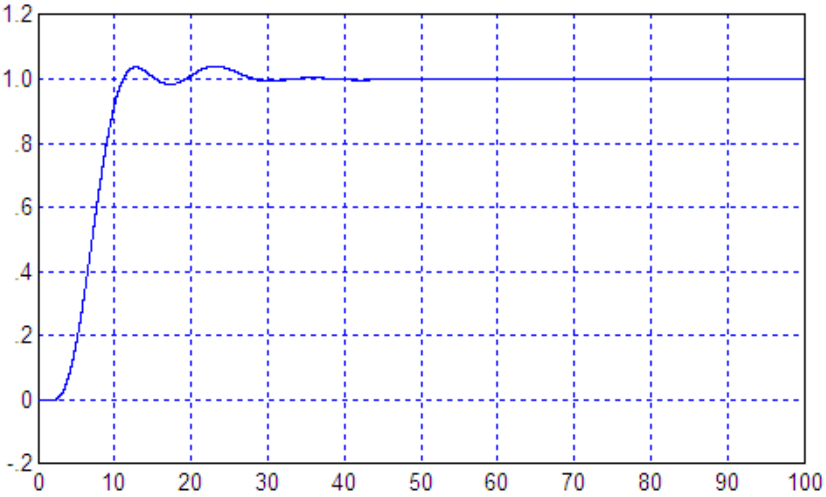

Fig. 20. Transient process in the system of Example 3

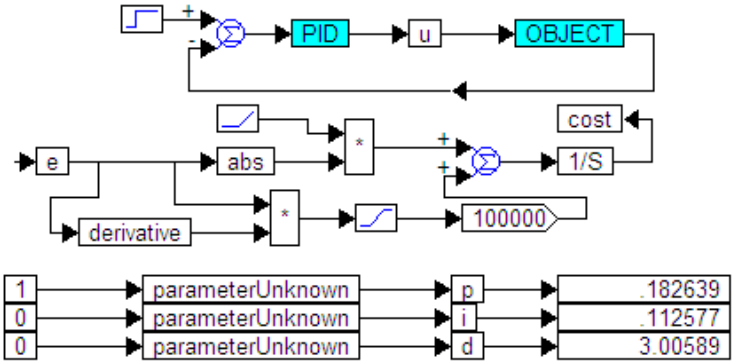

Fig. 21. The structure of the entire system of Example 3 using the error growth detector

Fig. 22 shows the output signal of the error detector (before integration), which took place in the structure of *Fig*.19. In the structure of *Fig*.21 this signal is practically zero (in the same axes the remnants of this signal merge with the axis).

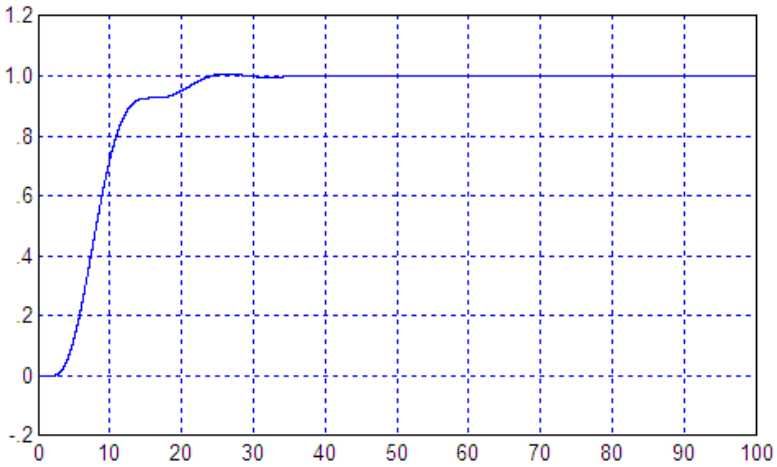

Fig. 22. The transient process in the system according to the structure of Fig. 21

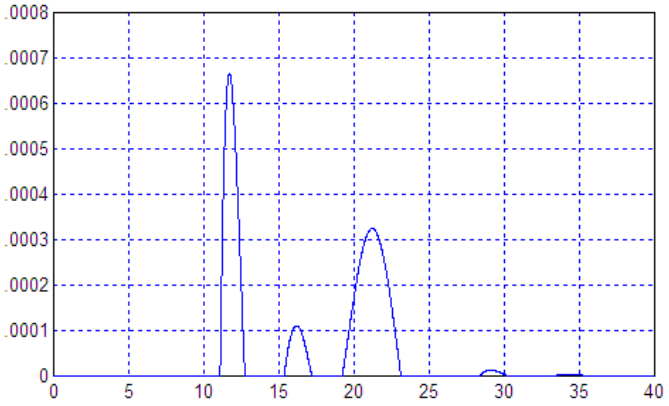

Fig. 23. The output signal at the output of the error detector delimiter (up to the integrator) in the system according to the structure of Fig. 19

VII. CONCLUSION

In this paper, we consider methods for calculating of regulators for controlling linear and nonlinear objects. Since analytical methods are inapplicable in the case of nonlinear objects, and even in the case of linear objects of great

complexity, for example, with elements of pure delay, numerical optimization methods are by now the only tools for solving these problems. The paper formulates the basic requirements for the system and the mathematical apparatus and gives the requirements for the physical feasibility of the model.

In this paper, we do not describe the control technique using local and pseudo-local feedbacks, did not give detailed classification of adaptive systems and authorial structures of adaptive systems, not considered systems with competitive quality criteria. The papers of the authors published in the journal "Automatics & Software Engineery", in the proceedings of international conferences and in other publication [1–10].

REFERENCES

[1] V. Zhmud., A. Liapidevskiy, E. Prokhorenko. "The design of the feedback systems by means of the modeling and optimization in the program vissim 5.0/6". 2010. Proceedings of the IASTED International Conference on Modelling, Identification and Control, pp. 27–32.

[2] V. Zhmud, O. Yadrishnikov, A. Poloshchuk, A. Zavorin. "Modern key techologies in automatics: Structures and numerical optimization of regulators". 2012. Proceedings - 2012 7th International Forum on Strategic Technology, IFOST 2012, paper № 6357804.

[3] A.A.Voevoda, V.A.Zhmud, R.Y. Ishimtsev, V.M. Semibalamut. "The modeling tests of the new pid-regulators structures". (2009) Proceedings of the IASTED International Conference on Applied Simulation and Modelling, ASM 2009, pp. 165–168.

[4] V. Zhmud, L. Dimitrov, O. Yadrishnikov. "Calculation of regulators for the problems of mechatronics by means of the numerical optimization method". 2014. 12th International Conference on Actual Problems of Electronic Instrument Engineering, APEIE 2014 - Proceedings, paper № 7040784, pp. 739–744.

[5] V. Zhmud, V. Semibalamut, A. Vostrikov. "Feedback systems with pseudo local loops". 2015. Testing and Measurement: Techniques and Applications - Proceedings of the 2015 International Conference on Testing and Measurement: Techniques and Applications, TMTA. 2015, pp. 411–417.

[6] G.V. Sablina, I.V. Stazhilov, V.A. Zhmud. "Development of rotating pendulum stabilization algorithm and research of system properties with the controller". 2016. 13th International Scientific-Technical Conference on Actual Problems of Electronic Instrument Engineering, APEIE 2016 - Proceedings, 3, paper № 7807046, pp. 165–170.

[7] V. Zhmud, O. Yadrishnikov. "Numerical optimization of PID-regulators using the improper moving detector in cost function". Proceedings of the 8-th International Forum on Strategic Technology 2013 (IFOST-2013), vol. II, 28 June – 1 July. Mongolian University of Science and Technology, Ulaanbaator, Mongolia. IEEE organized. 2013. P. 265–270. http://www.must.edu.mn/IFOST2013/

[8] V.A. Zhmud, A.A. Voevoda, R.Yu. Ishimtsev, V.M. Semibalamut. "New structures and methods of the scalar and multichannel regulators for non-

linear and/or delayed objects". Proceedings of DST-RFBR-Sponsored Indo-Russian Joint Workshop on Computational Intelligence and Modern Heuristics in Automation and Robotics. S. V. National Institute of Technology, Surat – 395 007, Gujarat, India. 20th - 22nd September 2010. pp. 63–67.

[9] V. Zhmud, L.Dimitrov. "Designing of complete multi-channel PD-regulators by numerical optimization with simulation". International Siberian conference on control and communications (SIBCON–2015): proc., Omsk, 21–23 May, 2015. – Omsk : IEEE, 2015. – Art. 129 (6 p.). ISBN 978-1-4799-7102-2. - DOI: 10.1109/SIBCON.2015.7147059.

[10] Zhmud V. A. Numerical Optimization of Locked Automatic Control System in Software VisSim: New Structures and Methods: monograph / V. A. Zhmud, L. V. Dimitrov, J. Nosek. - Novosibirsk: ZAO «KANT». https://www.researchgate.net/publication/325012120_Numerical_Optimization_of_Locked_Automatic_Control_System_in_Software_VisSim_New_Structures_and_Methods

A Sub-Nyquist Spectrum Sensing Method Based on Joint Recovery of Distributed MWCs

Jianxin Gai[1], Xiao Teng,[2], Hailong Liu[3], Ziquan Tong[4]
[1,2,3,4]*Harbin University of Science and Technology (HUST)*
jxgai@hrbust.edu.cn[1]

***Abstract*—The recently proposed sub-Nyquist spectrum sensing method based on Modulated Wideband Converter (MWC) can perform sampling at a rate far below Nyquist frequency, which relieves sampling pressure from wideband spectrum sensing. However, the success rate is far from satisfactory due to the influences of shadow effect and so on. In this paper, we present a distributed sub-Nyquist wideband spectrum sensing method using joint recovery technique based on multiple MWCs. The proposed sensing method can significantly improve the sensing performance with the increase of node numbers by making full use of the joint sparse structure across multiple signals and the diversity of sensing matrices. Numerical experiments show that, compared with separate sensing method, the proposed approach enhances the sensing performance in terms of success rate, and it even can achieve a success when the separate sensing for each MWC node fails.**

Keywords—sub-Nyquist, distributed spectrum sensing, joint recovery, sparse wideband signal

I. INTRODUCTION

Cognitive radio can achieve dynamic spectrum access, providing a new solution for efficient utilization of spectrum resources. Fast spectrum sensing for multiple channels in a wide frequency band is the premise and foundation for the realization of cognitive radio [1]. However, wideband spectrum sensing faces the pressure of high sampling rate [2-3]. The traditional method of spectrum estimation requires that the sampling rate is not less than the Nyquist frequency, which is undoubtedly a big problem for the radio signal with the bandwidth of GHz. The development of analog-to-digital conversion hardware has a certain distance from this requirement.

The recent emerging sub-Nyquist sampling approach named Modulated Wideband Converter (MWC) provides a new acquisition and processing method for sparse wideband signals. According to MWC, a sparse wideband signal can be recovered perfectly from fewer non-adaptive measurements than the number

prescribed by the Nyquist theorem, provided the sensing matrix conforms to some condition [4-5]. Compared with other sampling methods, MWC has the strength that it can be implemented using existing devices with a lower-dimensional sensing matrix, and the original signal can be perfectly recovered from samples at sub-Nyquist rate. The MWC has tremendous potential impact because of the longstanding, proven usefulness of spectral signal models in many engineering and scientific applications [6]. Although MWC can be employed to realize sub-Nyquist sampling on some condition, nevertheless the recovery performance of a single MWC is still far from satisfactory. Furthermore, spectrum sensing for cognitive radio requires multiple sensors to work in a cooperative manner to conquer the problem that a single sensor cannot do. The distributed system is expected to overcome the hidden terminal problem which is caused by the severe multipath fading and the shadowing effect [7]. However, the distributed sub-Nyquist sampling method based on MWC has not been researched sufficiently, and the existing methods are incompetent for the distributed sensing model of multiple MWCs.

In this paper, we present a distributed sub-Nyquist spectrum sensing method based on multiple MWCs. By exploiting the joint sparse structure across the signals, we propose a highperformance joint recovery algorithm. Numerical experiments demonstrate that, the proposed sensing approach based on joint recovery can significantly enhance the spectrum sensing performance.

II. MWC OVERVIEW

MWC is a sub-Nyquist sampling method for sparse wideband signals. It adopts spread-spectrum technique to deliberately alias all the subbands to the baseband, which allows the low rate samples to incorporate complete information of the original signal. As shown in Fig. 1, an MWC system has m parallel channels. The input signal $x(t)$ enters m channels simultaneously. In the ith channel $x(t)$ is mixed by Tp -period ($fp = 1/Tp$) pseudo-random signal $p(t)$.

After that, the signal is truncated in the frequency domain by an anti-aliasing lowpass filter and then sampled at the rate $f_s = 1/T$ which matches the cutoff $1/2T$ of the filter $h(t)$.

Applying classical Fourier analysis to MWC, the spectrum relation between the output and the input can be derived as follows in $f \in [-f_s/2, f_s/2]$,

$$Y_i(e^{j2\pi fT}) = \sum_{n=-\infty}^{\infty} y_i(n) e^{-j2\pi fnT} = \sum_{n=-l_0}^{l_0} c_{in} X(f - nf_p) \quad (1)$$

where c_{in} are the Fourier series coefficietns of $p_i(t)$.

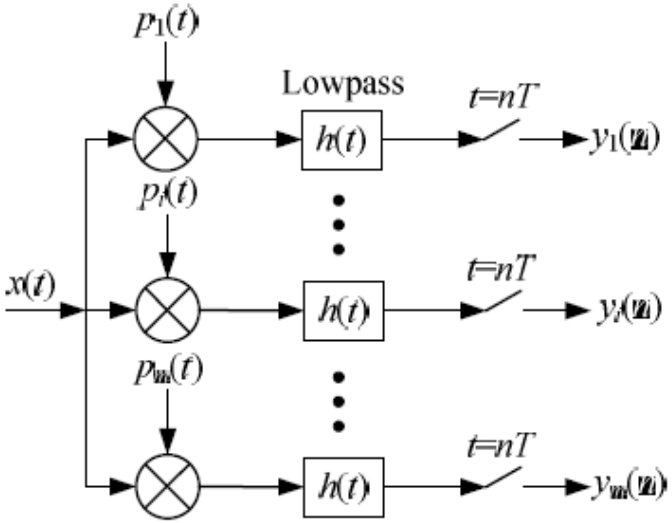

Fig. 1. Block diagram of the MWC system

From (1), it can be seen that the spectrum after being sampled by MWC becomes a linear combination of fp-shifted copy of the original spectrum $X(f)$ The shift interval f_p is the frequency of $p(t)$. If we consider $Y_i(e^{j2\pi fT})$ as the ith entry of an m-dimensional column vector $y(f)$ and $X(f-nf_p)$ as the nth entry of an L-dimensional ($L=2L_0+1$) column vector $z(f)$ then (1) can be reformulated as follows,

$$\boldsymbol{y}(f) = \boldsymbol{\Phi z}(f), \quad f \in [-f_s/2, f_s/2] \qquad (2)$$

where $\boldsymbol{\Phi}_{i,j} = c_{i,j}$, and $\boldsymbol{\Phi}$ is called sampling matrix with size $m \times L$ and $m < L$.

Fig. 2 gives the illustration of the relation between the unknown spectrum $\boldsymbol{z}(f)$ and the output signal spectrum $y(f)$. We can reconstruct $X(f)$ easily as long as the unknown vector $\boldsymbol{z}(f)$ is obtained by a specific recovery method.

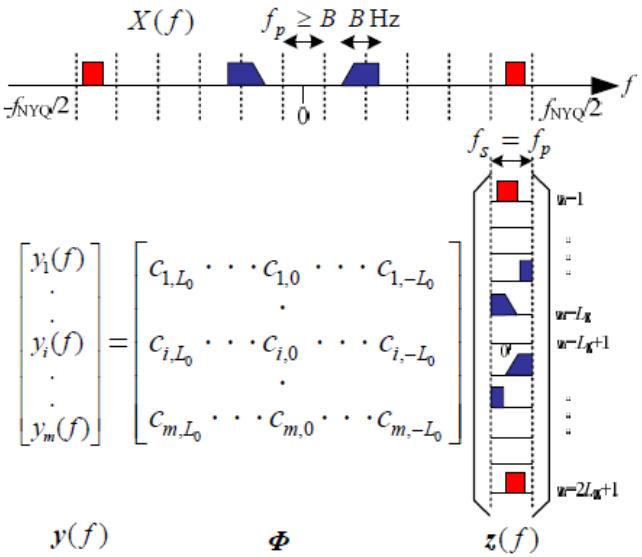

Fig. 2. Illustration of spectrum relations for input and output signals of MWC

From (2), the relation between the unknown time sequence *Z(n)* and measurements *Y(n)* can be developed by the inverse discrete time Fourier transform, and we have

$$\boldsymbol{Y}(n) = \boldsymbol{\Phi Z}(n) \quad (3)$$

where $\boldsymbol{Y}(n) = [\, y_1(n), y_2(n), \ldots, y_m(n)]^{\mathrm{T}}$

and $\boldsymbol{Z}(n) = [\, z_1(n), z_2(n), \ldots, z_m(n)]^{\mathrm{T}}$

Therein, $y_i(n)$ is the time sequence acquired from the ith channel, and $z_i(n)$ represents the unknown sequence corresponding to the ith unknown spectrum slice in $\boldsymbol{z}(f)$. Due to the condition $m<L$, both the matrix equations (2) and (3) are underdetermined so that we generally can not obtain the unique solution directly by inverse operations. Since the unknown $\boldsymbol{z}(f)$ or $\boldsymbol{Z}(n)$ has only few nonzero rows for sparse wideband signals, we can obtain the unique sparsest solution. We should first solve the support set of (3), and then perform the final recovery according to pseudo-inversion. It is noted that in spectrum sensing application, complete reconstruction of the signal is not needed, only the spectrum support is required to further judge the unused spectrum slices.

III. DISTRIBUTED SUB-NYQUIST SPECTRUM SENSING

For cognitive radio, uncertain channel fading and random shadowing would lead to varying signal strength at different receivers. Thus the distributed spectrum sensing approaches were considered in [7] and [8]. Such methods may significantly increase the reliability of the spectrum sensing process due to the comprehensive consideration. Although sub-Nyquist sampling method based on MWC has been proposed to sense the spectrum for cognitive radio, distributed sensing method using multiple MWCs have not yet been studied sufficiently. For distributed sub-Nyquist spectrum sensing, which is referred to as DSNSS (Distributed Sub- Nyquist Spectrum Sensing) later, both the sampling approach and recovery model differ from existing ones.

To achieve the potential strength of the distributed sensing, multiple MWC nodes can be separately placed on several locations of interest to acquire the different but correlated signals at sub-Nyquist rate of the same. Then the data obtained from these sensors is sent to a fusion center in which the final information is jointly recovered. Consider a distributed spectrum sensing system consisted of J MWCs. The sensing model can be formulated as follows,

$$\boldsymbol{Y}_j = \boldsymbol{\Phi}_j \boldsymbol{Z}_j \quad j \in \{1, 2, ..., J\} \qquad (4)$$

where the sensing matrix $\boldsymbol{\Phi}_j$ is of size $m \times L$ with $m < L$. Each unknown matrix $\boldsymbol{Z}_j$ with $j \in \{1, 2, ..., J\}$ consists of R sparse vectors, and all the matrices share $2N$ nonzero rows. That is, the joint sparsity level

$$\left| \bigcup_{j \in \{1,2,...,J\}} \mathrm{supp}(\boldsymbol{Z}_j) \right| = 2N$$

where $|S|$ represents the cardinality of the set S . Our task is to process the J MMV (Multiple Measurement Vector) problems [9] for the information of interest. For spectrum sensing, we do not need to recover each MMV problem exactly. We only need to find the support set to make a decision. Intuitively, we can solve (4) one by one through existing MMV recovery methods such as the OMPMMV and MUSIC algorithm. However, this cannot benefit the total recovery performance since the separate recovery process does not explore and take advantage of more information of the multiple measurement matrices. In (4), the unknown matrices have common nonzero rows, though the detailed entries of them are different. So in the following section, we attempt to utilize the joint sparse structure to seek a synchronous solving approach which can improve the sensing performance.

IV. JOINT-SPARSE RECOVERY ALGORITHM

In this section we introduce a new algorithm by exploring the correlation structures of the unknown matrices. We develop a method to recover the joint support of the signals. In [10], we adopted MUSIC algorithms to perform support recovery for a single MWC and achieved a good performance. Here, MUSIC can also be considered. We generalize this algorithm to multiple-MWC scenario. For MUSIC, in noisefree case the entries of support set decision $\boldsymbol{\Gamma}_{j,\downarrow l}$ of the jth MWC is zero for $l \in \Omega$ even when there is a certain noise, this value is relatively small. Hencre, if the l_2 norm is used to synthesize the decision matrix $\boldsymbol{\Gamma}_{j,\downarrow l}$ consisted of each decision vectors into one row vector γ the value of the element value at the index corresponding to the support set should also be relatively small. Conversely, we can judge the common support set by sorting the value of the elements in this vector. Table 1 gives the pseudo code of the DSNSS algorithm.

TABLE I. DSNSS Algorithm

Input: sampling matrices $\boldsymbol{\Phi}_j$, measurement matrices $\boldsymbol{Y}_j$, number of bands N ***Output***: Support set $\hat{\Omega}$ and final solutions $\hat{\boldsymbol{Z}}_j$
Step 1: Compute eigenvalues and eigenvectors of the correlation matrices of sampling value matrices $\boldsymbol{Y}_j(n)$ $j = 1, 2, ...J$; $n = 1, 2, ..., r$, respectively. Take eigenvectors corresponding to $2N$ maximum eigenvalues as the transformation matrices $\boldsymbol{T}_j = \boldsymbol{V}_j$. **Step 2**: Reduce the dimension of sampling value matrices through post-multiplying $\boldsymbol{Y}_j$ by $\boldsymbol{T}_j$, then we have: $\overline{\boldsymbol{Y}}_j = \boldsymbol{Y}_j \boldsymbol{T}_j$. **Step 3**: Find the kernel space matrix of each $\overline{\boldsymbol{Y}}_j$, that is, to solve $\overline{\boldsymbol{Y}}_j^{\mathrm{T}} \boldsymbol{W}_j = 0$ to achieve full-column-rank matrices: $\boldsymbol{W}_j \in \mathbb{R}^{m \times (m-2N)}$. **Step 4**: Calculate J MMV problems to obtain the preliminary support judge criterion $\boldsymbol{\Gamma}_{j,\downarrow \ell} = \| \boldsymbol{W}_j^{\mathrm{T}} \boldsymbol{\Phi}_{j,\downarrow \ell} \|_2$, $j = 1, 2, ..., J$, $\ell = 1, 2, ..., L_0 + 1$. Herein, $\boldsymbol{\Phi}_{j,\downarrow \ell}$ represents

the ℓ th column vector of the sensing matrix $\boldsymbol{\Phi}_j$.

Step 5: Compute the l_2 norm of each column vector of the matrix $\boldsymbol{\Gamma}$, and synthesize it into a row vector to form the final support judge criterion $\gamma_\ell = \left\| \boldsymbol{\Gamma}_{\downarrow \ell} \right\|_2$, $\ell = 1, 2, ..., L_0 + 1$.

Step 6: Find out the indexes related to N minimum values $\hat{\Omega}_0 = \min(\boldsymbol{\gamma}, N)$ in the vector $\boldsymbol{\gamma}$, which is taken as the first half of the support set.

Step 7: Obtain the complete support set element utilizing the conjugated symmetric relation the spectrum:

$$\hat{\Omega} = \hat{\Omega}_0 \bigcup (L + 1 - \hat{\Omega}_0).$$

In this algorithm, step 5 integrates the criteria of J support sets into a unified criterion through l2 norm. Therefore, the final support set criterion vector reflects the joint behavior of J-signals, which not only contains the diversity of different sparsity coefficients, but also includes the diversity of the sensing matrix. In addition, each support set criterion reflect the sparse structure of the corresponding unknown matrix to a certain extent. So the criterion fusion is equivalent to making full use of the sparse structure within the signal and the common characteristics between the signals. It is because of the above advantages that, in some cases, when the MWC isolation can not get the correct support set, the DSNSS joint sensing algorithm can still achieve the successful recovery of the support set.

V. EXPERIMENTS AND DISCUSSION

To evaluate the effectiveness of the proposed DSNSS spectrum sensing method, in this section we experimentally compare the joint recovery performance of DSNSS in terms of recovery rate with different numbers of MWCs, and show the potential strength in spectrum sensing application. In these experiments, the sparse wideband signals are generated by the following formula

$$x(t) = \sum \sqrt{E_n} B_n \operatorname{sinc}(B_n (t - \tau_n)) \cos(2\pi f_n (t - \tau_n)) + n(t)$$

where E_n, B_n, f_n and τ_n represent the energy coefficient, bandwidth, central requency and time offset of the nth band for a multiband signal, and $n(t)$ denotes additive white Gaussian noise.

In order to simulate the actual sampling process of MWC, the analog signal is represented by discretetime signal at Nyquist rate. In each experiment, the

following procedures are repeated for 500 times and the rate of success is computed according to the percentage of successful recoveries.

- ✧ The sign waveforms $p_i(t)$ are generated randomly with a uniform distribution.
- ✧ The central frequencies f_n are given randomly within the frequency interval $[-f_{NYQ}/2, f_{NYQ}/2]$.
- ✧ The support sets are jointly recovered using the DSNSS algorithm or separately recovered via MUSIC or OMPMMV.
- ✧ If the estimated support set $\hat{\Omega}$ is the same with the original one Ω, we announce a successful recovery. Moreover, if $\hat{\Omega} \supset \Omega$ and $\boldsymbol{\Phi}_{\hat{\Omega}}$ has full column rank, we also regard the recovery as a success.

We examine the recovery performance of DSNSS under different numbers of signals. Without loss of generality, we assume that there are J signals of interest, and for each, we take the number of bands $N = 6$ as an example. The time offset τ_n for the nth band of each signal is located randomly in the range of sampling duration. The central frequencies of bands distribute in the span $[-f_{NYQ}/2, f_{NYQ}/2]$ randomly, where the Nyquist rate $f_{NYQ} = 10$ GHz. The other parameters are fixed as: E_n={1, 2, 3}, B_n={50, 50, 50}MHz. According to [4], the parameters for each MWC are configured as follows: $f_s = f_p = f_{NYQ}/195 = 51.28$ MHz; $L_0 = 97$, $L = 2L_0+1 = 195$.

Since the performance enhancement of DSNSS is due to the use of more information across multiple signals, if the number of signals increases, the recovery performance is expected to be enhanced. To validate this, in this experiment, we shift the signal number $J \in \{1, 2, 4, 8\}$ and keep the other parameters unchanged. As shown in Fig. 3, when the channel number $m < 25$, the recovery rate increases with the rise of signal number J. For instance, when $m = 15$, the recovery rates are 22.0%, 61.5%, 85.0%, and 96.0% related to $J = 1, 2, 4, 8$, respectively. From the perspective of necessary minimum channel number, we can notice that the necessary channel number for exact recovery decreases with the increase of signal number J. We would guess that the theoretical lower bound of channel number ($m = 2N$) will be achieved when J is large enough.

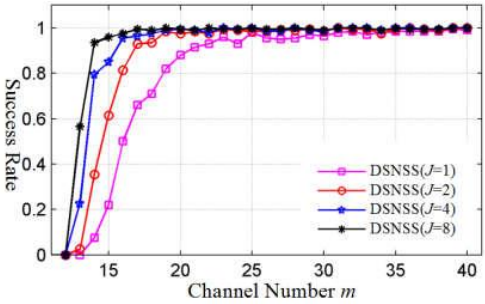

Fig. 3. Joint recovery rate curves of J signals with the shift of the number of channels m under signal-to-noise ratio of 10dB

The distributed spectrum sensing and joint recovery method based on DSNSS is expected to overcome severe fading and shadowing effect. To demonstrate this advantage of DSNSS, we consider a setting in which there are 6 transmission bands (3 pairs) and nevertheless partial transmissions are shadowed so as to the energy of corresponding bands becomes negligible at the specific receivers consisted of MWCs. We assume that two MWCs are adopted to sense the spectrum and for each the received bands are incomplete. The detailed setting is as the following table.

TABLE II. Signal parameters at the two MWCs

		Band #1	Band #2	Band #3
Signal Around MWC #1	E_n	**0.001**	5	2
	B_n	50 MHz	50 MHz	50 MHz
	f_n	2.4 GHz	3.5 GHz	4.8 GHz
	τ_n	0.2 μs	0.3 μs	0.5 μs
Signal Around MWC #2	E_n	4	**0.001**	1
	B_n	50 MHz	50 MHz	50 MHz
	f_n	2.4 GHz	3.5 GHz	4.8 GHz
	τ_n	0.3 uS	0.5 uS	0.7 uS

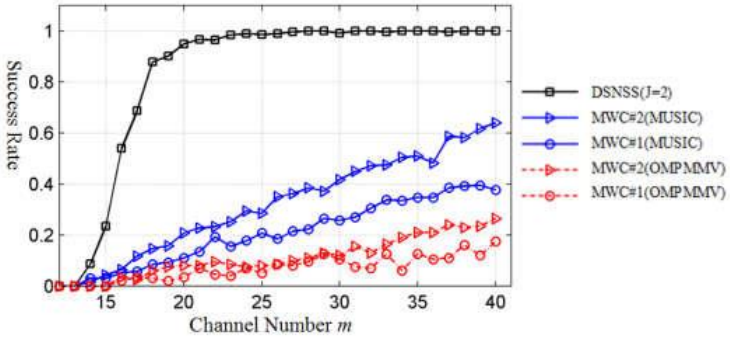

Fig. 4. Comparison of average success rates between separate recoveries using OMPMMV, DSNSS(J=1) and joint recovery using DSNSS(J=2)

Here because of the shadowing effect, the signal sensed by MWC #1 lacks band #1, and the signal around MWC #2 is short of band #2. Thus for each MWC the separate recovery result using MUSIC or OMPMMV fails to detect all the bands. Fig. 4 demonstrates the average success rates of the separate recovery using MUSIC and the joint recovery using DSNSS under SNR = 25dB. From this figure, we can see that, neither of MWC #1 or #2 can obtain all the band information due to the received incomplete information caused by the shadowing effect. In contrast, the DSNSS joint recovery algorithm can successfully detect all the bands with overwhelming probability when the number of channels is above 25. This shows the strength of the proposed DSNSS method for the spectrum sensing application.

VI. CONCLUSIONS

In this paper, we present a distributed sub-Nyquist spectrum sensing method based on multiple MWCs and a high-performance joint recovery algorithm. The proposed algorithm can improve the support recovery performance by using the joint sparse structure across multiple signals. Numerical experiments demonstrate that the joint recovery algorithm for multiple MWCs can significantly outperform the recovery approach for a single MWC in terms of sensing success rate. The success rate of joint recovery increases as the signal number rises, and the necessary number of hardware channels to achieve the same recovery rate deceases with the increase of the signal number. The proposed method can mitigate fading and shadowing effect owing to the cooperation between multiple nodes. Future works may include exploring a more efficient joint recovery algorithm for the distributed sub-Nyquist spectrum sensing problem.

ACKNOWLEDGEMENTS

This work was supported in part by the National Natural Science Foundation of China (NSFC) under grants 61501150, and the Youth Science Foundation of Heilongjiang Province under grants QC2014C074.

REFERENCES

[1] Kakalou I., Papadopoulou D., Xifilidis T., “A survey on spectrum sensing algorithms for cognitive radio networks”, 2018 7th International Conference on Modern Circuits and Systems Technologies (MOCAST), pp.1–4, 2018.

[2] Mashhour M. and Hussein A. “Sub-Nyquist wideband spectrum sensing based on random demodulation in cognitive radio”, 2017 12th International Conference on Computer Engineering and Systems (ICCES), pp.712–716, 2017.

[3] Qi P., Li Z., Li H., and Xiong T., “Blind Sub-Nyquist Spectrum Sensing With Modulated Wideband Converter”, IEEE Transactions on Vehicular Technology, vol.67, no.5, pp. 4278 - 4288, 2018.

[4] Mishali M., Eldar Y. C., “From theory to practice: sub-Nyquist sampling of sparse wideband analog signals”, IEEE Journal of Selected Topics in Signal Processing, vol. 4, no. 2, pp. 375–391, 2010.

[5] Adams D, Eldar Y C and Murmann B., “A mixer front end for a four channel modulated wideband converter with 62-dB blocker rejection”. IEEE Journal of Solid-State Circuits, vol.20, no.5, pp.1286-1294, 2017.

[6] Lexa, M. A., Davies M. E., Thompson J. S., “Reconciling Compressive Sampling Systems for Spectrally Sparse Continuous-Time Signals”, IEEE Transactions on Signal Processing, vol. 60, no. 1, pp. 155–171, 2012.

[7] Timalsina S. K., Moh S., and Lee J., “Cooperative Approaches to Spectrum Sensing and Sharing for Cognitive Radio Networks: A Comparative Study”, JNIT: Journal of Next Generation Information Technology, vol. 2, no. 4, pp. 10–23, 2011.

[8] Rasheed T., Rashdi A., Akhtar A. N., “Cooperative spectrum sensing using fuzzy logic for cognitive radio network”, 2018 Advances in Science and Engineering Technology International Conferences (ASET), pp.1–6, 2018.

[9] Cotter F. S., Rao D. B., Engan K, “Sparse solutions to linear inverse problems with multiple measurement vectors”, IEEE Transactions on Signal Processing, vol. 53, no. 7, pp. 2477–2488, 2005.

[10] Gai J., Fu P., Fu N., and Liu B. “Sub-Nyquist sampling reconstruction algorithm based on SVD and MUSIC”vol. 33, no. 9, pp. 2073-2079, 2012.